Plant specificities in rRNA processing

- From snoRNA to rRNA variations -

Dissertation

zur Erlangung des Doktorgrades

der Naturwissenschaften

vorgelegt beim

Fachbereich Biowissenschaften der

Goethe-Universität Frankfurt am Main

von

Deniz Streit

aus Wiesbaden

Frankfurt am Main 2022

(D30)

vom Fachbereich Biowissenschaften der Goethe-Universität als Dissertation angenommen.

Dekan: Prof. Dr. Sven Klimpel

Erster Gutachter: Prof. Dr. Enrico Schleiff

Zweiter Gutachter: Prof. Dr. Michaela Müller-McNicoll

Datum der Disputation: 21.07.2023

Für meinen Papa

Abstract

The production of ribosomes is a complicated multistep, that is susceptible to changes occurring within the cell and its environment. The process itself requires many proteins, known as ribosome biogenesis factors (RBFs) and many non-coding RNAs like the small nucleolar RNAs (snoRNAs). While RBFs are required for the accurate processing of the pre-rRNA into mature rRNAs, the snoRNAs act to coordinate and guide enzymes for post-transcriptional modifications, chiefly 2´-O-ribose methylation and pseudouridylation. While ribosome biogenesis is mostly described in human and yeast model eucaryotes, similar detailed studies in the model plant *Arabidopsis thaliana* are far less explored and understood. Furthermore, for many experimentally confirmed modification sites the according snoRNAs and for many pre-rRNA processing steps the responsible RBFs are missing. Therefore, it is expected that a high number of snoRNAs and RBFs are not identified till yet. For this reason, RNA-deep sequencing was performed in order to identify novel snoRNAs and MS analysis data of nucleoli and nuclei of *A. thaliana* from a former PhD student were used in order to find new proteins involved in pre-rRNA processing.

In here, it is shown that with RNA deep-sequencing still new snoRNAs and snRNAs can be identified and that detection of predicted snoRNAs can be fulfilled with a) antisense oligonucleotides tagged with fluorescence dyes and b) with radioactive labeled antisense probes. Furthermore, a secondary structure map of the 60S and 40S subunit highlighting the predicted and moreover verified modification sites in 5.8S, 25S and 18S rRNA was created. Especially, the correlation between the modification sites and the guiding snoRNA is highlighted further shedding light on overview about current pre-rRNA modification sites and corresponding guiding snoRNAs. The next chapter reveals the complex and multi-layered existence of the 5.8S rRNA and its numerous precursors. The mutant *prp24* (also known as *seap1*) encoding AtPRP24, is recognized as factor being important for splicing as it is promoting the recruitment of the U4 and U6 snRNAs to the spliceosome. In here, it was found that AtPRP24 is involved in processing of 5.8S rRNA precursors, recognizable by precursors that are over accumulating in the mutant. Moreover, it could be shown for the first time that the plant-specific precursor 5´-5.8S is exported to the cytoplasm, where final cleavage steps of 5.8S rRNA takes place. In the *prp24.2* mutant, this precursor is exported at an increased rate to the cytoplasm, where it can be detected in the actively translating ribosomes (polysomes). A lower sensitivity of the mutant seeds to cycloheximide (CHX) suggests that due to the extension at the 5´-end of 5.8S, the structure of the 60S subunit has altered CHX binding. In conclusion, this work highlights the importance and complexity of 5.8S rRNA and its precursors for ribosome biogenesis and displays new insights into pre-rRNA processing in *A. thaliana*.

Table of contents

Index of figures

Index of tables

Abbreviations

5´ETS/3´ETS	5´ and 3´ external transcribed spacer	NaCl	sodium chloride
2´-O-me	2´-ribose methylation	NaOH	sodium hydroxide
A. thaliana	*Arabidopsis thaliana*	NPET	nascent polypeptide exit tunnel
bp	base pairs	nt	nucleotide
ccDNA	circularized complementary DNA	*O. sativa*	*Oryza sativa*
cDNA	complementary DNA	PAA	polyacrylamide
crRNA	circularized RNA	PBS	phosphate-buffered saline
CHX	cycloheximide	PCI	phenol:chloroform:isoamylalcohol
cRT-PCR	circularized reverse transcription-PCR	PCR	polymerase chain reaction
Cy3/Cy2	cyanine 3/ cyanine 2	PE	pivoting element
ddH_2O	double distilled	PTC	peptidyl transferase center
DNA	deoxyribonucleic acid	PWS	Prader-Willi Syndrome
dNTP	desoxyribonucleotide	RBF	ribosome biogenesis factor
dT	deoxythymine	RNA	ribonucleic acid
DTT	dithiothreitol	RT-PCR	reverse transcription polymerase chain reaction
E. coli	*Escherichia coli*	*S. cerevisiae*	*Saccharomyces cerevisiae*
EDTA	ethylenediamine tetraacetic acid	SDS	sodium dodecyl sulfate
ES	expansion segment	snoRNA	small nucleolar RNA
EtBr	ethidium bromide	snoRNP	small nucleolar ribonucleoproteins
EtOH	ethanol	*S. lycopersicum*	*Solanum lycopersicum*
FLB	formamide loading buffer	SU	subunit
gDNA	genomic DNA	TBE buffer	Tris/Borate/EDTA
H	helix	Tris	Tris (hydroxymethyl) amino methane
H. sapiens	*Homo sapiens*	UV	ultraviolet
IPTG	isopropyl-beta-D-thiogalactopyranoside	X-DC	X-linked Dyskeratosis Congenita
ITS1/ITS2	internal transcribed spacer 1 and 2	X-Gal	5-bromo-4-chloro-3-indolyl-*beta*-D-galacto-pyranoside
$MgCl_2$	magnesium chloride	Ψ	pseudouridylation
mRNA	messenger RNA		
MS	murashige-Skoog		

Units

°C	degree Celsius	mM	millimolar
µg	microgram	nm	nanometer
µL	microlitre	ng	nanogram
µM	micromolar	pmol	picomole
das	days after stratification	rpm	rounds per minute
g	relative centrifugal force	sec	second
h	hour	U	unit
kDa	kilo Dalton	v/v	volume per volume
M	molar	V	volt
mbar	millibar	vol	volume
min	minute	w/v	weight per volume
ml	milliliter		

Nomenclature for genes and proteins

The nomenclature of genes and proteins in this thesis corresponds to the guidelines given by ´The Arabidopsis Information Resource´ (TAIR). Explanation on the example of Prp24 is given below. In the following work, *Arabidopsis thaliana* will be shortened to Arabidopsis for reasons of simplification.

PRP24	wild type allele
prp24	mutant plant line
prp24.1	mutant plant line #1
prp24.2	mutant plant line #1
atPRP24	protein

Zusammenfassung

Ribosomen sind hochkomplexe makromolekulare Maschinen, die notwendig sind für jede lebende Zelle. Ribosomen werden im Zytoplasma benötigt, um dort aus Messenger-RNA (mRNA) Proteine zu synthetisieren. Eukaryotische cytosolische Ribosomen bestehen aus einer 60S und 40S Untereinheit. Die pflanzliche 60S Untereinheit besteht aus der 25S, 5.8S und 5S rRNA zusammen mit 49 ribosomalen Proteinen und die 40S Untereinheit aus der 18S rRNA mit 30 ribosomalen Proteinen. Zusammen bilden sie das zytosolische 80S Ribosom.

Die Ribosomenbiogenese ist ein hoch komplexer Vorgang, der viele Proteine und RNAs benötigt. Die Proteine, die für die Herstellung funktionaler Ribosomen benötigt werden sind als Ribosomenbiogenesefaktoren (RBFs) bekannt. Es gibt ca. 250 verschiedene RBFs, die u.a. für die Modifizierung und der exo- und endonukleolytischen Trennung der pre-ribosomalen RNA (pre-rRNA) benötigt werden. Der Anfang einer jeden Ribosomenbiogenese findet im Nukleolus statt, wo die ribosomale DNA (rDNA) mithilfe der RNA-Polymerase I in die pre-rRNA transkribiert wird. Die pre-rRNA enthält nur drei der 4 rRNAs nämlich die 18S, 5.8S und die 25S. Die 5S wird unabhängig davon im Nukleus durch die RNA-Polymerase III transkribiert. Nach der Transkription findet in der Regel die posttranskriptionelle Modifizierung der pre-rRNAs mithilfe der ,,kleinen nukleolären Ribonukleinsäuren´´ (engl. small nucleolar RNAs; snoRNAs) statt. Dabei fungieren die snoRNAs als Leitelemente, um katalytisch aktive Proteine an die richtige Stelle an der rRNA zu bringen. Bisher sind über 200 verschiedene snoRNAs in *Arabidopsis thaliana* (*A. thaliana*) identifiziert. Nach der Modifizierung der pre-rRNA, werden enzymatische Proteine benötigt, deren Funktion es ist die pre-rRNA in einem hochkomplexen mehrstufigen Vorgang zu zerschneiden und in seine drei rRNA-Bestandteile aufzuteilen. Im Nukleus angekommen, fügt sich dann die 5S in die pre-60S Untereinheit ein und die Vorstufen beider Untereinheiten werden in das Zytosol exportiert. Im Zytosol findet dann die finale Reifung der rRNAs statt und ribosomale Proteine, die für die Reifung und Translation benötigt werden, stoßen in den letzten Schritten zu den Untereinheiten.

Die Prozessierung der pre-rRNA in die reifen rRNAs ist sehr komplex und erfordert daher das perfekte Zusammenspiel von snoRNAs, ribosomalen Proteinen und Ribosomenbiogenesefaktoren. Ein Teil dieser Dissertation handelt aus diesem Grund über die snoRNAs. Anlehnend an die snoRNAs wird im zweiten Teil eine umfangreiche Analyse der snoRNAs durchgeführt, indem Next-Generationen Sequenzierung und in-vitro Experimente zur Entdeckung und Verifizierung neuer snoRNAs geführt haben und im letzten Teil werden putative Ribosomenbiogenesefaktoren untersucht, die eine direkte bzw. indirekte Funktion in der pre-rRNA Prozessierung haben.

Die snoRNAs in *Arabidopsis thaliana*

Die snoRNAs werden in zwei Klassen unterteilt, die auf konservierten Sequenzen innerhalb der snoRNAs basieren. Die C/D Box snoRNAs besitzen eine C Box (RUGAUGA) und eine D Box (CUGA) und manchmal zwei weniger konservierte C´ und D´ Boxen. Während die C Box nahe am 5´ Ende der snoRNA vorliegt, ist die D Box in etwa mittig lokalisiert. Zwischen der C und B Box befindet sich eine 10-21 nt lange Sequenz, die komplementär zur rRNA-Position ist, die modifiziert werden soll. Etwa 5 nt vor der D Box findet dann die Modifizierung statt. Zur zweiten Klasse gehören die H/ACA Box snoRNAs. Hier findet sich eine H-Box (ANANNA) und eine ACA-Box, die zumeist am 3´-Ende der snoRNA zu finden ist. Die Stelle der Modifizierung findet hierbei etwa 15 nt vor der ACA-Box statt. Während C/D box snoRNAs die 2´-O-Ribose Methylierung anleiten, leiten die H/ACA Box snoRNAs die Konversion von Uridin zu Pseudouridin an. Beide snoRNA Klassen arbeiten in Kooperation mit Proteinen, die u.a. für die enzymatische Reaktion benötigt werden oder den Protein-snoRNA-Komplex stabilisieren. Dabei werden die C/D Box snoRNAs von den Proteinen Fibrillarin (Methyltransferase), Nop58, Nop56 und Snu13 unterstützt und die H/ACA Box snoRNAs von Nap57 (Hefe Cbf5), Nhp2, Nop10 und Gar1.

Für *A. thaliana* wurden bisher mehr als 200 snoRNAs identifiziert, die u.a. mittels RNA-Sequenzierungen in Verbindung mit computerbasierten Vorhersagen ermittelt wurden. Zudem führten verschiedene Methoden dazu, dass eine Vielzahl von Modifizierungsstellen an der ribosomalen RNA identifiziert werden konnten. So konnten bislang etwa 323 vorhergesagte modifizierte Stellen gefunden werden, zu denen 214 2´-O-ribose Methylierungen (2´-O-me) und 109 Pseudouridylierungen (Ψ) zählen. Durch verschiedenste experimentelle Ansätze konnten für die vorhergesagten 2´-O-me 132 und für die vorhergesagten Pseudouridylierungen 81 Stellen an der rRNA verifiziert werden. Die Lokalisierung der snoRNA Gene im Genom unterscheidet sich in mehreren Punkten von denen der Menschen und Hefe. Während menschliche und Hefe snoRNA Gene hauptsächlich im Intron von proteinkodierenden Genen liegen beziehungsweise unabhängig durch einen eigenen Promotor transkribiert werden, findet sich bei *A. thaliana* eine polycistronische Genorganisation, wobei mehrere snoRNA Gene über einen einzigen Promotor transkribiert werden. Kürzlich wurden zudem tRNA-snoRNA und snoRNA-miRNA Cluster in *A. thaliana* gefunden. Bisherige Analysen über die Funktion einzelner snoRNAs in *A. thaliana* zeigten, dass sie nicht nur eine Rolle in der Modifizierung haben, sondern davon abweichend ebenfalls in der Prozessierung der pre-rRNA mit involviert sein können, wie beispielsweise für HID2 gezeigt wurde. Genauso konnte gezeigt werden, dass obwohl die *HID2* Expression repremiert war, die Modifizierungsstelle, die von HID2 angesteuert wird, nicht betroffen war und immer noch modifiziert wurde. Diese Tatsache und die Tatsache, dass es für viele

Modifizierungsstellen in der rRNA von *A. thaliana* noch keine passende snoRNA gefunden werden konnte, die diese ansteuert, haben wir eine RNA-Sequenzierung der nuklearen RNA von *A. thaliana* durchführen lassen, die in einem zweiten Schritt von Bioinformatikern auf neue snoRNAs hin untersucht wurde. Dabei zeigten die Untersuchungen, dass u.a. eine große Anzahl der in Datenbanken geführten snoRNAs gefunden wurden und außerdem weitere Genloci für bereits zugewiesene snoRNAs entdeckt werden konnten. Einzelne snoRNAs wurden daraufhin weiteren Untersuchungen unterzogen, wobei mithilfe von Fluoreszenz- und Radioaktiv-markierten Antisense-Oligonukleotiden die Lokalisation innerhalb der Zelle analysiert wurde. Hierbei zeigte sich, dass einige der bereits bekannten snoRNAs nicht nur im Nukleus der Zelle detektiert werden konnten, sondern auch, was unüblich ist, im Zytosol. Des Weiteren, konnte gezeigt werden, dass es eine unterschiedliche Verteilung der snoRNAs innerhalb der Pflanze gibt. So wurden einige snoRNAs vor allem in reproduktiven Geweben, wie den Blüten, gehäuft vorgefunden. Hinzukommend, wurden für manche der neu annotierten snoRNAs rRNA-Alignments durchgeführt, um potenzielle Modifizierungsstellen zu identifizieren.

Die Modifizierungen der rRNA von *A. thaliana*

Die Anzahl der posttranskriptionellen Modifizierungen der rRNAs von *A. thaliana* nehmen mittlerweile immer mehr zu. Dazu führte u.a. die neuartige Herangehensweise für die Identifizierung neuer Stellen. So werden für 2´-O-Methylierungen RiboMethSeq angewendet, dass es erlaubt innerhalb kürzester Zeit RNA-Methylierungen zu erfassen und zu Quantifizieren. Für Pseudouridylierungen wird die RNA mit N-Cyclohexyl-N´-(2-morpholinoethyl)-carbodiimid-methyl-p-toluolsulfonat (CMC) behandelt, um neue Stellen mittels der Next-Generation Sequenzierung zu identifizieren. Die große Anzahl an neu identifizierten Modifizierungsstellen an der rRNA, führte zum zweiten Teil dieser Arbeit. Hierbei wurde eine aktualisierte Karte der Sekundärstruktur der rRNAs mit den gegenwärtig bekannten Modifizierungsstellen von *A. thaliana* erstellt, die gleichzeitig auch die snoRNAs, die die jeweilige Stelle ansteuert, aufgelistet. So kann gezeigt werden, wo an der rRNA wichtige und funktionale Modifizierungen vorliegen und gleichzeitig mit den Modifizierungen aus Menschen und Hefe verglichen werden. Außerdem wurden die bekannten Modifizierungsstellen und dazugehörige snoRNAs in einer Tabelle mit denen verglichen, die es in Menschen und Hefe gibt, sodass ein schneller und direkter Abgleich stattfinden kann. Auf diese Weise zeigte sich, dass obwohl mehrere Stellen konserviert sind von Menschen zu Hefe zu Pflanzen, einige Modifizierungsstellen speziell nur in *A. thaliana* gefunden werden können, wobei die Ursache dafür nicht herausgefunden werden konnte, und noch untersucht werden muss in der Zukunft. Zur Vereinfachung wurde die Struktur der 60S und 40S rRNAs in mehrere Teile gegliedert, die

einzelne Domänen aufzeigen. Für die Diskussion wurde die Struktur dann wieder zusammengesetzt.

AtPRP24 und die Prozessierung der 5.8S rRNA in *A. thaliana*

Die Hauptfunktion von Prp24/SART3(p110) in Hefe bzw. Menschen ist die Rekrutierung der U4 und U6 snRNA im Nukleus zum Spliceosom und trägt damit zum korrekten Splicing verschiedenster pre-mRNAs bei. Für das Arabidopsis Homolog AtPRP24 ist diese Funktion noch nicht vollständig untersucht worden aber Daten deuten darauf hin, dass diese Funktion auch in Arabidopsis vorliegt. Mehr noch scheint AtPRP24 mehrere andere Rollen innerhalb des Zellkerns wahrzunehmen. So konnte gezeigt werden, dass AtPRP24 bzw. SEAP1 (Serrate-Associated Protein 1) in der Biogenese von miRNAs eine entscheidende Rolle spielt.

In dieser Arbeit wurde AtPRP24 ausgesucht, da es zum einen mehrere RNA-Bindestellen aufweist und zum anderen nur im Nukleus vorliegt und somit eine mögliche direkte oder indirekte Funktion in der rRNA Prozessierung wahrnehmen könnte. In der Tat zeigen Untersuchungen von T-DNA Insertionslinien, dass Störungen in der pre-rRNA Prozessierung vorliegen, die mitunter erheblich erhöht werden, wenn die T-DNA Insertion bereits im Exon 4 von *PRP24* vorliegt (*prp24.2*) als wenn es in Intron 14 (*prp24.1*) vorliegt. So wurde *prp24.2* für alle weiteren Experimente ausgesucht. Besonders auffällig an der Mutante ist, dass die pflanzenspezifische 5.8S Vorstufe 5´-5.8S pre-rRNA angehäuft wird. Diese Beobachtung führte zur Frage ob und wie die Anhäufung in den Subkompartimenten der Zelle auftreten. Wildtyp und *prp24.2* Pflanzen wurden daher einer Subfraktionierung unterzogen und die cytosolische mit der nukleären RNA mittels Northern Hybridisierung vergleichend analysiert. Dabei zeigte sich, dass die 5´-5.8S pre-rRNA bereits im Zytosol des Wildtyps vorkommt, und in *prp24.2* in fast 2-facher Menge vorliegt. Des Weiteren, wurde beobachtet, dass neben der 5´-5.8S pre-rRNA auch mehrere andere 5.8S Vorstufen mit derselben Sonde im Nukleus detektiert werden konnten. Diese zusätzlichen, bisher nicht beschriebenen Vorstufen, wurden in *prp24.2* ebenso akkumuliert wie die 5´-5.8S pre-rRNA. Dieses deutet darauf hin, dass ein grundlegender Schritt während des Prozessierungsweges in *prp24.2*, betroffen sein muss. Ein Vergleich mit *rrp6l2*, der Mutante der 3´-5´ Exosom-Komponente AtRRP6L2, zeigte das mehrere dieser unbekannten Vorstufen auch hier im Nukleus akkumulieren, obwohl *rrp6l2* vorwiegend 3´ verlängerte 5.8S pre-rRNAs akkumuliert.

Die Erkenntnis, dass viele Vorstufen der 5.8S rRNA noch nicht oder nur geringfügig in der Literatur beschrieben wurden, führte zu intensiven Untersuchungen dieser Vorstufen im Zellkern von *prp24.2* und Wildtyp. Dabei zeigte sich, dass etwa sechs verschiedene Vorstufen von der 5.8S rRNA gebildet werden. Außerdem, werden einige dieser Vorstufen entweder nur

im Wildtyp oder nur in *prp24.2* gebildet. So konnte die A_3-5.8S-3´ Vorstufe nur in *prp24.2* gefunden werden und A_2-5.8S und A_3´-5.8S Vorstufen nur im Wildtyp detektiert werden. Diese unterschiedliche Zusammensetzung lässt darauf schließen, dass erstens die Prozessierung der 5.8S rRNA grundlegend komplexer und aufwendiger zu sein scheint als bisher angenommen und zweitens *prp24.2* einen etwas veränderten Prozessierungsweg einschlägt als der Wildtyp. Denn obwohl die 5.8S pre-rRNA Prozessierung in *prp24.2* gestört zu sein scheint, lässt sich kein Unterschied in der Menge der reifen 5.8S rRNA feststellen. Diese Annahmen führten zu einem neuen vorgeschlagenen Prozessierungsweg, sowohl für den Wildtyp als auch einen für *prp24.2*. In diesem neuen theoretischen Weg wird die 5´-5.8S pre-rRNA dem rRNA Prozessierungsweg 1 zugeordnet, wie bereits früher schon vermutet. Die große Anzahl an verschiedenen 5.8S Vorstufen mit unterschiedlichen 5´-Verlängerungen, führte dabei dazu, dass die 5.8S pre-rRNA Prozessierung in einen Haupt- und Nebenweg gegliedert wurde, die beide aus der A_2-C_2 Vorstufe hervorgehen. Auf Grundlage der Sequenzierungshäufigkeit der einzelnen Vorstufen, wurden pre-rRNAs mit großer Häufigkeit in den Hauptweg, und pre-rRNAs mit niedriger Häufigkeit in den Nebenweg eingegliedert. So scheint es, dass der Hauptweg im Wildtyp mit insgesamt vier Vorstufen komplexer verläuft als in *prp24.2* mit nur zwei Vorstufen. Dieses führt zu der Annahme, dass Grundlegende Schritte der Prozessierung in *prp24.2* betroffen sind, die dazu führen, dass die 5´-Prozessierung über einen schnelleren Weg erfolgen. Interessanterweise findet sich in den Polysomen von *prp24.2* gehäuft die 5´-5.8S pre-rRNA, was darauf schließen lässt, dass der letzte Prozessierungsschritt zur Reifung der 5.8S rRNA teilweise übersprungen wird und stattdessen eine 5´-Verlängerte 5.8S rRNA in den Ribosomen verbleibt. Um einen Einblick zu bekommen, wie sich so eine Verlängerung auf die Struktur der 60S Untereinheit auswirken könnte, wurden hypothetische Strukturbilder angefertigt, die die Verlängerung und alle ribosomalen Proteine in der Nähe aufzeigt. Hieraus erschließt sich, dass besonders Proteine, die sich am 5´-Ende der 5.8S rRNA befinden am meisten von der Verlängerung betroffen wären. Dabei lässt sich aber nicht ausschließen, dass auch im inneren der 60S Untereinheit grundlegend Veränderungen auftreten, die u.a. die Translation beeinflussen könnten. So könnten diese heterogenen Ribosomen, die zu einem kleinen Teil auch im Wildtyp vorkommen, für die Translation von spezifischen mRNAs benötigt werden. Letzteres könnte man untersuchen, wenn man in der Lage wäre, diese 5´-Verlängerten Ribosomen zu isolieren, um dann eine Ribosomen Sequenzierung durchzuführen, die aufzeigen könnte, ob im Vergleich zu normalen Ribosomen andere mRNAs überwiegend bevorzugt werden. Die Isolation mittels einem Antisense-Oligonukleotids erwies sich als schwer durchführbar und bedarf einiger Verbesserungen, um in Zukunft solche heterogenen Ribosomen besser isolieren zu können.

1 Introduction

Ribosomes are catalytic machineries important for the production of polypeptides from a messenger RNA (mRNA) sequence. The generation of functional and intact ribosomes requires an intricate process, by which multiple proteins and RNAs must work together to orchestrate this process. Ribosomes are multiprotein ribonucleoprotein particles having a molecular weight ranging from 2.3 MDa (70S ribosomes in bacteria) to 4.3 MDa (80S ribosomes in eukaryotes), with two-thirds of the mass composed of RNA and one-third of protein (Rostom et al., 2000; Khatter et al., 2015; Pilla et al., 2019). The Arabidopsis ribosomes have an approximate mass of 3.2 MDa, with the 60S subunit (large subunit, LSU) having a mass of 2.01 MDa and the 40S subunit (small subunit, SSU) with a mass of 1.16 MDa (Chang et al., 2005). The 60 subunit of Arabidopsis consists of the 5S, 5.8S and 25S rRNA and approximately 46 ribosomal proteins (RPs), while the 40S subunit contains only the 18S rRNA and approximately 33 RPs (Konikkat and Woolford, 2017; Pillet et al., 2017). Although both subunits are required for translation, each subunit has its own specific role in the process. The 60S subunit contains the peptidyl transferase center (PTC), harboring the aminoacyl- and peptidyl-tRNA binding sites (A and P site) and is necessary for peptide bond formation and peptide release (Beringer and Rodnina, 2007; Polacek and Mankin, 2008). In contrast, the 40S subunit harboring the decoding center (DC), a binding site for mRNAs and tRNAs, is essential for codon-anticodon interaction and translocation (Liang et al., 2009; Schluenzen et al., 2000). The regions PTC and DC, which are comprised of rRNA, are extensively decorated with modifications (Decatur and Fournier, 2002; Liang et al., 2009; Streit and Schleiff, 2021). The ribosomal RNAs are arranged in the nucleolar encoded polycistronic unit 35S pre-rRNA containing 18S, 5.8S and 25S in the so-called 90S particle (Figure 1). This precursor is extensively processed during ribosome biogenesis in a process called pre-rRNA processing within the nucleolus. In subsequent steps, rRNA modifications usually takes place within the nucleolus, with the assistance of nuclear encoded small nucleolar RNAs (snoRNAs) in collaboration with a specific subset of proteins known as small nucleolar ribonucleoparticles (snoRNPs). The pre-66S and pre-43S subunits are exported to the nucleus, where the nuclear encoded 5S rRNA is loaded onto the pre-60S subunit. Both pre-subunits are then exported to the cytoplasm, where during or after export, rRNA maturation is accomplished by last cleavage steps (Figure 1). A first test drive shows if both subunits are correctly folded and functional. The following chapters provide detailed insights into the topics of rRNAs, snoRNAs, posttranscriptional modifications of rRNAs, processing of pre-rRNAs and the role of the 5.8S rRNA in the ribosome.

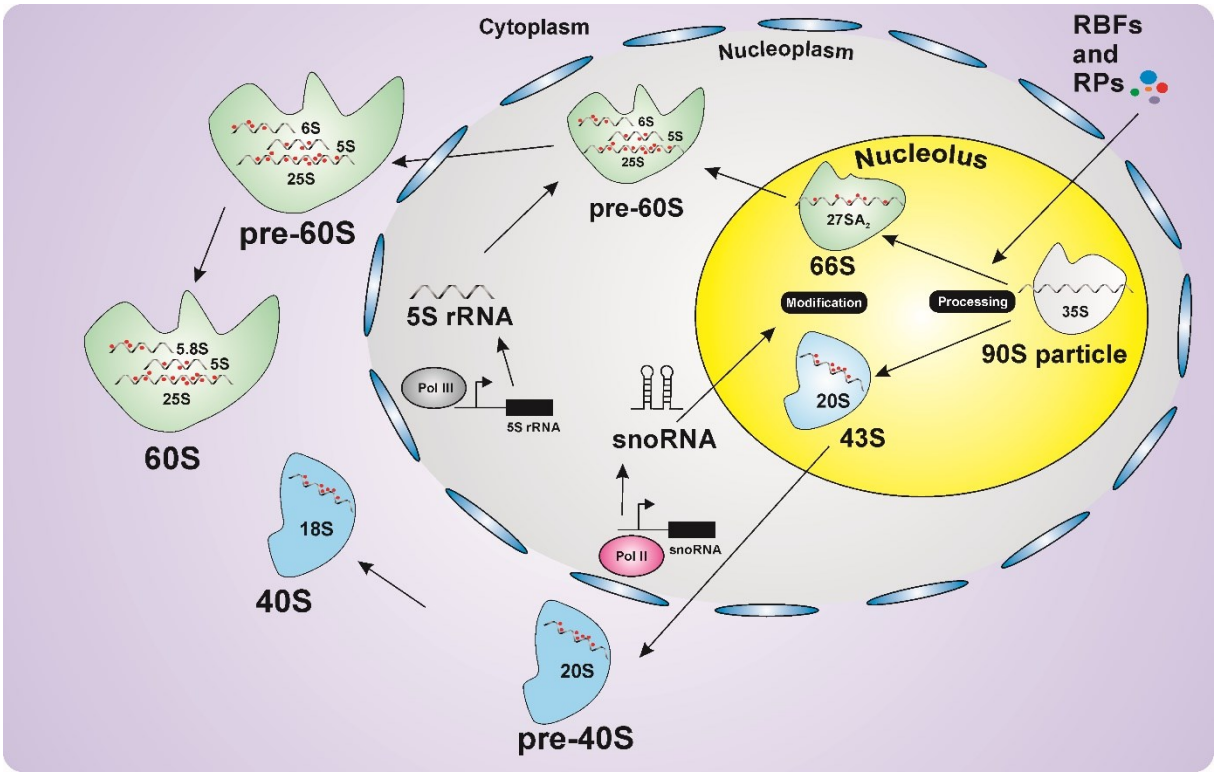

Figure 1. Ribosome biogenesis in eucaryotes.
The 90S particle is formed after transcription of rDNA, with the help of ribosome biogenesis factors (RBFs) and snoRNAs, the 35S pre-rRNA is processed and modified within the nucleolus. The pre-66S and pre-43S subunits are exported to the nucleus and 5S rRNA is joining pre-60S subunit. Subsequently, subunits are exported to cytoplasm. After finalization, both subunits are joining in the cytoplasm. Adapted from Lafontaine (2015).

1.1 post-transcriptional modifications of rRNA and snoRNAs

In the last decades, it has been shown that ribosomal RNA is extensively modified. Most modifications can be grouped in four forms: methylation of the ribose backbone (2´-O-ribose methylation), conversion of uridine to pseudouridine (Ψ), base methylation, and acetylation of cytidines (Decatur and Fournier, 2002; Lafontaine, 2015; Ito et al., 2014). Usually, these modifications are carried out by the 60-300 nt short snoRNAs with the substantial assistance of a specific subset of proteins, known as snoRNPs (Liang et al., 2019). The latter ones are grouped in two classes: namely the C/D box and H/ACA box snoRNPs (Figure 2). The C/D box snoRNPs are comprised of an exchangeable snoRNA, which specifically binds to a region on the rRNA by antisense elements and the proteins Fibrillarin /Nop1p (methyltransferase), NOP58/Nop58p, NOP56/Nop56p and 15.5K/Snu13p (Brown et al., 2003) (Figure 2A). The C/D box snoRNAs contain the conserved C (RUGAUGA; R is any purine) and D (CUGA) boxes and sometimes the two less conserved C´ and D´ boxes (Brown et al., 2001). The C box is located close to the 5´-region of the snoRNA, followed by an antisense element of approximately 10-21 nt for rRNA binding, where the fifth nucleotide upstream of the D box is used to be the nucleotide to be methylated (Barneche et al., 2001; Kiss, 2001; Kruszka et al.,

2003). A second antisense element can be found closer to the 3´-region between C´ and D´ boxes (Figure 2A).

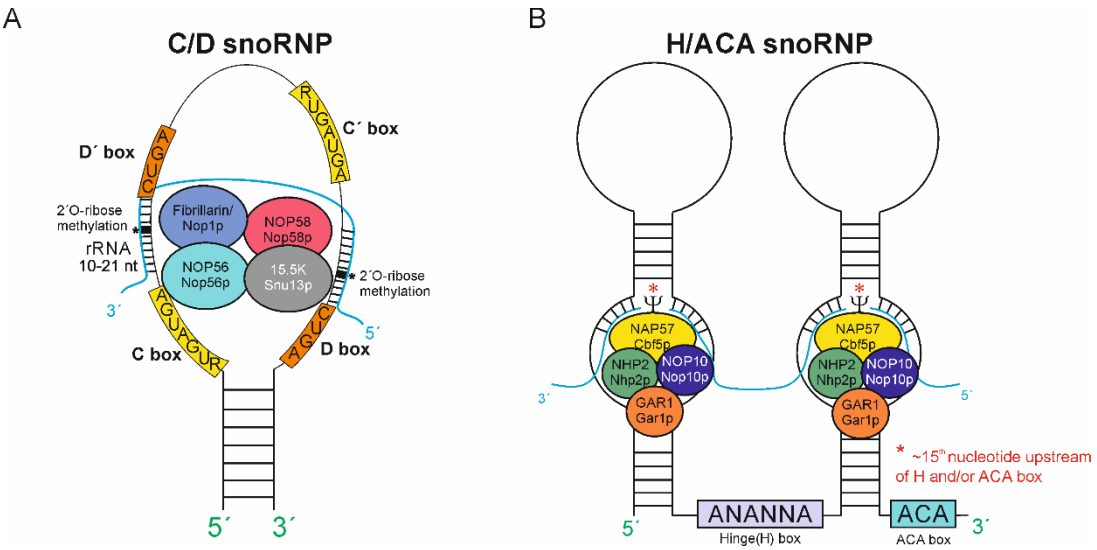

Figure 2. The C/D and H/ACA snoRNPs.
A) C/D snoRNPs consist of four core proteins, namely Fibrillarin/Nop1p (methyltransferase), NOP58/Nop58p, NOP56/Nop56p and 15.5K/snu13p and a C/D box snoRNA. The snoRNA is characterized by the two conserved boxes C (RUGAUGA) and D (CUGA) and two lesser conserved boxes C´ and D´. the guiding snoRNA is 10-21 nt of the rRNA region, by which the fifth nucleotide upstream of the D or D´ box is targeted for 2´-O-methylation. **B)** The H/ACA box snoRNPs are composed of the proteins NAP57/Cbf5p, NHP2/Nhp2p, NOP10/Nop10p and GAR1/Gar1p together with a H/ACA snoRNA. The snoRNA is characterized by a Hinge (H) box with the consensus sequence (ANANNA) and the ACA box, three nucleotides upstream of the 3´-end. The site of pseudouridylation happens approx. 15 nt upstream of the H and/or ACA box, respectively. Adapted from Streit and Schleiff (2012).

The H/ACA box snoRNPs are composed of an H/ACA box snoRNA, which usually forms a hairpin-hinge-hairpin-tail structure, containing the Hinge (H) box with the consensus sequence ANANNA (N stands for any nucleotide) and the 3´ located ACA-box (Dragon et al., 2006) (Figure 2B). The H/ACA box snoRNPs are formed by an exchangeable snoRNA and the proteins dyskerin (NAP57)/Cbf5 (pseudouridine synthase), NHP2/Nhp2, NOP10/Nop10 and GAR1/Gar1 (Rodor et al., 2011). Alike C/D box snoRNPs, H/ACA box snoRNPs are able to simultaneously convert two U to Ψ, whereby the U to be modified is usually located ~15 nt upstream of the H and/or ACA box (Lindsay et al., 2013; Figure 2B).

The C/D-box and H/ACA-box snoRNPs are necessary for the majority of rRNA modifications. Although, it is well known that single stand-alone enzymes like methyltransferases or pseudouridine synthases do have a considerable impact on modifications of the rRNA (Penzo et al., 2016; Sharma and Lafontaine, 2015). Although the type of rRNA modification differs, the function of rRNA modification is quite conserved. Due to the high abundance of modifications in functionally important regions of the ribosome it is likely that these modifications have an impact on the translational fidelity and on the structural stability of the ribosome (Sloan et al., 2017). However, the type and frequency of rRNA modifications varies in different eucaryotes and as described in the following sections.

1.1.1 The human rRNA modifications and snoRNAs

The human 80S ribosome consists of the 5S, 5.8S, 18S and 28S rRNAs (25S in yeast and plants). So far 947 snoRNA genes are annotated, where only 50% of the snoRNAs could be identified as being actively expressed (Fafard-Couture et al., 2021). Furthermore, it could be shown that subsets of snoRNAs are differently expressed in different human tissues (Fafard-Couture et al., 2021). The human snoRNA organization is concentrated on intronic regions (~91%) while only a small number of the expressed genes are located in intergenic regions (~9%) (Fafard-Couture et al., 2021; Figure 3).

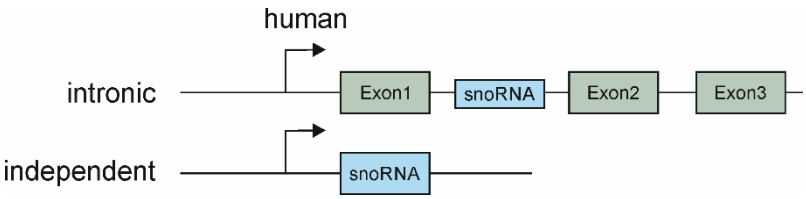

Figure 3. Localization of human snoRNA genes.
Most of the human snoRNAs are concentrated in intronic regions of protein coding genes. A small number can be found in intergenic regions. Adapted from Streit and Schleiff (2021).

To date, 229 modified rRNA sites are known, with 110 2´-O-ribose methylations, 12 base modifications and 107 Ψ-sites, which are guided from 216 snoRNAs arising from up to 700 snoRNA genes (Taoka et al., 2018; Motorin et al., 2021; Jorjani et al., 2016; Dieci et al., 2009). Remarkably, while 5.8S, 18S and 28S contain many modified nucleotides, the 5S rRNA, which carries one pseudouridylation site in yeast, carries no modification site in human (Motorin et al., 2021). In recent years, it could be shown that snoRNAs, apart from the guidance of rRNA modifications, are involved in several processes like gene transcription or RNA splicing and mutations or altered expression can lead to cancer in vertebrates (Liang et al., 2019). Furthermore, several disorders resulting from defective snoRNP members are known, like the neurological disease Prader-Willi-Syndrome (PWS), where loss of imprinted snoRNAs in chromosome 15 leads to cognitive and physical impairments (Runte et al., 2001; Zhang et al., 2014). Another disease known as X-linked Dyskeratosis Congenita (X-DC), is based on a mutation on the pseudouridine synthase and H/ACA snoRNP enzymatic member DKC1 (dyskerin), which in turn leads to e.g. abnormal mucocutaneous appearance and due to disorders in pseudouridylation levels on rRNA, affected patients are more prone to cancer as shown on the mice model (Dimitrova et a., 2019; Sridhar et al., 2008; Haruehanroengra et al., 2020; Penzo et al., 2013). In cancer cells, ribosome biogenesis is strongly increased due to the fact, that oncogenes are overexpressed and tumor suppressors like p53 are inactivated (Marcel et al., 2013). Interestingly, p53 is known to be a negative regulator of ribosome biogenesis by binding to RNA-Polymerase I and by that inhibiting rDNA transcription and most interestingly p53 was found to interact directly with fibrillarin, which in turn reduces rRNA 2´-

O-ribose methylation. But defective p53 leads to increased rDNA transcription and increased FBL expression, leading to the production of altered ribosomes with modified rRNA methylation pattern, which are more prone to translate mRNAs of pro-oncogenic and anti-apoptotic proteins (Marcel et al., 2013). All together these examples from humans shows the importance of the fine regulation of snoRNAs, the enzymatic proteins within the snoRNP complexes and the rRNA modifications.

1.1.2 The yeast rRNA modifications and snoRNAs

The modifications of rRNA in yeast are very diverse and can be grouped in 12 types: four types of 2´-O-methylation on one of the four bases A, C, G or U and eight modifications on nucleobases (Sharma and Lafontaine, 2015). The latter account for the conversion of uridine to pseudouridine, five base methylations, acetylated cytosines and hypermodified nucleotides (Sharma and Lafontaine, 2015). Until now 112 modified nucleotides were found in the yeast model *Saccharomyces cerevisiae*, most of them belonging to the modification group of 2´-O-methylation and pseudouridylation (Baudin-Baillieu and Namy, 2021). These modifications are guided from approximately 75 snoRNAs expressed from 76 genes (Dieci et al., 2009). The acetylation of cytidines on the 18S rRNA (C_{1773} and C_{1280}) are unique to *S.cerevisiae* and is fulfilled by the two orphan snoRNAs snR4 and snR45 together with the RNA acetyltransferase Kre33p (Rra1p) (Ito et al., 2014; Sharma et al., 2017b; Baudin-Baillieu and Namy, 2021). The snoRNA gene organization is similar to the human counterpart, but the independent gene organization is more abundant than the intronic localization. Moreover, yeast snoRNA genes are also organized in polycistronic clusters, which are transcribed from one promoter (Brown et al., 2003; Streit and Schleiff, 2021) (Figure 4).

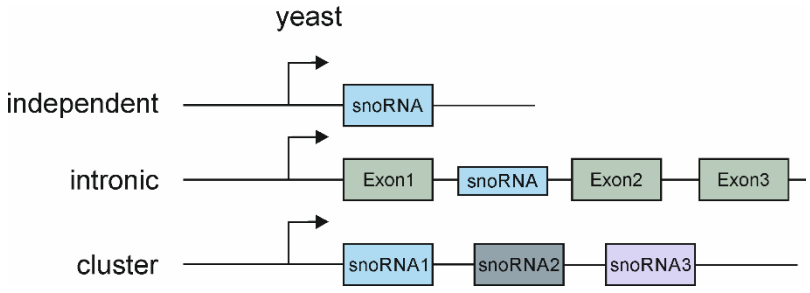

Figure 4. Localization of yeast snoRNA genes.
Most of the yeast snoRNAs are independently expressed by its own promoters. Another subset is expressed in intronic regions of protein coding genes and very few snoRNAs are expressed in snoRNA-clusters with their own promoter. Adapted from Streit and Schleiff (2021).

Most of the snoRNAs are known to guide modifications, but some snoRNAs also act in rRNA folding, like snR35 in rRNA folding (Huang and Karbstein, 2021) or like U3, U13, U14 and U8 in rRNA processing (Ojha et al., 2020). Although they originate in the nucleus and function in the nucleolus, where rRNA modifications takes place, the C/D box snoRNA located in the intron

of Rpl13 in yeast is also present in the cytoplasm upon oxidative stress (Holley et al., 2015). It is suggested that the reason for this could be the requirement of C/D box snoRNAs as regulatory factors for modifications of certain mRNAs as it was found for H/ACA snoRNAs targeting a subset of mRNAs for pseudouridylation (Holley et al., 2015; Schwartz et al., 2014). Indeed, molecules like snoRNA-derived small RNAs (sdRNAs), known for their participation in microRNA pathways, were found in the cytoplasm of yeast albeit the lack of their microRNA machinery (Mleczko et al., 2019). Moreover, it could be shown that these sdRNAs and snoRNAs are associated with translating ribosomes, and especially upon stress in increasing manner, which in turn is leading to inhibitory effects during translation (Zywicki et al., 2012; Mleczko et al., 2019). The significance of rRNA modifications is shown on the effect of growth retardation, decreased amino acid incorporation and the lack of free 40S subunits upon deletion of several modification sites in the functionally important decoding center (DC), while single deletions have no or very low effects (Liang et al., 2009). Alike humans, yeast is also affected by rRNA modification deletions as well as from disturbances in snoRNA formation.

1.1.3 *Arabidopsis thaliana* rRNA modifications and snoRNAs

The Arabidopsis 80S ribosome consists alike yeast of the 5S, 5.8S, 18S and 25S rRNAs. The rRNAs of Arabidopsis contain in contrast to human and yeast only 2´-O-ribose methylations or pseudouridylations (Piekna-Przybylska et al., 2008). To date more than 200 snoRNAs are known in Arabidopsis (Azevedo-Favory et al., 2021). Different approaches have led to a repertoire of 323 predicted modified nucleotides namely 214 2´-O-ribose methylation sites, and 109 pseudouridylation sites, of which 132 predicted 2´-O-me and 81 predicted Ψ-sites were experimentally confirmed (Barneche et al., 2001; Qu et al., 2001; Chen and Wu, 2009; Kim et al., 2010; Sun et al., 2019; Azevedo-Favory et al., 2020; Streit et al., 2020). The snoRNA gene organization is akin to human and yeast, with few exceptions: The overall gene organization is majorly orientated in snoRNA gene clusters, while only few cases are known for intronic, independent loci (Leader et al., 1997; Brown et al., 2003; Dieci et al., 2009), tRNA-snoRNA (Kruszka et al., 2003) or even snoRNA-miRNA dicistronic (Qu et al., 2015) organization (Figure 5). Unfortunately, only little is known about snoRNA or rRNA modification deficiencies in Arabidopsis. To date only one snoRNA has been functionally analyzed, namely HIDDEN TREASURE 2 (HID2), which is assumed to target G2620 on the 25S rRNA (Zhu et al., 2016). However, the modification was not altered under reduced *HID2* expression, while rRNA processing seemed to be delayed in the *hid2* mutant (Zhu et al., 2016). This shows exemplary, that snoRNAs do not only guide post-transcriptional modifications but also have functions in processing. Consequently, it is discussed that *HID2* has other functions in ribosome biogenesis, although it contains an antisense region for 25S, which in turn could also be helpful

for proper folding of 25S rRNA (Zhu et al., 2016). Alike human 5S rRNA, Arabidopsis 5S rRNA contains no methylation (Wu et al., 2021).

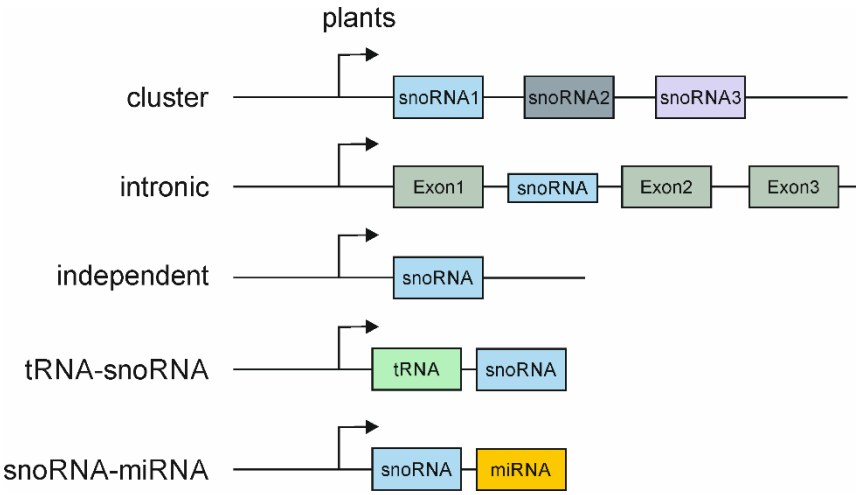

Figure 5. Localization of plant snoRNA genes.
Most of snoRNAs are organized in clusters. Few cases are also known for intronic organization and independent gene organization. Furthermore, tRNA-snoRNA and snoRNA-miRNA dicistronic organization was described. Adapted from Streit and Schleiff (2021).

1.2 rRNA processing in *Arabidopsis thaliana*

Next to the post-transcriptional modification of rRNA, the processing of rRNA is another essential process to obtain intact and functional ribosomes. While modifications are usually taking place within the nucleolus of the cell, processing of rRNA is initiated in the nucleolus by transcription of the 45S rDNA into the 35S pre-rRNA by RNA-Polymerase I and by the assistance of general transcription factors (GTFs), is continued in the nucleus and finalized in the cytoplasm (Tsang et al., 2003; Layat et al., 2012; Sáez-Vásquez and Delseny, 2019). The primary rRNA transcript is 10 kb long and 570-750 rDNA gene copies are tandemly arranged at the nucleolus organizer region (NOR) on the short arms of chromosome 2 and 4 (Copenhaver and Pikaard, 1996) and encodes as polycistronic unit for the 18S, 5.8S and 25S rRNA. However, the 80S ribosome consists of four rRNAs, the 5S rDNA is akin to the 45S rDNA arranged in arrays containing roughly 1000 copies on chromosomes 3, 4 and 5 and is transcribed independently by RNA-Polymerase III (Layat et al., 2012). Though, the rDNA loci on chromosome 3 and partly chromosome 5 are inactive, whereas loci on chromosome 4 and partly chromosome 5 are transcribed (Cloix et al., 2002; Layat et al., 2012). The 5S rDNA is approximately 500 bp long and contains the 120 bp long 5S rRNA and an intergenic spacer of about 380 bp (Layat et al., 2012). The 35S pre-rRNA transcript contains the 18S, 5.8S and 25S rRNAs, which are flanked by 5´- and 3´- external transcribed spacers (5´ETS/3´ETS) and separated by internal transcribed spacer 1 and 2 (Tomecki et al., 2017; Figure 6). To separate the rRNAs from ITS and ETS regions and to allow proper maturation, the pre-rRNA contains several cleavage sites as points of attack for exo- and endonucleases, two classes of proteins

being part of the huge group of ribosome biogenesis factors (RBFs) with more than 200 members (Kressler et al., 1999; Ebersberger et al., 2014). Apart from cleavages and digestions of rRNA, RBFs fulfill many essential tasks during ribosome biogenesis as e.g. methyltransferases, ATPases, GTPases, RNA helicases or phosphatases (Woolford and Baserga, 2013). The first endonucleolytic cleavage, which produces the pre-rRNA, happens co-transcriptionally in the 3´ETS at site B_0 through the RNaseIII-like protein AtRTL2, (Comella et al., 2007; Tomecki et al., 2017). The subsequent step involves most-probably a splicing-like event, by which the 1083 nt insertion is removed to produce the $35S_{A123B}$ rRNA (Weis et al., 2015a). The next step includes the involvement of the exonucleases XRN2/XRN3 by trimming the pre-rRNA at the 5´ETS, followed by the endonucleolytic cleavage at site P by XRN2 and U3 snoRNP forming the 35S precursor (Zakrzewska-Placzek et al., 2010; Weis et al., 2015a; Tomecki et al., 2017). From now on, different pathways are described, leading to different rRNA precursors but finally to the same mature rRNAs (Figure 6). The minor processing pathway (Pathway 1) in Arabidopsis is comparable to the yeast system and is characterized by the first cleavage site occurring in the 5´ETS (5´ETS-first) and the main rRNA processing pathway shows similarities to the mammalian system with the first cleavage site occurring in ITS1 (ITS1-first) (Weis et al., 2015a). However, under different circumstances, like increasing temperatures (Shanmugam et al., 2021), auxin treatment of mutants with involvement in rRNA processing or even under control conditions in Arabidopsis cell suspension cultures (Palm et al., 2019), an additional pathway was observed, which by-passes the latter two pathways by producing the precursor P-C_2, resulting from an early cleavage in the ITS2 (Shanmugam et al., 2021). Though, this precursor seems not to be implicated in functional ribosomes as the C_2-end was found to be polyadenylated, which indicates that the precursor is undergoing degradation (Shanmugam et al., 2021; Sikorski et al., 2015). The current model on pathway 1 shows, that the 35S pre-rRNA is cleaved at site P´ and B_2, producing the 33S (P´) pre-rRNA, which is further cleaved at site P_2 to produce the 32S pre-rRNA (Weis et al., 2015a). The upcoming step separates pre-60S subunits from pre-40S subunits through a cleavage at site A_2, generating the $27SA_2$ and most probably 20S pre-rRNA (Weis et al., 2015b). The next step involves a cleavage at site B_1 which is required for 5´-maturation of the 5.8S rRNA and production of 27SB pre-rRNA (Figure 6). The latter is cleaved at site C_2 to separate 7S and the not detectable C_2-25S pre-RNA (Shanmugam et al., 2021), which is probably directly cleaved at C_1 site to directly mature 25S rRNA. The 7S pre-rRNA is digested at first to 5.8S + 70nt and then trimmed exonucleolytically to E´ to produce the 6S pre-rRNA. A final cleavage at site E produces the mature 5.8S rRNA. The 20S (18S-A_2) rRNA is then cleaved by the endonuclease AtNOB1 at site D for proper maturation of the 18S rRNA (Missbach et al., 2013).

Pathway 2 starts with the direct separation of pre-40S and pre-60S subunits by a cleavage at site A_3 (Weis et al., 2015a/b). The precursor characterized for this pathway, $27SA_3$ is produced and cleaved at site B_1 to generate 27SB pre-rRNA. The subsequent steps are similar to Pathway 1. Nevertheless, 18S precursors are completely different from pathway 1. Here, a P-A_3 precursor is formed by cleavage at site P_1 , P´ and P_2 to form 18S-A_3 precursor, which is either digested to 18S-A_2 or directly cleaved at site D to form mature 18S rRNA (Weis et al., 2015a; Weis et al., 2015b; Figure 6). Interestingly, the precursor 5´-5.8S pre-rRNA, which is only present in plants under native conditions, has not been assigned to the right position in the current models of rRNA processing in Arabidopsis (Weis et al., 2015b; Palm et al., 2019; Sáez-Vásquez and Delseny, 2019). It is currently discussed whether it might be a precursor arising from pathway 1 (5´ETS-first) or even from the ITS2-first bypass pathway (Palm et al. 2019; Sáez-Vásquez and Delseny, 2019).

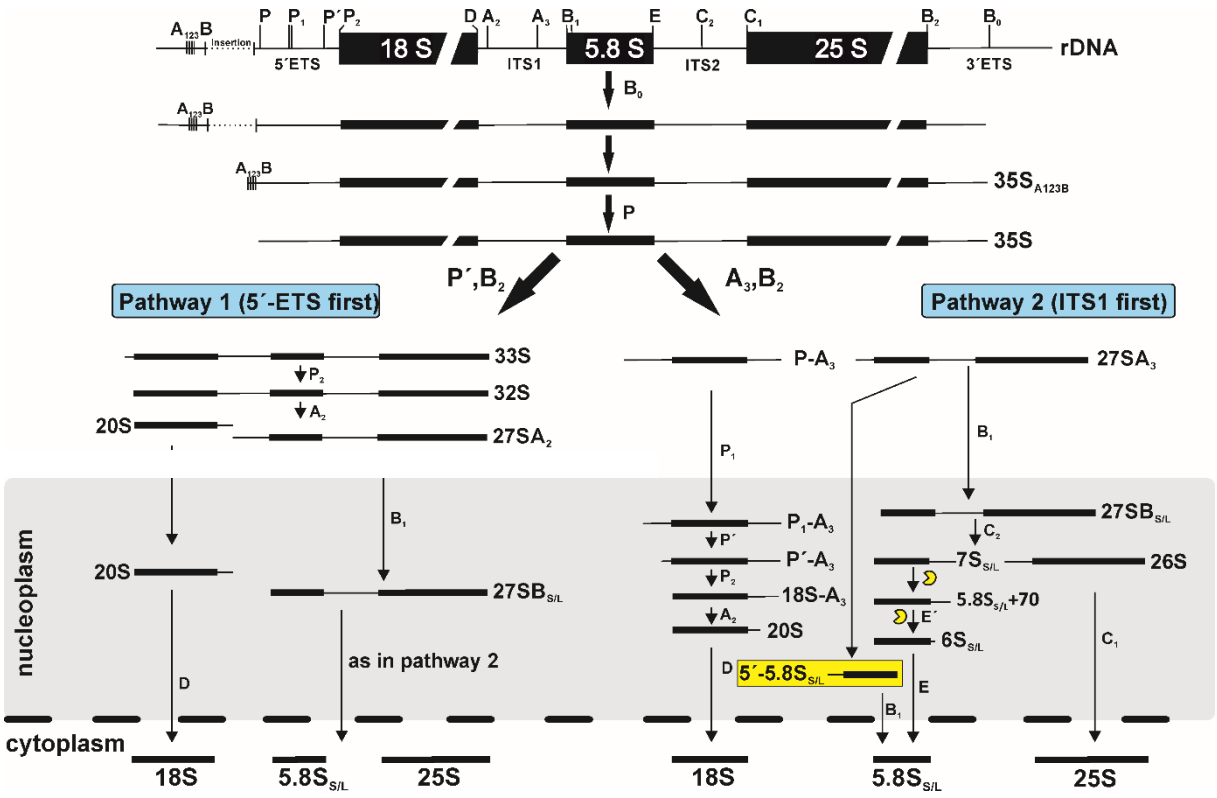

Figure 6. The rRNA processing scheme of Arabidopsis.
After transcription the 35S pre-rRNA is cleaved extensively in coordinated manner to generate mature 5.8S, 18S and 25S rRNA in the cytoplasm. rRNA processing can be separated in two alternative pathways, producing partly different precursors. Pathway 1 is characterized by a late separation of pre-40S and pre-60S particles and a first cleavage at the 5´-ETS, while pathway 2 directs an early separation of the pre-40S and pre-60S subunits with a first cleavage happening in the internal transcribed spacer 1 (ITS1). The plant-specific precursor 5´-5.8S pre-rRNA is highlighted in a yellow box. For further information see the main text. Adapted from Streit and Schleiff (2021).

1.3 The role and biogenesis of 5.8S rRNA

1.3.1 The function of 5.8S rRNA within the ribosome

The 5.8S rRNA is the smallest nucleolar encoded rRNA of the cytoplasmic 80S ribosomes in eucaryotes. With a size of about 160 nt (164 nt in *Arabidopsis thaliana*) it forms two conserved hairpins and three short stems in the secondary structure (Figure 26) (Nazar, 1984). Bacteria lack the 5.8S rRNA, however, the 23S rRNA contains at its 5´ end a sequence like the 5.8S rRNA (Nazar, 1980). Possible reasons for the separation could be that the 5.8S has evolved from a non-functional sequence to a sequence with more importance in the ribosome or simply the maturation pathway has changed over evolution (Nazar, 1984). The 5´ and 3´ helices of mature 5.8S are base pairing with 25S rRNA (28S in human) of the 60S subunit (Piekna-Przybylska et al., 2007). Interestingly, cell-free extracts of mutated 5.8S rRNA of *Schizosaccharomyces pombe* resulted in increased polysome size and enhanced sensitivity against the antibiotics cycloheximide and diphtheria toxin affecting translation elongation (translocation), a process by which tRNAs and the mRNA are moved by three nucleotides (codon) inside the ribosome (Elela and Nazar, 1997; Belardinelli et al., 2016). Due to that, it is believed that the 5.8S rRNA plays a significant role in ribosomal translocation (Elela and Nazar, 1997). Moreover, by affinity chromatography, it could be shown that 5.8S rRNA is binding to 40S subunit proteins making it possible that 5.8S is located at the ribosomal interface (Nazar, 1984; Toots et al., 1979). Even more interesting is the fact, that modifications on 5.8S rRNA, especially in helix 7 (H7) may enable protein or RNA binding sites, as this region was observed to contain reactive sites upon treatment with dimethyl sulphate (Nazar, 1984). It is also proposed that 5.8S rRNA might have a role in tRNA binding, as the sequence G-A-A-C (mammalian residues 42-45 and 104-107) might bind the G-T-Ψ-C at the T-loop of tRNAs (Lo and Nazar, 1982). However, these sites were not readily accessible in 80S ribosomes, further supporting the idea that parts of 5.8S rRNA are buried in the ribosome playing a role in the subunit interaction (Lo and Nazar, 1982). A different and interesting aspect for the function of 5.8S rRNA concerns its modifications. Mammals have four modified sites (Um14, Ψ55, Ψ69 and Gm75), yeast only one (Ψ73) and Arabidopsis contains at least four modified sites (Ψ22, Am47, Ψ78 and Gm79; Gm155 is not verified yet) (Piekna-Przybylska et al., 2008; Streit and Schleiff, 2021). So far only in mammals it could be shown that some modifications are only partly present and that modifications levels were dependent on the tissue to be analyzed. By that it was found that two sites (Um14 and Ψ55) appeared in submolar amount (Nazar et al., 1975; Nazar, 1984). Especially in fast growing tumor lines like HeLa cells or the Novikoff hepatoma revealed lower methylation status as compared with normal differentiated cells (Nazar, 1984). This could lead to the conclusion that some of the modifications are used as a sensor for rRNA quality and the absence of a modification could change ribosomal activity and

by that affect cell growth and development (Nazar, 1984). Apart from the latter function, recently it has been shown that the 5.8S rRNA was released during hemolysis in zebrafish and human plasma to activate coagulation (Alharbi et al., 2021). Since neither 18S nor 28S was found in the lysate, it is very likely that 5.8S was either dissociated from 28S or it gets released from a free pool (Alharbi et al., 2021).

1.3.2 The 5´- processing of 5.8S in different eucaryotes

The processing of 5.8S rRNA in eucaryotes is as complicated as the precursors from which it is formed, and the massive repertoire of factors being involved in the maturation of this relatively small rRNA. In general, two forms of mature 5.8S rRNA are formed in eucaryotes distinguishable by their size and designated as "short" and "long" form ($5.8S_{S/L}$) (Weis et al., 2015b). In yeast, the long form contains 7-8 nt more than the short form (Mitchell et al., 1995) and interestingly, the short form is more abundant than the long form with a ratio in budding yeast of 80:20 (Schillewaert et al., 2012). Human 5.8S also possess three forms, the shorter form lacking ~5 nt at the 5´ end, the long form and the 5.8S cropped form, lacking 10 nt at the 3´ end (Venturi et al., 2021). Here the ratio of short to long form is about 60:40 (Schillewaert et al., 2012). However, in Arabidopsis the ratio is 40:60 from short to long (Zakrzewska-Placzek et al., 2010; Tomecki et al., 2017). In yeast the short and long form of 5.8S are produced in two different pathways. The short form is built by endonucleolytic cleavage of the $27SA_2$ pre-rRNA at site A_3 in ITS1 by the RNase MRP, followed by a 5´→3´ exonucleolytic trimming achieved by Rat1 and its cofactor Rai1 and Rrp17 (Oeffinger et al., 2009; Henras et al., 2015; Schillewaert et al., 2012). The pathway producing the minor long form of 5.8S is almost unexplored, however it is suggested that a currently unknown enzyme performs endonucleolytic cleavage of the $27SA_2$ pre-rRNA at site B_{1L} (Faber et al., 2006; Henras et al., 2015). The alternative processing ways for the two forms of 5.8S in plants are yet not fully understood (Asha and Soniya, 2017). Although, AtXRN2 and AtXRN3 are involved in cleavages occurring at site A_2 and A_3 and subsequent exonucleolytic trimming to the 5´region of 5.8S, it is not clear whether they are also required to produce the two 5.8S forms, as absence of AtXRN2 alone does not influence the ratio of $5.8S_L$ to $5.8S_S$ in Arabidopsis, which could be due to the compensatory effect of AtXRN3 (Zakrzewska-Placzek et al., 2010). Alike in Arabidopsis, depletion of human XRN2 caused no change of the $5.8S_L$ to $5.8S_S$ ratios, but depletion of BOP1 led to increased levels of $5.8S_L$ and depletion of NOL12 impairs ITS1 processing and maturation of $5.8S_{S/L}$ (Sloan et al., 2013). BOP1 and NOL12 are the yeast homologues of Erb1 and Rrp17 and are required for exonucleolytic trimming from site 2 (A_3 in yeast and plants) to $B1_S$ site (Pestov et al., 2001; Sloan et al., 2013).

Besides these diversities at the 5´-end of 5.8S, several 5´-extended versions are documented. The best-known form is the 5´-5.8S pre-rRNA (Zakrzewska-Placzek et al., 2010; Weis et al.,

2015b; Missbach et al. 2013; Palm et al., 2019; Figure 7). This precursor is naturally occurring in plants (Zakrzewska-Placzek et al., 2010), while yeast shows a similar precursor, when the exoribonucleases Rat1, Xrn1 or Rrp17 are mutated (Henry et al., 1994; Oeffinger et al., 2009). In Arabidopsis the endonucleases AtXRN2 and AtXRN3 are known to be involved in A_2 and A_3 cleavages and for the exonucleolytic trimming till B_{1S} of 5.8S pre-rRNA (Zakrzewska-Placzek et al., 2010; Tomecki et al., 2017). However, it is believed that another enzyme has to exist, which is taking over the major part in processing the 5´-part of 5.8S pre-rRNA, since the *xrn2/xrn3* mutant accomplishes normal levels of mature 5.8S (Zakrzewska-Placzek et al., 2010).

Finally, in human cells it could be shown that depletion of the RNA-induced silencing complex (RISC) proteins Drosha and Dicer, multiple forms of 5´ and 3´ extended 5.8S precursor were accumulated, indicating that these RNase III endonucleases beside their role in miRNA biogenesis, are also involved in pre-rRNA processing (Liang and Crooke, 2011).

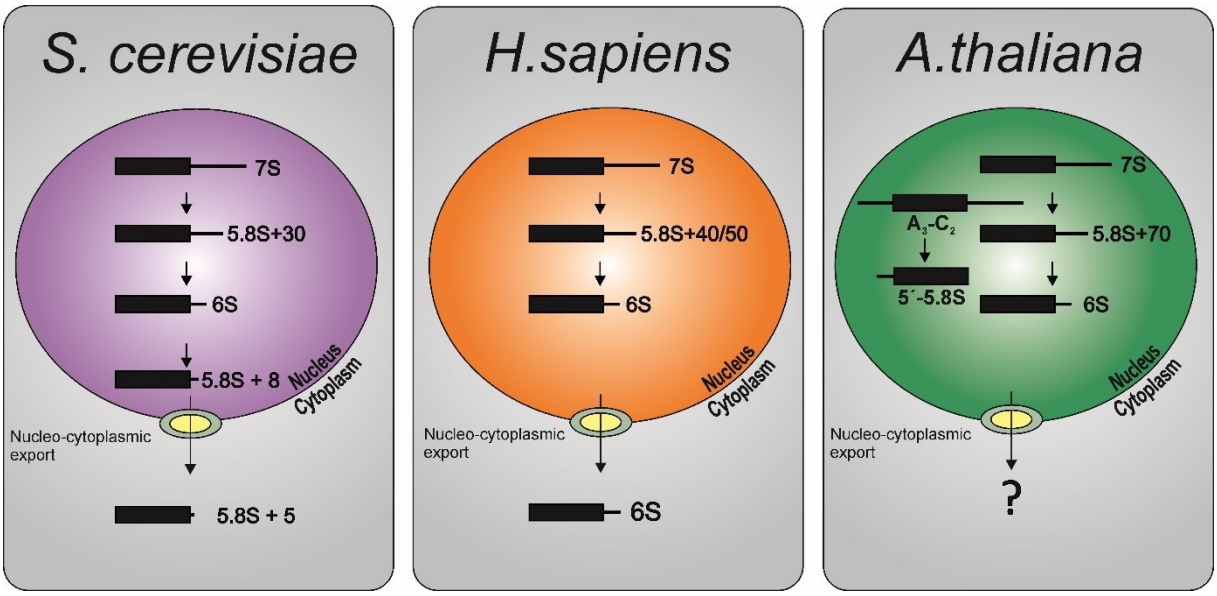

Figure 7. Processing of 5.8S rRNA in different eucaryotes.
Maturation of 5.8S rRNA is dominated by 3´-extended precursors in yeast (*S. cerevisiae*), human (*H. sapiens*) and *Arabidopsis thaliana*. All three species have common precursors like the 7S pre-rRNA, a shorter form like 5.8S+30 (yeast), 5.8S+40/50 (human) and 5.8S+70 (Arabidopsis) and the 6S pre-rRNA. In yeast and human, the shortest forms 5.8S+8 (yeast) and 6S (human) are exported to the cytoplasm, where final cleavage or digestion is taking place. For Arabidopsis, the evidence for immature 5.8S export was not described so far. Figure adapted and modified from Tomecki et al. (2017) and Thomson and Tollervey (2010).

1.3.3 The 3´- processing of 5.8S in different eucaryotes

In contrast to 5´-processing, the 3´-processing of 5.8S rRNA is well understood. In yeast, processing within ITS2 leads to separation of 5.8S and 25S as soon as B_1 processing has been fulfilled. The separating cleavage of the 27SB pre-rRNA happens at C_2 (site 4 in human) and is carried out by the endonuclease Las1 and in complex with Grc3, Rat1 and Rai1 both

ends of ITS2 are further processed (Gasse et al., 2015; Tomecki et al., 2017). The resulting 7S pre-rRNA is trimmed sequentially by the exosome components Dis3 and Rrp6, both supported by the helicase Mtr4 to produce the 5.8S+30 nt and 6S pre-rRNA (Figure 7). Additional trimming by the Rex exonucleases generates the 5.8S+5 nt, which is exported to the cytoplasm, where final cleavage or trimming with Ngl2 produces mature 5.8S rRNA (Tomecki et al., 2017; Briggs et al., 1998; Rodríguez-Galán et al., 2015; Allmang et al., 1999; Thomson and Tollervey, 2010).

In human, first ITS2 cleavage appears at site 4, an additional cleavage site, which is not present in yeast or plants. However, it is similar to yeast and plant C_2 site, since it is the first cleavage site separating precursors of 5.8S from 25S/28S rRNA (Tomecki et al., 2017). Similar to yeast, human Las1 is believed to be required for separation of 5.8S from 28S rRNA, because 32S pre-RNA accumulated and 12S pre-rRNA levels were decreased in the mutant (Castle et al., 2010; Figure 7). Exonucleolytic trimming of the 12S pre-rRNA to the 7S pre-rRNA is performed by the enzyme ISG20L2 (Coute et al., 2008). However, it seems as ISG20L2 can be substituted by the exosome complex including DIS3 and RRP6 or trimming is accomplished in a successive coordinated manner by these enzymes (Preti et al., 2013). The 7S pre-rRNA is further trimmed sequentially by the action of the exosome and probably MPP6 and RRP47 to 5.8S+40/50nt and by the exosome and RRP6 to the 6S pre-rRNA (Schilders et al., 2007). The 6S pre rRNA is alike in yeast exported to the cytoplasm and the final trimming is fulfilled by ERI1 as shown for mice (Ansel et al., 2008; Figure 7).

In plants, no endonucleolytic enzyme was found so far to be involved in C_2 cleavage. However, for exonucleolytic trimming of the 7S to 5.8S+70 nt and 6S pre-rRNA (corresponding to 7S, 5.8S+30 nt and 6S in yeast), several candidates have been found to act as 3´-5´ exonucleases namely, AtSMO4 (Micol-Ponce et al., 2020), AtRRPL6L2 and AtMTR4 (Lange et al., 2011) and AtRRP44a, a homologue of yeast Rrp44/Dis3 (Kumakura et al., 2013). The *mtr4* mutants displayed reduced rRNA processing rates, hence ribosome biogenesis is delayed in the mutant (Lange et al., 2011). More intriguingly, AtXRN2 (Rat1 in yeast) and AtXRN3, besides their role in ITS1 processing also has an indirect role in 3´-maturation of 5.8S rRNA, as precursors with extended 3´ extremities are accumulating in the double mutant *xrn2/xrn3* (Zakrzewska-Placzek et al., 2010). This indicates that processing in ITS1 and ITS2 proceeds in a coordinated manner, as folding of the 5.8S rRNA brings the 5´ and 3´ end closely together (Schillewaert et al., 2012). Interestingly, there is no data available, if 5.8S rRNA maturation is finalized within the nucleus before pre-60S subunit export or if as shown for yeast and human 6S pre-rRNA or other precursors are finally processed in the cytoplasm (Figure 7).

2 Objectives

The process of ribosome biogenesis in plants is not well understood, particularly as the complexity, shown by the presence of higher number of RBF orthologues to human and yeast is much higher. Furthermore, the regulation and role of snoRNAs in the process has not been experimentally determined, as at stage sites of modifications are predictions from *in silico* analysis. So far, we know that more than 200 snoRNAs exists in Arabidopsis. It is known from many modified rRNA sites, that there is no snoRNA so far that could target these modified regions. Thus, the first objective was to find new snoRNAs, that might have the potential to target those sites, where no snoRNA was described so far and secondly to confirm the existence of novel snoRNAs. Furthermore, due to the fact that snoRNAs of yeast was found to move within the cell due to changing environmental conditions, the distribution of novel snoRNAs and snRNAs within the cell compartments were analyzed.

The processing of pre-rRNAs require a huge repertoire of proteins involved in different parts of processing. In yeast 255 RBFs are known and for approx. 30% of these proteins no orthologues proteins could be assigned (Ebersberger et al., 2014; Simm et al., 2015). In a recent study, several newly identified proteins were described to be "involved in rRNA processing" or simply IRP (Palm et al., 2019). Though, for many processing steps including cleavages and digestions of the pre-rRNAs, the according RBFs have not been curated and thus the second objective deals with the identification of not yet discovered ribosome biogenesis factors in Arabidopsis, by analyzing mutants of putative RBFs on processing of pre-rRNAs based on high resolution northern blotting.

As shown for yeast and human, the processing of 5.8S rRNA, the smallest nucleolar encoded rRNA, involves a highly complex process that is only surpassed by the complexity and variety of proteins involved. During maturation, many precursors are formed that are especially in yeast and human extended to the 3´ sites belonging to ITS2 (Gasse et al., 2015; Castle et al., 2010). In plants a different mechanism has evolved, which contributed to precursors, having a 5´-extension belonging to ITS1 and a distinctive precursor called 5´-5.8S pre-rRNA that is specific to plants (Palm et al., 2019). There is not much known about this precursor and how it fits to the current rRNA processing pathway model in *Arabidopsis thaliana*. For that reason, the third objective was to analyze in detail the maturation steps of 5.8S rRNA processing in Arabidopsis and to find more precursors, which are not detectable under normal conditions and to determine the role of such not yet discovered precursors within the known processing pathways. Additionally, the discovery of new factors being involved in the maturation of 5.8S rRNA are of special focus.

3 Materials

3.1 Oligonucleotides

Table 1. Anti-sense oligonucleotides used for northern blotting of pre-rRNAs and snRNAs.

name	species	position on pre-rRNA (relative to TIS)	sequence (5´ → 3´)
p4	A.t.	+3893 - +3914	CGTTTTAGACTTCAGTTCGCAG
p5	A.t.	+4068 - +4092	GGATGGTGAGGGACGACGATTTGTG
p42	A.t.	+3716 - +3736	CCACGGATCCGGCGGGCAAGG
p43	A.t.	+3834 - + 3855	ATGCCAGCCGTTCGTTTGCATG
p3	A.t.	+3643 - +3667	GGTCGTTCTGTTTTGGACAGGTATC
p1	A.t.	+613 - +637 / +925 - +949 / +1237 - +1261	CCTAGGCGGATCCATGCTTTCCAAC
p52	A.t.	+4154 - +4177	GTACGCTCCAGGCGTCCTTGGCTC
5.8S	A.t.	+3917 - +3938	GCCGAGATATCCGTTGCCGAGA
p4	S.l.		CGTTTGTGTTAACAGAGCAGCG
p5	S.l.		GAGGGGGCGACGCGATGCGTG
p4	O.s.		CGTGTGGATTTAACTCGTGGTATC
S9	O.s.		GCGCCCTCCCGGATAGGGGGGGCGCG

Solanum lycopersicum (S.l.), *Arabidopsis thaliana* (A.t.), *Oryza sativa* (O.s.), Transcription initiation site (TIS)

Table 2. Anti-sense oligonucleotides for RNA-FISH in *Arabidopsis thaliana.*

name	sequence (5´ → 3´)
SNORD72	Cy3-TCTCATAAGTCCAGACATATATATTAGCAACATCATCATCGCAACCAAAG-Cy3
snoR29	Cy3-AACGCCTAATTCCGGTCTGTTGAGCTTGAAATTTCCGAGTCATCACTGCC-Cy3
U3	Cy3-TCTAGCCGCACGGTCATGGTTCATCAACCAGGGTAAAAGGCCTGTCTCTT-Cy3
snoR100	Cy3-CAAAGAACCAATAAGGAACTCAGAGCAGGCACAGACATTTGAAACCCATG-Cy3
snoR106	Cy3-CCTTCAAGCAACTTAGATCAAAGTGTCATCAAGAAACTCCGAGATCAAAT-Cy3
U49-1	Cy3-TGTTGTGTAAAGTGTCATACGGCACTTCCTATCTATGGGA-Cy3
U31a	Cy3-GTATCAACACTGTATTTCAGATTTGCAGACGTATGGAATTACATCCTCAT-Cy3
snoR135	Cy3-TTTGTAGACGGTAACAACCATGCAAATAGAATTAAAGAAGAAAAATAAAC-Cy3
AT2G03875	Cy3-TTATCTTTTAACAGATGTGCCGCCCCAGCCAAACTCCCCACCTGACAATG-Cy3
5´-5.8S	Cy3-GAGAGTCGTTTTAGACTTCAGTTCGCAGCACAGCATCCGC-Cy3

Table 3. Anti-sense oligos used for northern blotting of snoRNAs/snRNAs

snoRNA/snRNA probe	species	sequence (5´ → 3´)
U3-3	A.t.	GTTCATCAACCAGGGTTAAG
U3-5	A.t.	ATCCTCTACAGCACCGGATG
U24-2	A.t.	AGATCTTGGTGGTAAATATC
U27-1 (1)	A.t.	CAACAAGGATTAATTCAGACATA
U27-2 (2)	A.t.	GACATATGCTTGTCTATTTT
U31a	A.t.	GTCAGATGGTAGTGCATGTC
U49-1	A.t.	AGTGTCATACGGCACTTCCT
snoR100	A.t.	GGAACTCAGAGCAGGCACAGAC
snoR106	A.t.	GTGTCATCAAGAAACTCCGAGATC
snoR160	A.t.	AGTCTGTCTCTTGACTTACT
SNORD72	A.t.	GCTCAGAAGGTTGCACAATC
snR77	A.t.	TGTTCTACTCCAGCAATTCC
SNORD31	A.t.	CAGACTGGGTGTCACAAAAC
U25	A.t.	ACTCAGTCCCTTAGATGTTCA
U2	A.t.	AGGCGACTCGTGAAAGTCC
U2	S.l.	TGAGGCCGAGAAAGGTAT
U2	O.s.	AGCCAAGGCGACACATGAGG

Solanum lycopersicum (S.l.), *Arabidopsis thaliana* (A.t.), *Oryza sativa* (O.s.)

Table 4. Oligonucleotides used for detection of T-DNA in mutant lines.

name	sequence (5´ → 3´)	AGI	position on gDNA
prp24.2-fw	CTTTATGAACGGGGACTTTCTG	At4g24270	913 - 934
prp24.2-rv	GTCTGCAGATTCCGAATCTTTC	At4g24270	1964 - 1985
Salk LB1	TGGTTCACGTAGTGGGCCATCG		
Salk LB3	ATTTTGCCGATTTCGGAAC		

Table 5. Oligonucleotides used for circular RT-PCR and sanger sequencing.

name	sequence (5´ → 3´)	position on pre-rRNA (relative to TIS)
cRT-F1	GCAGAATCCCGTGAACCATCGAG	+3987 - +4009
cRT-R1	GCCGAGAGTCGTTTTAGACTTC	+3902 - +3923
cRT-RT	CACACCAAGTATCGCATTTCGCTACG	+3957 - +3982
cRT-R2	CCAGCCGTTCGTTTGCATGTTC	+3831 - +3852
M13-f	TGTAAAACGACGGCCAGT	
M13-r	CAGGAAACAGCTATGACC	

Transcription initiation site (TIS)

3.2 Antibodies

Table 6. Antibodies used in this study

name	dilution	host animal	source	reference
α-ENP1	1:10,000	rabbit	raised	Missbach et al., 2013
α-NOB1	1:15,000	rabbit	raised	Missbach et al., 2013
α-FIB1	1:400	mouse	Thermo Fisher Scientific, USA	Missbach et al., 2013
α-RPL10AB	1:10,000	rabbit	raised	Shanmugam et al., 2021
α-RPS3-2	1:10,000	rabbit	raised	Shanmugam et al., 2021
α-RPS10	1:10,000	rabbit	raised	Palm et al., 2016
α-BRX1-1/BRX1-2	1:5,000	rabbit	raised	Weis et al., 2015b

3.3 Chemicals

All chemicals were purchased in high quality from VWR (Darmstadt, Germany) and Roth (Karlsruhe, Germany). Chemicals for northern blotting and RNA-FISH were purchased in highest purity from Merck (Darmstadt, Germany). Media and enzymes for plants were purchased from Duchefa Biochemie (Haarlem, Netherlands). Radioactive nucleotides were purchased from Hartmann Analytic (Braunschweig, Germany).

3.4 Plant lines

All plant lines were ordered from Nottingham Arabidopsis Stock Centre (NASC) or were kindly provided (Table 6). Besides, wild-type seeds of *Arabidopsis thaliana* (accession Col-0), *Oryza sativa* (var. japonica) and *Solanum lycopersicum* (var. moneymaker) were used.

Table 7. Plant lines used in this study.

name	AGI number	stock center ID	reference
prp24.1	At4g24270	SALK_045810	this study
prp24.2	At4g24270	SALK_040327	this study
xrn2-1/xrn3-3	At5g42540		Gy et al. (2007) Zakrzewska-Placzek et al. (2010)
rrp6-l2	At5g35910	SALK_113786	Sikorski et al. 2015
pcp2	At1g18850	SAIL_35_C07	This study
RNA-polymerase II degradation factor-like protein	At1g29350	SALK_152117	This study

3.5 Media

Growth media for bacteria were made according to standard protocols (Sambrook and Russel, 2001). For selection of transformed bacteria using the blue/white screening solid media plates with Ampicillin (50 µg/ml) were supplemented with 0.5 mM IPTG and 80 µg/ml X-Gal. Solid media plates for Arabidopsis plants contained half-strength MS salts including vitamins (Duchefa Biochemie), 2 % (w/v) sucrose and 0.3 % (w/v) gelrite. For mutant plant selection solid media was supplemented with Kanamycin (50 mg/L). For sugar stress, salt stress and auxin stress, media was supplemented with either 200 mM (w/v) glucose, 150 mM (w/v) NaCl or 10 µM (v/v) 2,4 dichlorophenoxyacetic acid, respectively. Liquid media for Arabidopsis root suspension culture (kindly provided by A. Batschauer, Phillips-Universität, Marburg) contained 1x MS salts, 3% (w/v) sucrose, 1 mg/L 2,4 dichlorophenoxyacetic acid, 4 mg/L nicotinic acid, 4 mg/L pyridoxine hydrochloride, 40 mg/L thiamine hydrochloride and 400 mg/L myo-inositol. The cell culture was maintained at 25°C and 150 rpm in the dark and subcultured every week.

3.6 Plasmids and bacterial strains

For circular RT-PCR analysis first-strand synthesized cDNA of pre-rRNA were cloned into the pGEM-T vector (Promega, USA). Cloning and propagation of plasmids were performed in a chemical competent *E.Coli* (DH5α) strain (Life technologies).

4 Methods

4.1 Molecular biological and biochemical methods

4.1.1 RNA extraction using Guanidinium thiocyanate-phenol-chloroform method

RNA was extracted of either plant tissue, cultured cells or subcellular compartments with an adapted protocol of Chomczynski and Sacchi (1987). Fine powder of plant material ground in liquid nitrogen (500-1,000 mg) was resuspended in 3 ml of Solution D (4 M guanidinium thiocyanate, 25 mM sodium citrate pH 7.0, sodium lauryl sarcosinate and 147 mM ß-mercaptoethanol). After addition of 300 µl 2 M sodium acetate pH 4.0, 3 mL acidic phenol and 600 µL chloroform, the sample was vigorously mixed and incubated on ice for 15 min on a rotary shaker at 100 rpm. Afterwards sample is centrifuged at 5,000 rpm for 20 min at 4°C. The RNA containing aqueous phase was transferred to a new tube and 1 vol of phenol/isoamyl alcohol/chloroform (PCI; 25:24:1) was added. After centrifugation at 5,000 rpm for 10 min at 4°C, the upper phase was further extracted with 1 vol chloroform, followed by a last centrifugation as in the latter step. The RNA from the aqueous phase was precipitated overnight with 1 vol isopropanol at -20°C. RNA was pelleted by centrifugation at 20,000 g for

20 min at 4°C. The pellet was washed twice with 70% (v/v) cold Ethanol, air-dried for 10 min and resuspended in RNase-free ddH_2O and stored at -80°C until further use.

4.1.2 Reverse transcription (RT) for polymerase chain reaction (PCR)

1,000 – 2,000 ng of RNA from plant tissue was treated with RNase-free DNase I according to manufacturer's protocol (Thermo Scientific) and reverse transcribed using RevertAid reverse transcriptase according to manufacturer's protocol (Thermo Scientific). In brief, 1,000 ng RNA were incubated with 1 U DNase I at 37°C for 30 min. The enzyme was inactivated by addition of 5 mM EDTA and incubation at 65°C for 10 min. Subsequently, 100 pmol of Oligo(dT) were annealed to the RNA by incubation at 70°C for 5 min and samples were cooled for 5 min on ice. Reverse transcription was performed in the presence of 200 U reverse transcriptase and 1 mM dNTPs for 1 h at 42°C. The enzyme was heat inactivated for 10 min at 70°C. the complementary DNA (cDNA) was diluted to 50 ng with H_2O and stored for short-storage at 4°C or for long-storage at -20°C until further use.

4.1.3 RNA gel electrophoresis and northern blotting

The detection of pre-rRNAs of different plant species was performed with Northern Blotting (Sambrook & Russell, 2001) using anti-sense oligonucleotides (Table 3). Glassware was washed once with 2 % bentonite and H_2O before use. For separation of large RNAs, denaturing agarose gels were loaded with 5-10 µg RNA filled with RNase-free ddH_2O to 10 µl and mixed with 1 vol glyoxal loading buffer (Sambrook & Russell, 2001). Samples containing 20 µl volume were incubated at 55°C for 1 h, followed by colling one ice for 5 min and addition of 1.5 µl of formamide loading buffer (FLB; 95 % deionized formamide, 0.025 % bromophenol blue, 0.025 % xylene cyanole FF, 0.025 % SDS and 5 mM EDTA) (Sambrook & Russell, 2001). The separation on a 1.2 % agarose gel in 1 x BPTE-buffer (30 mM Bis-Tris, 10 mM PIPES and 1 mM EDTA). Gels were run for 18 h at 50 V. Mature RNAs were visualized by staining with ethidium bromide (EtBr), then gel was washed with H_2O for 15 min under gentle shaking. Afterwards, gel was treated with 0.1 M NaOH for 25 min to partially degrade the RNA, then washed with H_2O and neutralized twice with Tris-NaCl-buffer (0.5 M Tris, pH 7.5, 1.5 M NaCl) for 20 min. The gel was equilibrated in 6 x SSC (20 x SSC: 3 M NaCl and 300 mM sodium citrate, pH 7.0) for 10 min. Gel was blotted on a HyBond Nylon membrane (RPN303B, GE Healthcare, Buckinghamshire, UK) in 6 x SSC with vacuum blotting at 70-100 mbar for 3-4 h. For short pre-rRNAs (20 – 500 nt), denaturing polyacrylamide gels were used. Whereby, 2-5 µg RNA in a maximum of 10 µl RNase-free H_2O were mixed with 1 vol FLB to a volume of 20 µl and heated at 85 °C for 5 min. The samples were separated on 12 % polyacrylamide/ 8 M urea gels in 1 x TBE buffer (89 mM Tris, 89 mM Boric acid and 2 mM EDTA) for 2 h at 25 Watt. Mature rRNAs were visualized by staining the gel with EtBr. Gel was washed for 10 min with

H_2O and equilibrated for 10 min in 1 x TBE buffer. Blotting was performed on HyBond Nylon membrane with electroblotting using the wet-blot-technique in 1 x TBE at 15 V for 16 h or at 50 V for 4 h. After blotting, the membranes were UV-cross-linked using the Stratalinker 2400 two times at auto-crosslink settings (two-times 1,200 µJoules x 100). After cross-linking, membranes were stained with methylene blue staining solution (0.02 % (w/v) methylene blue, 0.3 M sodium acetate, pH 5.2) for 2 min and destained with 0.2x SSC, 0.1 % SDS. For detection of specific pre-rRNAs, 2.5 µM of probe (Table 1 and 3; Missbach et al., 2013; Weis et al., 2014; Streit et al., 2020) was radiolabeled with [γ-^{32}P]-ATP (SRP 201, Hartman Analytic) and T4 Polynucleotide kinase (Thermo Scientific, Darmstadt, Germany) for 30 min at 37°C, while membrane was equilibrated in hybridization buffer (6x SSC, 1 % (w/v) SDS, 2x Denhardt's solution (2 % bovine serum albumin, 2 % Ficoll 400, 2 % polyvinylpyrrolidone), 0.1 mg/mL Fish DNA) at 37°C. The labelled probe was added to the membrane in hybridization solution and incubated for 16 h at 37°C. Afterwards membrane was once washed in wash-buffer 1 (6x SSC) and once in wash-buffer 2 (2x SSC, 0.1 % SDS) for at least 30 min (up to one hour). Immediately, membranes were air-dried, wrapped in transparent foil and incubated in Storage Phosphor Screens (GE healthcare, USA). Incubation on screens was dependent on signal-strength and varied between one day and 2 weeks. Screens were scanned with a Typhoon 9400 scanner (GE healthcare, USA). Quantification was performed with ImageJ.

4.1.4 Circularized-RT-PCR (cRT-PCR) and sequencing

Circular RT-PCR was performed as described with slight modifications (Shanmugam et al., 2017). In detail, 5 µg of RNA from total, cytoplasmic or nuclear RNA was denatured at 70°C for 5 min, chilled on ice and allowed to circularize in a total volume of 50 µl with 30 U of T4 RNA Ligase I (NEB), 1x RNA T4 ligase buffer, 1 mM ATP, 40 U RiboLock (Thermofisher Scientific, Germany) and RNase-free H_2O. Samples were incubated at 37°C for 2 h, enzymes were deactivated at 65°C for 15 min and circularized RNA (crRNA) was precipitated overnight with 0.1 vol of 3M sodium acetate and 2.5 vol of ice cold 100% EtOH. Samples were centrifuged at maximum speed at 4°C, once washed with 70 % EtOH, air-dried and pellet was resuspended in 50 µl RNase-free H_2O. Reverse transcription was performed with 1 µg crRNA, 0.5 mM of a gene specific oligonucleotide (Table 5), 1 mM dNTPs and RNase-free H_2O in a total reaction volume of 10 µl. Samples were incubated at 70°C for 5 min and immediately chilled on ice for 3 min. In the meanwhile, reaction mixture was prepared for circularized complementary DNA (ccDNA) synthesis in a total of 10 µl with 1x SuperScript III RT-buffer, 10 mM $MgCl_2$, 80 U RiboLock, 10 mM DTT, 200 U of SuperScript III RT (Thermofisher Scientific, Germany). Samples were incubated at 42°C for 1 h and enzymes deactivated at 85°C for 5 min. Finally, ccDNA was diluted to 50 µl with H_2O. The ccDNA was used for RT-PCR with cRT-F1/cRT-R1 and cRT-F1/cRT-R2 (Table 5). The major DNA bands were excised from agarose

gel and eluted with E.Z.N.A. Gel Extraction Kit (Omega, Bio-Tek, USA) and subsequently cloned into pGEM-T vector (Promega, USA), followed by transformation into the *E. coli* DH5α strain. Positive colonies containing the vector and insert were selected by using blue/white screening (see section 3.5 Media). For further purification, colony PCR was performed, the DNA of correct size was excised from the gel and eluted. Subsequently, DNA was sent for sanger sequencing with M13-F or M13-R oligonucleotides (Table 5). Sequenced DNA was aligned to pre-rRNA with Clone Manager 10.

4.1.5 RT-PCR and colony PCR

RT-PCR was performed as described (Sambrook & Russell, 2001). For colony PCR, single colonies were picked with pipette tip and transferred into 10 µl water in PCR tubes. Afterwards, 10 µl of reaction mixture was added and mixed thoroughly. The PCR was performed with 32-35 cycles.

4.1.6 Sucrose density gradient fractionation

The ribosomal fractionation of *A. thaliana* plants was performed with modifications as described (Hsu et al., 2014; Weis et al., 2014; Firmino et al., 2020). In detail, 400 mg of pulverized tissue of 10 das old seedlings were resuspended on ice in 200-400 µl ribosome extraction buffer (REB; 200 mM Tris-HCl, pH 8.8, 200 mM KCl, 25 mM EGTA, pH 8.3, 36 mM $MgCl_2$, 1 % (w/v) Brij-35, 1 % (v/v) Triton X-100, 1 % (v/v) Igepal CA 630, 1 % (v/v) Tween 20, 1 % (v/v) polyoxyethylene 10 tridecyl ether, 1 % (w/v) sodium deoxycholate, 50 µg/ml Cycloheximide, 1 mg/ml Heparin, 50 µg/ml Chloramphenicol, 5 mM DTT, 1 mM PMSF, 10 µl protease inhibitor cocktail/ml buffer). To avoid that polysomes are degrading, tissue was allowed to slowly thaw in REB, just by pipetting up and down. Samples were incubated on ice for 20 min under gentle rotation (35 rotations per minute) and centrifuged at 14,000 rpm for 2 min for cleaning the supernatant from cell debris. A first indication for the quantity of ribosomes was obtained with a Bradford assay (Bradford, 1976). A sample was found to be good when 1 µl of sample yielded an OD_{595} of ≥ 0.4. The gradient was prepared with 15 – 60 % sucrose in 1x polysome buffer (10x; 400 mM Tris/HCl, pH 8.0, 200 mM KCl, 100 mM $MgCl_2$, 100 µg/ml cycloheximide) in 14 ml polypropylene tubes (Beckman Coulter, Marburg, Germany) and pre-chilled in the fridge until samples were ready. For loading 200 – 500 µl of sample were loaded onto the gradients, tubes ere balanced and placed into the buckets of a TST41.14 rotor. Samples were centrifuged at 23,500 rpm for 18 h at 4°C. Gradients were read out using a gradient collector with continuous UV absorption measurement at 254 nm (Wöhnert Lab, Frankfurt, Germany) with 70 % sucrose solution. For isolation of RNA from fractions 300 µl of the fractions were mixed with 300 ml Solution D (see 4.1.1), 60 µl NaOAc, pH 4, and 600 µl PCI (25:24:1). After centrifugation at full speed for 5 min at RT, 500 µl of aqueous phase was

mixed with 500 µl chloroform, mixed vigorously and centrifuged at full speed for min 5 min at RT. Then 400 µl of aqueous phase was mixed with 1 ml 100 % EtOH and RNA was allowed to precipitate over night at -20°C. Next, RNA was pelleted by centrifugation at full speed for 20 min at 4°C, pellet was washed once with 70% EtOH, centrifuged again for 5 min and pellet was air-dried for max. 15 min, before resuspension with 20 µl ddH_2O. For protein isolation, 175 µl of each fraction was mixed with 700 µl methanol, 175 µl chloroform and 525 µl ddH_2O. Samples were vigorously mixed and centrifuged at full speed for 5 min. Aqueous phase was discarded and 700 µl methanol was added to the lower phase, mixed vigorously, and centrifuged at full speed for 5 min. Supernatant was discarded completely, and pellet allowed to air-dry. Then, pellet was resuspended with 50-100 µl cracking solubilization buffer (4.1.10). Samples were incubated for 10 min at 60°C and 1400 rpm.

4.1.7 Extraction of genomic DNA

The crude genomic DNA was extracted from *A. thaliana* leave tissue as described (Edwards et al., 1991). In brief, the plant leaves were disrupted by using an Eppi-Pistil (Schuett Biotec, Göttingen, Germany) in gDNA isolation buffer (200 mM Tris, pH 7.5, 250 mM NaCl, 25 mM EDTA, pH 8.0, 0.5 % SDS). The samples were incubated at room temperature for at least 10 min and centrifuged at 10,000 rpm for 10 min. The supernatant was mixed 1:1 with isopropanol and DNA was allowed to precipitate at -20°C for 1 h. The DNA was pelleted at 14,000 rpm for 15 min at 4°C. The pellet was dried at 42°C for 5 min and finally resuspended in TE-buffer (10 mM Tris-HCl, pH 7.5, 1 mM EDTA, pH 8.0). DNA was stored at 4°C until further use.

4.1.8 T-DNA screening and mapping

For screening of T-DNA insertion in mutant gDNA, oligonucleotides listed in Table 4 were used for PCR. In a total reaction volume of 20 µl, 50 ng gDNA were mixed with 20 µM of each forward and reverse oligonucleotides, 4 mM dNTPs, 1 X Taq buffer and 0.25 µl Taq polymerase and PCR program was adjusted to 30 cycles with 56°C as annealing temperature. In brief, for detection of the left border region of T-DNA *prp24.2*-fw and Salk LB1 were used. For detection of the right border of the T-DNA *prp24.2*-rv and Salk LB1 were used. To check whether there is still a wildtype copy of the gene, *prp24.2-rv* and *prp24.2-fw* were used. For mapping the position of the T-DNA in the mutant, PCR product corresponding to the left border region of the T-DNA and the genomic region were eluted from agarose gel and send for sanger sequencing with Salk LB3. The same was performed for the right border region of the T-DNA. The sequenced regions were aligned to the gDNA of *PRP24* with Clone Manager 10.

4.1.9 Fluorescence in situ hybridization (FISH)

FISH was performed as described (Duncan et al., 2017) with minor modifications. For detection of snoRNAs and pre-rRNAs in *A. thaliana* roots and cultured root cells, 40-50 nt long antisense oligonucleotides labelled at 5´ and 3´ position with cyanine 3 (Cy3) (Sigma-Aldrich, Darmstadt, Germany) were used. In brief, *A. thaliana* Col-0 plants were grown vertically for 4-5 days under long-day conditions. Root-tips were cut and fixed in 4% paraformaldehyde in 1x PBS (12 mM Phosphate, 137 mM NaCl, 2.7 mM KCl) for 30 min. Root-tips were washed twice in 1x PBS for 5 min, afterwards placed on a microscope slide under a cover glass to gently squash the roots with a rubber. Immediately, root-tips were shock frozen for 5 sec in liquid nitrogen, the cover glass was flipped off and the root-tips were allowed to air-dry at room temperature for at least 30 min. Afterwards, samples on microscope slides were permeabilized with 70 % EtOH for one hour at room temperature and stored for a maximum of 7 days in 70 % EtOH at 4°C before hybridization with probes. For hybridization, respective FISH-probe was diluted to 250 nM in hybridization solution (100 mg/ml dextran sulphate, 10 % deionized formamide, 2x SSC). The root-tips and root cells were immersed with hybridization solution containing the probe (200 µl) and covered with a glass-slide. The samples were placed in a humid chamber and incubated overnight at 37°C or 55°C, for snoRNA or pre-rRNA detection, respectively. Next day, samples were washed twice with wash buffer (10 % deionized formamide and 2x SSC) and incubated in wash-buffer for 30 min at room temperature. Subsequently, samples were incubated with 100 µl DAPI solution (100 ng/µl DAPI, 10 % formamide, 2x SSC) for 10 min at 37°C. DAPI solution was rinsed off twice with 2x SSC and 100 µl anti-fade GLOX buffer without enzymes (0.4 % glucose, 10 nM Tris-HCl, 2x SSC) was added for 1-2 min for equilibration. Excess anti-fade GLOX buffer was removed and anti-fade GLOX buffer with enzymes (0.4 % glucose, 10 nM Tris-HCl, 2x SSC, 1 µl glucose oxidase,1 µl bovine liver catalase) was added. Immediately, samples were closed with a cover glass and sealed with nail-varnish. Images were taken subsequently after sample preparation to avoid fluorescence bleaching.

4.1.10 SDS-PAGE and Western blotting

Protein samples of isolated nuclei, cytoplasm and total cells of *A. thaliana* cell suspension culture, plant leaves and liquid fractions after sucrose density gradient fractionation were denatured using cracking solubilization buffer (8M Urea, 5 % (w/v) SDS, 40 mM Tris-HCl pH 7.5, 0.1 mM EDTA, 0.04 % (w/v) bromophenol blue, 150 mM ß-mercaptoethanol, 1 mM PMSF; Yeast Protocols Handbook, Clontech). Samples were further processed by heating at 60°C for 10 min and 1400 rpm. Protein samples were separated by SDS-PAGE (Laemmli, 1970). Subsequently, SDS-gel was blotted on nitrocellulose membrane (GE healthcare) by electro blotting using semi-dry buffer (0,037 % (w/v) SDS, 96 mM Tris, 39 mM glycine, 20 % (v/v) methanol) for 90 min at 1 mA cm^{-2}. Afterwards, membrane was stained with Ponceau Red for

5 min to visualize blotted proteins and protein marker. For blocking, 5 % milk powder was dissolved in 1x PBS and incubated with the membrane for 1 h at room temperature while shaking. After that, membrane was incubated with first antibody overnight at 4°C. Antibodies and dilutions are given in Table 6. Next day, after removing first antibody the membrane was washed three times with 1x PBS for 5 min before secondary antibody (dissolved in 5 % milk in 1x PBS) was incubated with the membrane for 1 h at room temperature. After washing three times each 5 min with 1x PBS, the membrane was incubated with enhanced chemiluminescence reagents (ECL) for 5 min before images were taken with the ChemoStar ECL imager (INTAS, Göttingen, Germany).

4.1.11 Confocal laser scanning microscopy (CLSM)

Fluorescent images were taken with the Zeiss LSM780 Confocal Laser scanning microscope. The fluorescent dyes DAPI and Cy3 were excited at 405 nm and 543 nm, respectively. Emission was recorded at 460 nm and 570 nm, respectively. The fluorophores GFP and mCherry were excited at 488 nm and 568 nm and emission was recorded at 505-525 nm and 580-610 nm, respectively. Images were prepared with ImageJ (Schneider et al., 2012).

4.1.12 RNA-sequencing

RNA sequencing was performed to identify new snoRNAs. For that reason, subcellular fractionation of *A. thaliana* cell suspension culture was performed (see 4.2.3 Subcellular fractionation of *A. thaliana* cell culture). The RNA of each fraction (total, cytoplasm, nucleus and nucleolus) was quality checked by using agarose gels (Figure 8).

4.1.13 Structure analysis

The RNA sequence of the 64 nt extension at the 5´end of the 5.8S rRNA structure models were folded with RNAfold and illustrated with the FORNA tool (Kerpedjiev et al., 2015; Hofacker, 2003). The 64 nt extension of 5´-5.8S pre-rRNA was converted with RNAcomposer to a PDB-file (Popenda et al., 2012). The structures were presented with PyMol 2.0 (Schrödinger LLC.). The 80S pictures was created based on the structure from PDB ID: 5TGM (Melnikov et al., 2016).

4.1.14 Immuno-FISH

For immuno-FISH, 2 ml of *A. thaliana* root suspension culture was pelleted with 200 rpm for 5 min at RT. Cells were prepared as described (chapter 4.1.9; Heerklotz et al., 2001). After fixation, cells were washed twice with 1x MTSB (100 mM PIPES [piperazine-N,N´9-bis(2-ethanesulfonic acid] pH 6.9, 2 mM EGTA, 1mM $MgSO_4$). Cells were allowed to attach to poly-L-lysin coated cover glasses. Subsequently, cells were permeabilized with 0.5 % Triton X-100

in MTSB for 15 min. Due to the stringent conditions, FISH was performed first with hybridization as described in chapter 4.1.9. Immediately, after washing off the FISH probe, the residual aldehyde groups were blocked with 100 mM glycine in PBS for 15 min and cells were incubated in PBS-1 % bovine serum albumin (BSA) for 30 min. Then, cells were incubated with the primary α-AtRPS3-2 antibody in 1:500 dilution in PBS-1 % BSA overnight at 4°C. After washing with 1x PBS, cells were incubated with the secondary Cy2-conjugated antiserum for 1.5 h in the dark. After washing with 1x PBS, cells were incubated with 100µl DAPI solution in 1x PBS for 15 min at RT. The cover glasses were sealed with nail varnish on glass slides and images were taken subsequently after sample preparation to avoid fluorescence bleaching.

4.1.15 Statistical analysis

For the comparison of genotype (*prp24*, WT) and treatment (CHX 1µg/ml; CHX 2µg/ml; CHX 3µg/ml) factor differences on the root growth we tried to perform a Two-Way ANOVA (Analysis of Variance). Based on the failed normality test (Shapiro Wilk $p<0.05$) and passed equal variance test we had to perform instead the non-parametric all pairwise multiple comparison procedure of Holm-Sidak. The overall significance level was =0.05 and we observed significant differences in the genotype comparison (*prp24* vs WT) and for the treatments CHX 1µg/ml vs CHX 3µg/ml and CHX 2µg/ml vs CHX 3µg/ml of the genotype *prp24* and overall. Within the treatment differences of genotype WT we did not observe any significance.

4.1.16 RNA sequencing, analysis and snoRNA detection

RNA sequencing of total and nuclear RNAs were prepared as follows: The RNA was extracted and DNAse treated. Subsequently a size separation of the RNA on polyacrylamide gel was performed, in which RNA of a size of about 200 nt or smaller were extracted. The RNA sequencing and rRNA-depletion was prepared by GenXPro (Frankfurt, Germany). Reads of stranded single-ends with a size of 100 nt were generated on Ilumina NextSeq 500 and quality controlled by FASTCQ (www.bioinformatics.babraham.ac.uk/projects/fastqc). The program NextGenMap (Sedlazeck et al., 2013) was used to map the reads to the genome of *A. thaliana* (TAIR10) (Berardini et al., 2015) with standard parameter settings. The mapped reads were analyzed with HTSeq (Anders et al., 2015). Analysis of known snoRNAs were performed using the snoRNA databases snOPY (Yoshihama et al., 2013) and snoRNA db (Brown et al., 2003), for tRNA the database plantRNA (Cognat et al., 2013) and for rRNA sequences in SILVA (Quast et al., 2013) were used to assign the reads to these RNA classes. New snoRNAs were detected through a filterd set of reads of nuclear samples, purified from all annotated genes in the GFF file of *A. thaliana* (TAIR10). Reads with continuous read coverage in all three biological replicates were treated as "contigs" of putative ncRNAs and used as input for Infernal (Nawrocki and Eddy, 2013) for identification of similar sequence and structure predictions in

the covariance models to RNAs deposited in RFAM (Kalvari et al., 2018). If contigs showed similarities to a snoRNAs, they were extracted and classified as H/ACA or C/D box snoRNAs.

4.2 Plant methods

4.2.1 Plant growth conditions

Plant growth conditions were performed as described with little variations (Palm et al., 2019). For plant growth on solid ½ MS media in plates, seeds were surface sterilized with 6 % sodium-hypochlorite for 2 min, followed by 70 % EtOH for 2 min and washed five times with sterilized ddH_2O. For stratification seeds were kept in sterilized ddH_2O for three days at 4°C in the dark. The seeds were cultivated at long day conditions (16/8 h light/dark cycle) for 10 - 20 days.

4.2.2 Subcellular fractionation of plants

The subcellular fractionation of plants was performed as described before (Palm et al., 2016). In brief, frozen plant tissue (14 days old) was grinded in liquid nitrogen to a fine powder. Approximately, 2 g of powder was transferred to a 15 ml conical tube and 2 ml of HEPES-nuclear buffer (HNB; 25 mM HEPES, pH 7.5, 5 % (w/v) sucrose, 5 % glycerol, 25 mM NaCl, 5 mM $MgCl_2$, 1 mM EDTA, pH 8.0, 2 mM $CaCl_2$ and 10 µl/ml Plant protease Inhibitor Cocktail (PIC; Sigma, Rödermark, Deutschland) was added. The sample was allowed to thaw in the buffer on ice and incubated for 15 min. Samples were filtered through Miracloth to remove larger cell debris. To the homogenate 1 % Nonidet-P40 was added and mixed thoroughly. A sucrose cushion (10 % sucrose in HNB) was laid under the homogenate and the sample was centrifuged at 2150 x g for 10 min at 4°C. The pellet containing the nuclei was washed with HNB buffer and centrifuged once again for 5 min before RNA and/or protein extraction was performed. The supernatant containing the cytoplasmic fraction was recovered and directly used for RNA and/or protein extraction.

4.2.3 Subcellular fractionation of *A. thaliana* cell culture

The fractionation of Arabidopsis root culture was performed as described with minor modifications (McKeown et al., 2008). In brief, 100 ml of three-day-old cell culture was centrifuged at 134 x g at room temperature for 5 min. The pellet was gently resuspended in 50 ml Protoplast Isolation Buffer (PIB; 0.5 M sorbitol, 10 mM MES/KOH, pH 5.5, 1 mM $CaCl_2$) with 1 % Cellulase Onozuka R-10 (Duchefa, Haarlem, Netherlands) and 0.25 % Macerozym (Duchefa, Haarlem, Netherlands). The cell suspension was gently shaken at 25 °C for approx. 1.5 h until the cells released nuclei. Protoplasts were pelleted at 134 x g for 5 min. Protoplasts were resuspended in 40 ml flotation buffer (60 % Percoll, 0.5 M sorbitol, 10 mM MES/KOH, pH 5.5, 1 mM $CaCl_2$). A Percoll step gradient is formed by overlaying 20 ml of protoplasts with 5

ml of 45 % Percoll, 5 ml of 35 % Percoll and 5 ml of 0 % Percoll, which are dilutions of flotation buffer with PIB. Samples are centrifuged at 134 x g for 5 min and intact protoplasts will float between the 35 % and 0% Percoll interface. All subsequent steps need to be performed one ice or in the cold room. Intact protoplasts are removed carefully with a large pipette tip and transferred into a new tube. For washing, protoplasts are resuspended in 20 ml PIB and centrifuged at 134 x g at 4°C for 5 min. Protoplasts are counted using a counting chamber. For isolation of nuclei, protoplasts are pelleted and resuspended in Nuclear Isolation Buffer (NIB; 10 mM MES/KOH, pH 5.5, 0.2 M sucrose, 2.5 mM EDTA, 2.5 mM DTT, 0.1 mM spermine, 0.5 mM spermidine, 10 mM NaCl, 10 mM KCl, 10 µl/ml PIC) with 1 x 10^6 protoplasts/ml of NIB. Samples were incubated for 5 min on ice and afterwards sonified (Bandelin, Sonopuls, HD70; 20 sec with a cycle of 5 sec on and 5 sec off with an amplitude of 20 %) until many nuclei were released as judged by phase contrast microscopy. An aliquot of nuclei fraction was saved for RNA and protein extraction. The remaining nuclei fraction was sonified more often until nuclei released nucleoli as judged by microscopy. Nucleoli were centrifuged 200 x g for 5 min and used for RNA and protein extraction.

4.2.4 Stress treatments on plates

For stress treatments of Arabidopsis seedlings, surface sterilized seeds of wild-type (Col-0) or mutants were sown on ½ MS plates with 2 % sucrose and kept for 14 days in growth chambers under long-day conditions before heat treatment in water bath or cold treatment at 4°C was performed. Optimal cycloheximide conditions have been identified by testing concentrations ranging between 50 ng/ml and 3 µg/ml, thus for treatment with cycloheximide, ½ MS media without sucrose was supplemented with CHX before pouring into plates with either 1, 2 or 3 µg/ml as those concentrations severely affected the germinate rate of the plants. Plates with seeds were kept under log-day conditions in growth chambers for at least 17 days. On day 17, seeds were photographed using a stereo microscope (Zeiss, Oberkochen).

5 Results

5.1 Content of snoRNAs and snRNAs in *Arabidopsis thaliana*

Many modified sites on rRNA could not be assigned to a snoRNA and furthermore many snoRNAs were just predicted but not experimentally confirmed. Thus, to identify and verify predicted novel snoRNAs, RNA deep sequencing was performed in combination with northern blotting and FISH. The protoplasts of Arabidopsis cell suspension culture were isolated and fractionated into cytoplasmic, nuclear and nucleolar fractions as judged by light microscopy, northern blotting and western blotting (Figure 8). After protoplasting (Figure 8A), cells were ruptured for release of nuclei (Figure 8B), an additional rupturing of the nuclei released the nucleoli (not shown). From each fraction of total cells, nuclei and nucleoli enriched fractions, RNA and proteins were extracted. The RNA was loaded on a 1.2% agarose gel and EtBr staining revealed two RNA species larger than mature 25S rRNA (Figure 8C). A subsequent northern blotting with complimentary probes (Table 1) shows that the highest RNA molecule unveiled the 35S* pre-rRNA, as the probe p1 is binding to one of the very first pre-rRNA transcripts (Figure 8C). The pre-rRNA appearing just above mature 25S rRNA, could be assigned to the $27SB_{S/L}$ pre-rRNA as proven with the probe p5 (Figure 8C). Western hybridization verified nucleolar enrichment of AtFIB1 (nucleolar marker) in the corresponding fraction (Figure 8D).

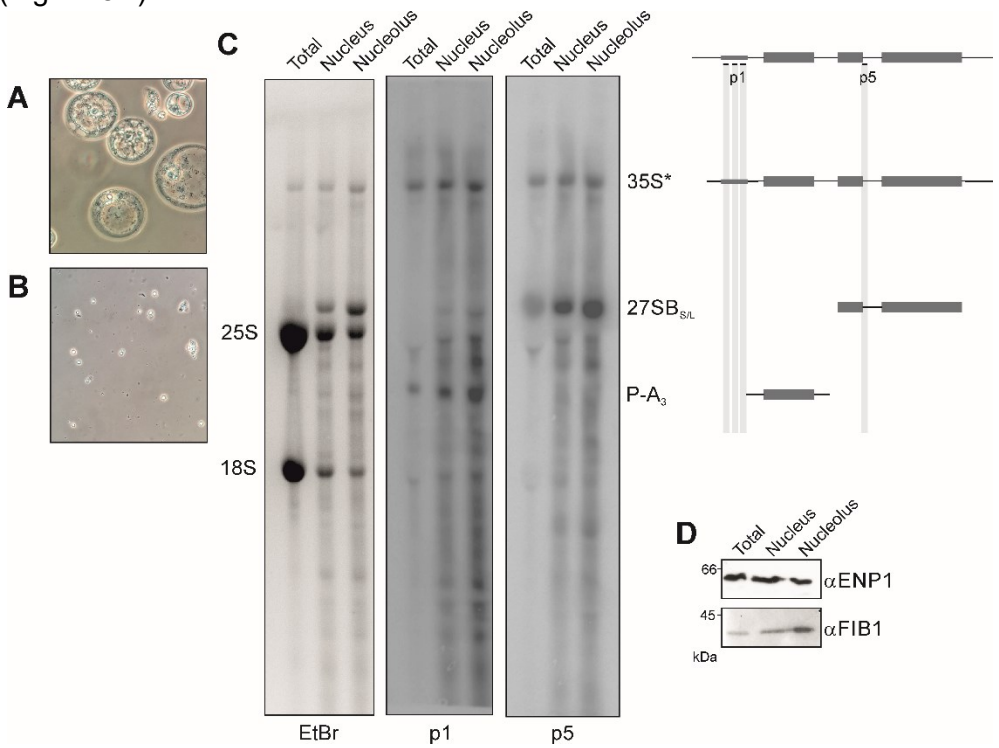

Figure 8. Analysis of nuclear and nucleolar integrity after fractionation.
A) Protoplasts of Arabidopsis root suspension culture. **B)** Isolated nuclei from protoplasts. **C)** 1.2 % agarose gel, loaded with RNA from protoplasts (total), nucleus and nucleolus. Probes (Table 1) for detection of 35S and 27SB pre-rRNAs were used. **D)** Proteins from each fraction (Figure 8C) were used for western blotting. Confirmation of enrichment of nuclear and nucleolar proteins were evaluated with α-ENP1 and α-FIB1 (Table 6).

For RNA-sequencing, three biological replicates of nuclei were prepared. For total cell lysate, a total of 12 million reads and 7 or 15 million reads for the nuclear fractions, were obtained, and mapped to the genome of *A. thaliana* (Table 8). The number of identified snoRNAs annotated in the Arabidopsis Information Resource (version 10; TAIR10; Berardini et al., 2015) is higher in the nuclear fractions compared to the total cell lysate (Table 8). The number of reads mapped to mRNA were higher for nuclear fractions, although the total number of mRNAs were higher in cell lysate. The total numbers are comparable amongst rRNA, tRNAs and ncRNAs, while reads are higher in the total lysate (Table 8).

Table 8. Distribution of coding and non-coding RNAs in Arabidopsis thaliana cells.
The number of reads (top) and of detected molecules (bottom) is presented. Adapted from Streit et al. (2020)

reads

	Total	Mapped	mRNA	ncRNA	rRNA	tRNA	miRNA	snRNA	snoRNA
Lysate	16,810,729	12,170,663	813,230	5,188	2,815	2,314	23	59	76
Nucleus 1	9,537,942	7,304,410	942,534	331	1,665	373	1	32	82
Nucleus 2	9,188,824	6,779,108	689,495	934	961	439	3	34	72
Nucleus 3	19,595,258	15,182,429	1,591,891	861	1,675	715	5	72	130

total number

	mRNA	ncRNA	rRNA	tRNA	miRNA	snRNA	snoRNA
Lysate	5,485	164	13	37	7	9	28
Nucleus1	1,354	74	12	23	1	5	28
Nucleus2	2,007	105	13	25	2	4	28
Nucleus3	2,242	108	12	32	2	8	38
Total nucleus	3,559	136	13	39	3	9	49
total	6,530	182	13	51	8	10	53

By comparison, nearly all predicted and earlier identified snoRNAs (53 H/ACA box and 155 C/D box) were found in at least one of the three replicates (Figure 9A). Interestingly, also 11 putative snoRNAs without a known fold were identified (Figure 9A). For identification of novel and not yet assigned snoRNAs, the longest read frame with reads of small ncRNAs in the nuclear fraction was used to identify known snoRNAs based to RFAM (Kalvari et al., 2018). By this tactic 34 snoRNAs (21 C/B box and 13 H/ACA box) were found, that do not occur in databases like TAIR10 or snOPY and thus are assigned as new (Figure 9B). These snoRNAs are distributed equally throughout the five chromosomes of Arabidopsis and are not clustered in one region (Figure 9C).

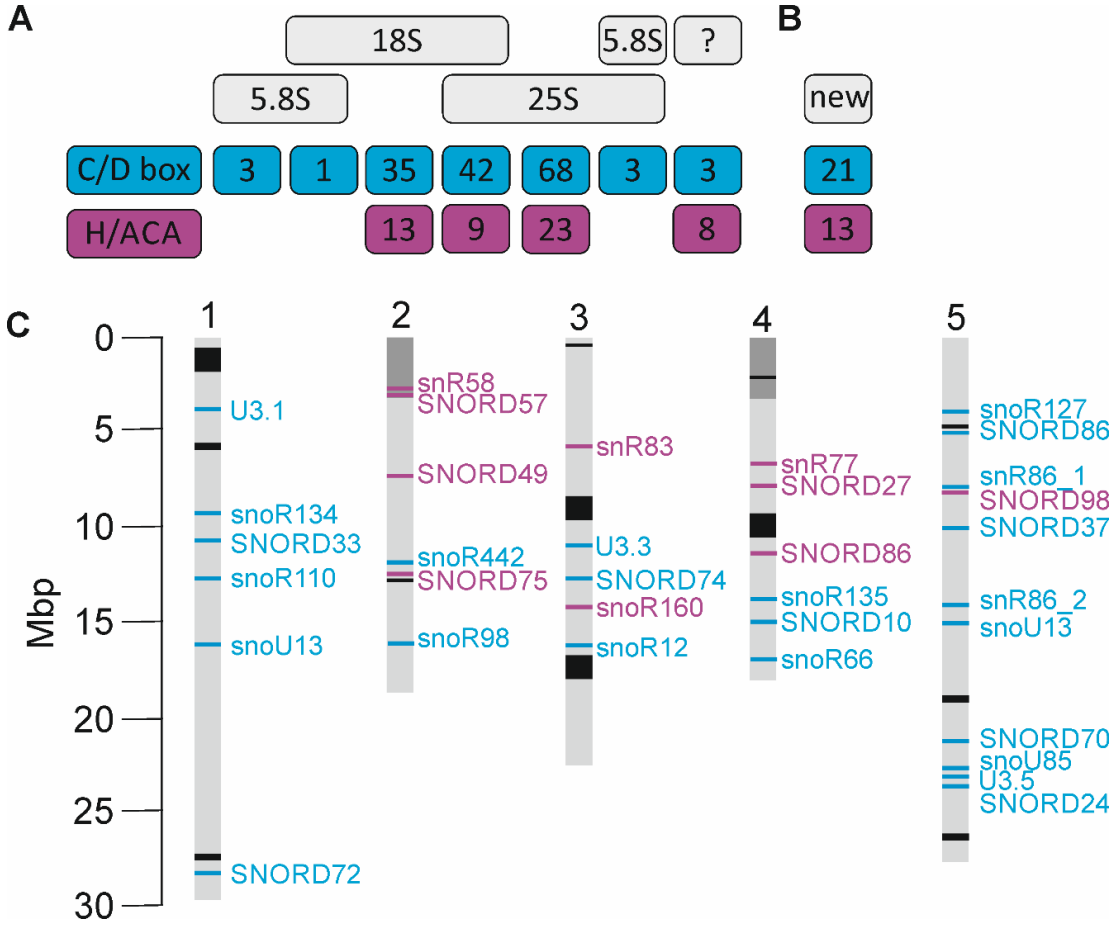

Figure 9. Distribution of detected snoRNAs of *Arabidopsis thaliana*.
A) Known snoRNAs based on comparison to snOPY (blue: C/B box; violet: H/ACA box). **B)** Number of newly identified snoRNAs of C/D box and H/ACA box family. **C)** Chromosomes of Arabidopsis were depicted indicating the regions were newly assigned snoRNA were found. Grey boxes indicate rDNA regions and black regions contain high snoRNA frequency. Adapted from Streit et al. (2020).

5.1.1 Localization of Arabidopsis U3-like snoRNAs

The NGS analysis revealed the existence of three U3-like snoRNAs with typical C/D box elements. Comparisons of secondary structure predictions shows that U3.1 (located on chromosome 1) is most comparable to the yeast counterpart (Figure 10A; Zhang et al., 2013). The U3.3 (located on chromosome 3) and U3.5 (located on chromosome 5) snoRNAs contain the C/D boxes as well, but predictions uncover many differences in the secondary structure (Figure 10A). The sub-cellular localization of these snoRNAs were analyzed in Arabidopsis root tips using FISH analysis. Since all three U3 snoRNA share almost the same sequence, the probe designed for FISH is most probably detecting all existing U3 snoRNAs (Figure 10B). FISH probe detected the snoRNAs in the nucleolus and RNase A treated samples confirmed the specificity of the probe (Figure 10B). The microscopic localization with FISH was further confirmed by northern blotting with cytoplasmic and nuclear RNA (Figure 10C). The purity of the nuclear fraction was evaluated with U25 snoRNA (Figure 10C, left). While U3.3 was only slightly detectable in the nuclear fractions (Figure 10C, middle), U3.5 is strongly abundant in the nucleus and present in the cytoplasm (Figure 10C, right). In addition to the most abundant

U3.5 snoRNA of 300 nt, four fragments were detected. Almost all of these fragments are present in the cytoplasm, although in lower amounts. The existence of U3.1 could not be shown in these experiments, presumably due to very low expression.

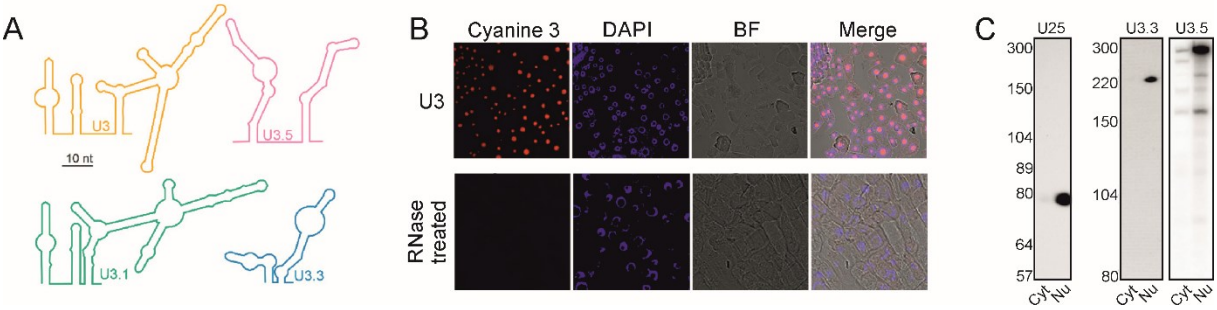

Figure 10. Analysis of U3-like snoRNAs in *Arabidopsis thaliana*.
A) Prediction of secondary structure models of U3-like snoRNAs according to yeast (Zhang et al., 2013) **B)** FISH analysis in Arabidopsis root tip cells with an antisense probe (Table 2) against U3-like snoRNAs before and after RNase A treatment. **C)** Northern blotting of U3.3 and U3.5 in cytoplasmic and nuclear fractions of Arabidopsis cell culture. Adapted from Streit et al. (2020).

5.1.2 Localization of C/D and H/ACA box snoRNAs in *Arabidopsis thaliana*

For confirmation of the computationally predicted snoRNAs, the cellular distribution was analyzed with FISH (Table 2) and by northern blotting (Table 3). First, the known C/D box snoR29 was examined in Arabidopsis root tips and was found exclusively in the nucleolus (Figure 11A). A control sample pre-treated with RNase A for 30 min, excluded an unspecific binding of the probe (Figure 11B). The C/D box snoRNA U49-1 shows a clear localization in the nucleolus and hybridization confirms the findings with FISH (Figure 11C, J). The U33a snoRNA, another C/D box snoRNA is as well localized in the nucleolus and designing the probe for this snoRNA was difficult as gene duplication has led to several variants, which cannot be targeted specifically due to high sequence similarities thus leading to three unique signals with northern hybridization (Figure 11D, E, J). The new member of C/D box snoRNAs is SNORD72 (Figure 11F). Distribution analysis by FISH revealed an exclusive localization in the nucleolus (Figure 11F). However, northern blotting shows that a very small amount can be observed also in the cytoplasm (nuclear depleted) fraction (Figure 11J). A special case with a different distribution for a snoRNA was observed for the earlier assigned snoR106. The snoRNAs are found only in the nucleolus, where rRNA modifications usually take place. FISH analysis showed that snoR106 is localized to the cytoplasm and nucleus (Figure 11G). To confirm that probe design was not faulty, a probe against At2g03875 was designed, which is only found in the cytoplasm (Figure 11I). In contrast, northern blotting reveals that a 300 nt RNA can be found in the nuclear fraction, but two smaller RNA fragments of ~140-150 nt were observed in the cytoplasm (Figure 11J). Another cytoplasmic snoRNA, snoR135 (Figure 11H) was detected in nucleus and nucleolus. However, NGS results revealed that it was less

abundant and 9 ± 3-fold enriched in the total cell lysate (Table S1). Nevertheless, detection by northern analysis did not yield a signal presumably due to their low levels. Identification of H/ACA class snoRNAs is hindered, due to their less conserved and more variable box sequences. We analyzed the two selected candidates snoR100 and snoR160. FISH analysis of snoR100, shows that it is majorly found in the nucleolus (Figure 11K) with faint signal detected in the cytoplasm.

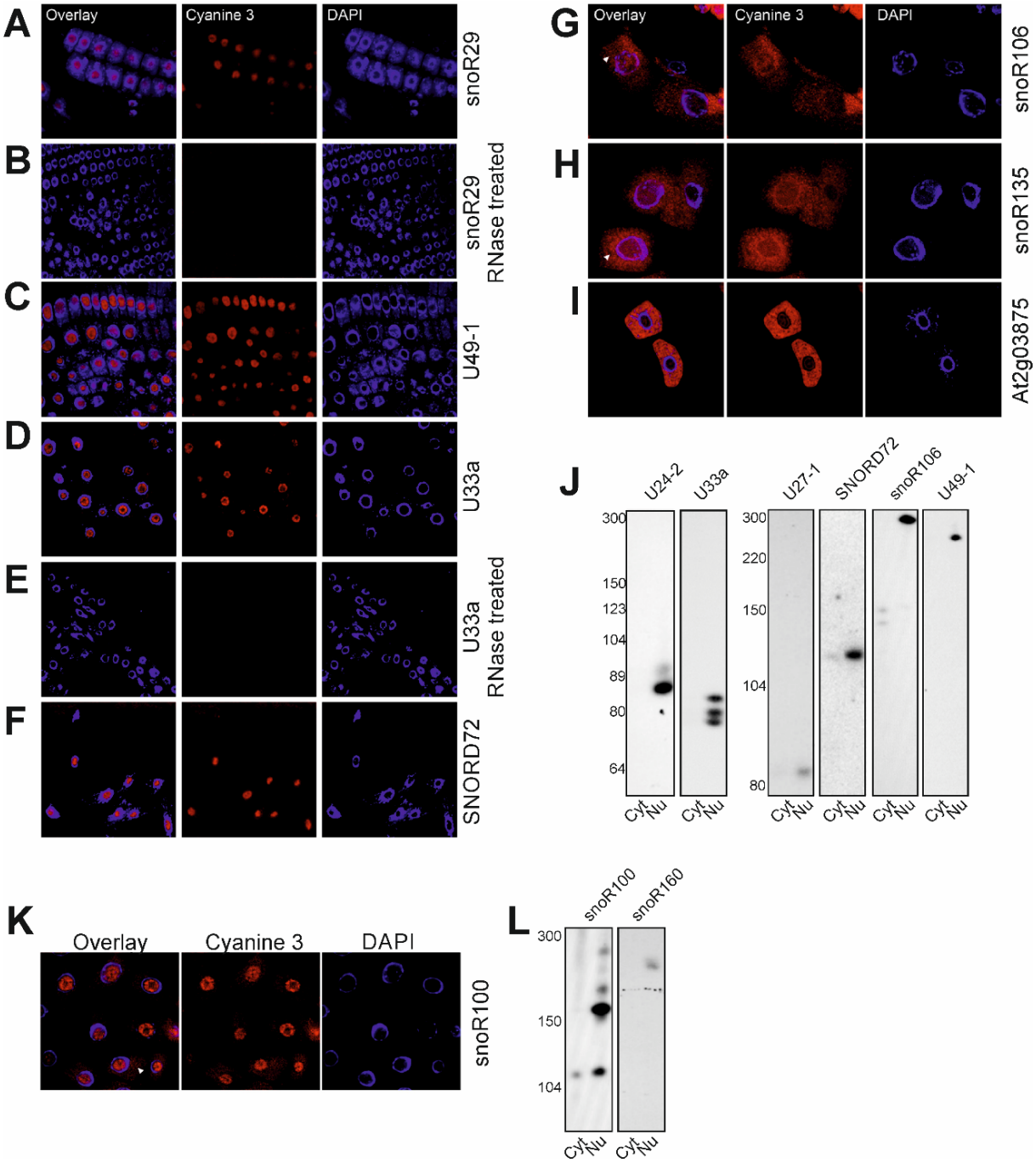

Figure 11. Distribution of snoRNAs in *Arabidopsis thaliana*.
(A-I) Fish probes (Table 2) against known and newly discovered C/D box snoRNAs, were incubated with Arabidopsis root tips. First panel shows overlay of DAPI staining and cyanine 3 labeled antisense oligonucleotide. Second panel shows cyanine 3 oligonucleotide and third panel only DAPI staining. **(B, E)** RNase A treated root tips are shown exemplarily for snoR29 and U33a. **J)** Northern blots of C/D box snoRNAs. **K)** FISH analysis of H/ACA box snoRNA snoR100. **L)** Northern blot of the two H/ACA snoRNAs snoR100 and snoR160. Adapted from Streit et al. (2020).

A direct comparison with northern blotting reveals that this snoRNAs is indeed partly in the cytoplasm (Figure 11L). However, several fragments are detected and only the smallest fragment (approx. 110 nt) seems to be exported to the cytoplasm. The most abundant RNA has a size of ~160 nt and is exclusively in the nucleoplasm, but also higher size RNA was found (Figure 11L). For snoR160, an exclusive nucleoplasm localization was observed (Figure 11L).

5.1.3 Distribution of snoRNAs in different tissues of *A. thaliana*

Next, the distribution of few selective snoRNAs were analyzed in roots (R), shoots (S) and flowers (F) tissues of *Arabidopsis thaliana* by northern hybridization with complementary probes (Table 3). A representative EtBr staining of polyacrylamide gel shows the intact mature rRNAs in the different tissues (Figure 12A). While 5.8S and 5S rRNA, components of the cytoplasmic 80S ribosomes are detectable in all tissues, the chloroplastic 4.5S rRNA is not present in roots and only faintly present in flowers, while it is more abundant in shoots (Figure 12A). The probe for detection of the newly discovered H/ACA snoR160 shows high abundance in roots and flowers, while in shoots this is only weakly detectable (Figure 12B, first).

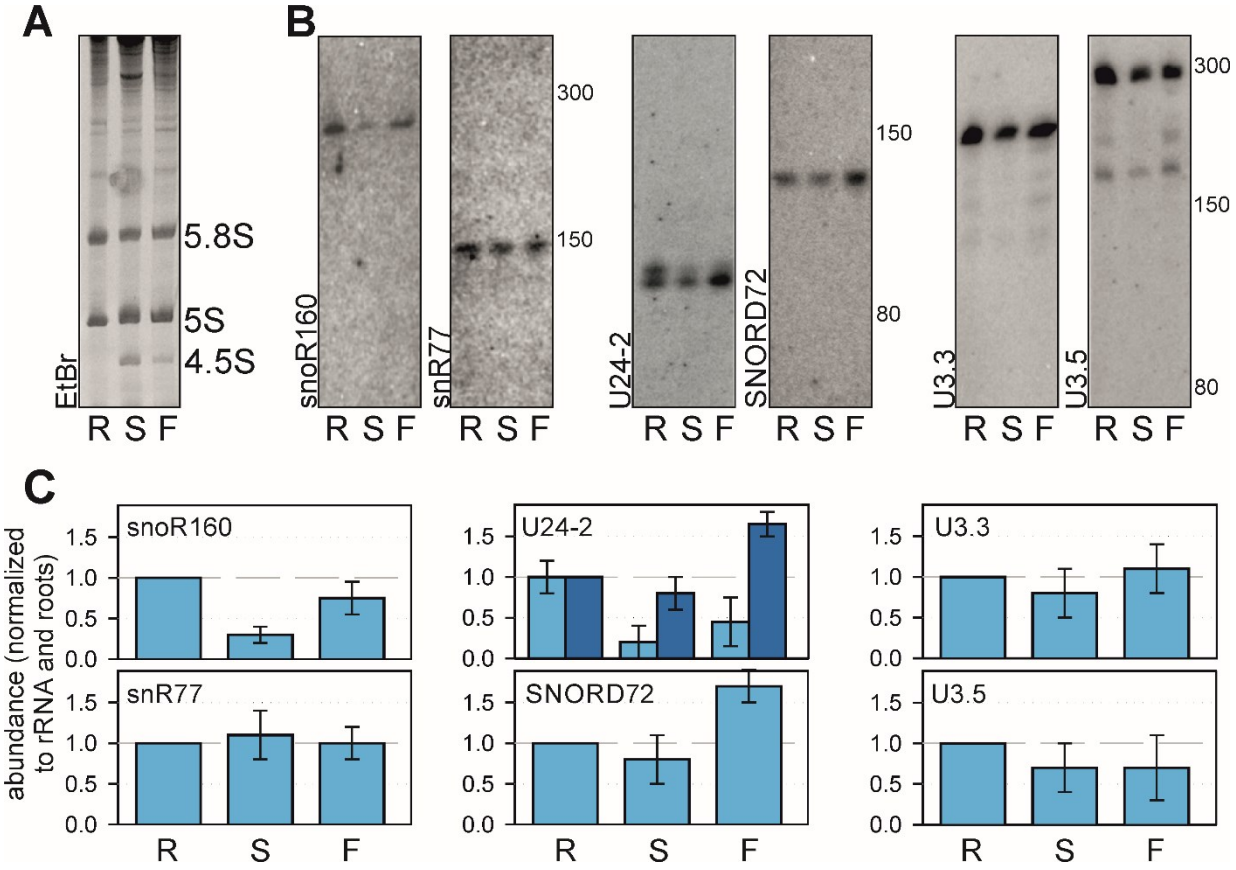

Figure 12. Distribution of snoRNAs in different tissues of *Arabidopsis thaliana*.
A) Representative polyacrylamide gel stained with ethidium bromide showing mature rRNAs used for quantification. **B)** Northern blots probed for selected known or newly identified snoRNAs. **C)** Quantification of band intensity was analyzed and normalized to the abundance in roots and to 5.8S and 5S rRNA. For U24-2 the lower band is illustrated in dark blue and the higher band in light blue, both values were normalized to the density of the lower band. R: root, S: shoot and F: flower. Adapted from Streit et al. (2020).

Quantification of the signal intensities normalized to the signal from roots and the mature 5S and 5.8S rRNAs, emphasizes the findings of northern hybridization (Figure 12C). The other newly discovered snR77, which was not detectable in root cell culture of Arabidopsis was found in plant tissues with northern blotting (Figure 12B, second). As quantifications underlines, this snoRNA is almost equally distributed across different tissues (Figure 12B, second and C). The known snoRNA U24-2 appears in cell culture in two forms, one minor larger form and one major smaller form (Figure 11J). Interestingly, in root tissue an almost equal amount of longer to smaller form is observed (Figure 12B, third). While in shoots the smaller form is dominating and in flowers is most abundant (Figure 12C). The novel snoRNA, SNORD72 is present in all tested tissues and mostly abundant in flowers (Figure 12B, fourth and C). The U3 snoRNAs U3.3 and U3.5 have an almost equal abundance in all tissues (Figure 12B, fifth and sixth and C).

5.2 The role of 5´-5.8S pre rRNA in plants

Processing of 5.8S precursor is a highly complicated process as discussed in chapter 1.3.2 and 1.3.3. Surprisingly, plants have evolved a 5.8S precursor which is extended to the ITS1 regions and is therefore called 5´-5.8S pre-rRNA. This precursor is only detectable in Arabidopsis under normal growth conditions. Although, it has only been described in Arabidopsis, their existence in other species has not been analyzed. Also, the question whether this precursor is finally cleaved within the nucleoplasm or in the cytoplasm to mature 5.8S rRNA remains elusive. Thus, this chapter deals with the existence of 5´-5.8S in other plant species and their distribution.

5.2.1 The 5´-5.8S pre-rRNA is localized in the cytoplasm of Arabidopsis

To determine the subcellular distribution of 5´-5.8S the total RNA from cytoplasmic fraction (Cyt), nucleoplasm (Nu) and nucleolus (No) were size separated and used for northern hybridization (Figure 13, C). The EtBr-stained agarose gel shows, that the cytoplasmic fraction contains only mature rRNAs from 80S and 50S ribosomes, while nucleolar und nucleoli fraction is enriched in pre-rRNAs like 27SB and 35S (Figure 13C). To determine the purity, pU2 and pU25 probes were used for Nu and No fraction, respectively (Figure 13A). The snoRNA U25 is highly abundant in No fraction with low levels in Nu fraction. The snRNA U2 is more abundant in Nu and No and cytoplasmic fraction contains slight contamination with U2 (Figure 13A). Interestingly, the 5´-5.8S pre-rRNA detection with p4 clearly shows, that this precursor is localized in the cytoplasm. Moreover, several smaller and larger precursors appear, that seem to mainly localize to the nucleoplasm (Figure 13A).

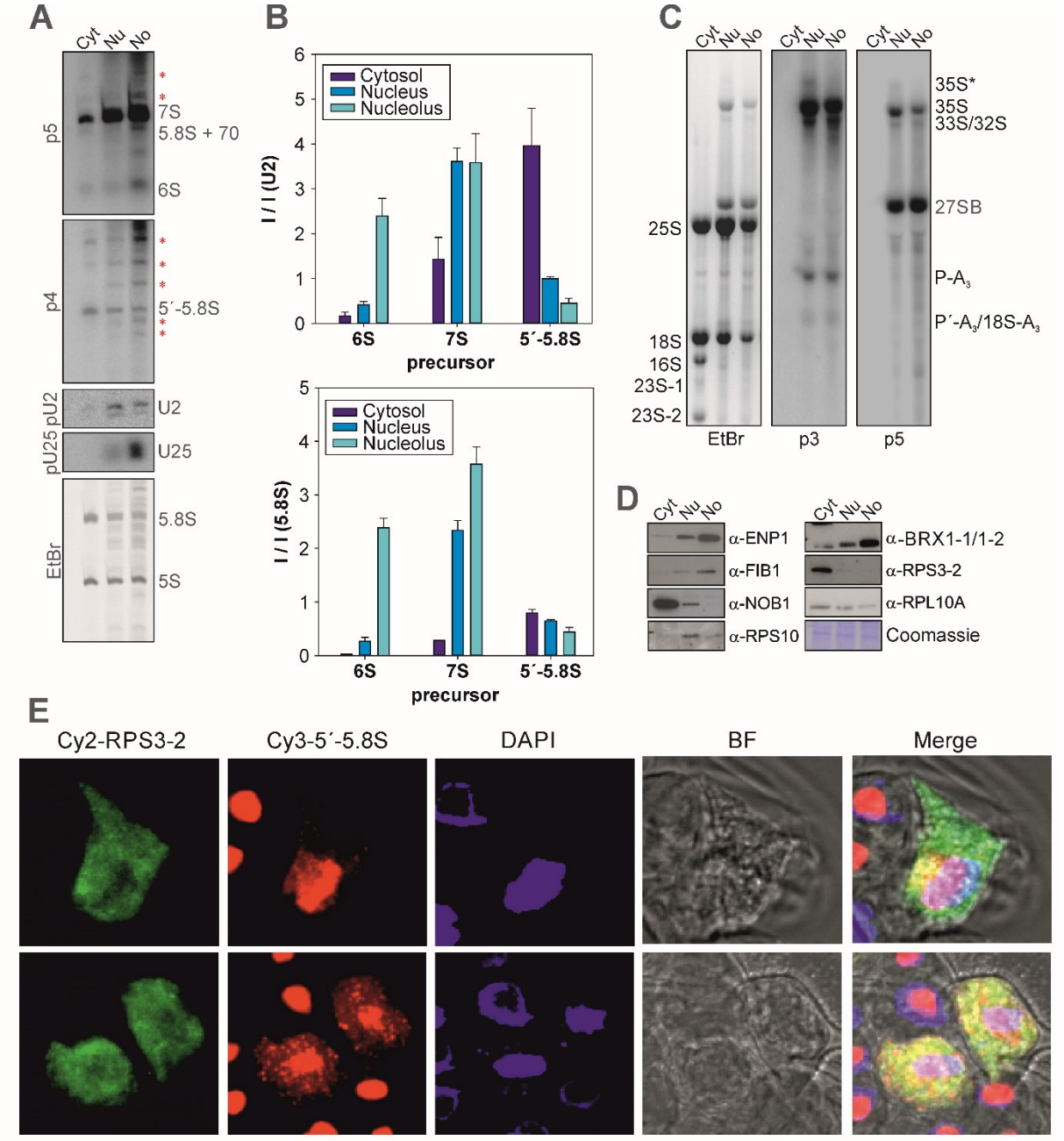

Figure 13. Analysis of 5´-5.8S pre-rRNA in Arabidopsis cell suspension culture.
A) RNA isolated from cytoplasm (Cyt), nucleoplasm (Nu) and nucleoli (No) were separated on a 16% polyacrylamide gel and blotted on a membrane. Membrane was incubated with pU25, pU2, p4 and p5. **B)** Quantifications of 6S, 7S and 5´-5.8S pre-rRNAs in relation to U2 and mature 5.8S rRNA. Three biological replicates were used for calculation of the standard deviation. **C)** The same RNA as in A) was loaded on a 1.2% agarose gel and blotted for northern hybridization with p3 and p5. **D)** Proteins were extracted from each fraction from A) for western blotting. Coomassie blue staining was used as loading control. **E)** Immuno-FISH analysis was performed in Arabidopsis root suspension culture cells. Secondary antibody labeled with Cy2 was used for detection of α-AtRPS3-2 antibody, for detection of 5´-5.8S an anti-sense oligo labeled with Cy3 was used. Nuclei were stained with DAPI. BF: brightfield.

The 3´-extended precursor like 6S and 7S pre-rRNA are concentrated in the No and Nu fractions. When intensities of 6S, 7S and 5´-5.8S pre-RNAs were normalized to intensities of nucleoplasmic U2, 6S pre-rRNA is predominantly present in nucleoli, whereas 7S is mainly localized in Nu and No and 5´-5.8S is mostly present in the cytoplasm (Figure 13B). When the intensities are compared to mature 5.8S rRNA, 6S is a precursor present in nucleoli while 7S

seems to diffuse to nucleoplasm and 5´-5.8S is located in the cytoplasm. Western hybridization analysis was performed in addition to verify purity of each fraction (Figure 13D). Indeed, the nucleoplasmic AtENP1 is present in nucleoplasm, the nucleolar AtFIB1 is mainly present in No fraction and the cytoplasmic AtNOB1 mainly appears in the cytoplasm. The AtRPS10 protein was recently found to be associated to ribosome already in the nucleoplasm (Palm et al., 2018) and is also here majorly present in the Nu fraction (Figure 13D). The proteins AtBRX1-1 and AtBRX 1-2 are associated to nucleolar pre-60S ribosomes and therefor majorly present in the No fraction (Weis et al., 2015b; Figure 13D). The 40S protein AtRPS3-2 is exclusively present in cytoplasmic ribosome and AtRPL10 is equally distributed in different fractions (Figure 13D). An immuno-FISH analysis was performed to determine the observed localization of 5´-5.8S pre-rRNA and to ensure that this precursor is indeed associated with cytoplasmic ribosomes. In here the cytoplasmic AtRPS3-2 was used as control for the 80S ribosome. Immunofluorescence was performed with an antibody against AtRPS3-2 and a secondary antibody coupled to Cyanine 2 (Cy2), targeting the primary antibody. For FISH, a 50 nt long Cy3-labeled complimentary oligo was used. The merge of Cy2 and Cy3 channels shows regions with overlapping spots of AtRPS3-2 and 5´-5.8S within the cytoplasm and verifies the preceding experiments (Figure 13E).

5.2.2 Presence of the 5´-5.8S pre-RNA is conserved in dicots and monocots

Previous analysis with Arabidopsis cell suspension culture, showed that 5´-5.8S pre-rRNA is exported to the cytoplasm albeit to a limited extent. Next the existence of the 5´-5.8S pre-rRNA was determined in other plant species. For this purpose, tomato plants (*Solanum lycopersicum* var. Moneymaker), rice plants (*Oryza sativa* var. japonica) and Arabidopsis plants (*Arabidopsis thaliana*, Col-0 accession) were subjected to subcellular fractionation according to chapter 4.2.2. Quantification of precursor distribution of *A. thaliana* shows that, 50 % of 5´-5.8S precursor is present in the cytoplasm (Figure 14A, B, E). Moreover, along with 5´-5.8S pre-rRNA, the probe p4 is detecting precursors of longer size in the nucleoplasm as seen before. As control for the purity of the cytoplasmic fraction the detection of the U2 snRNA was used. The probe p5 binding to the 3´-end of 5.8S rRNA, shows high abundance of 7S and 6S in the nucleoplasm as expected, while only 16 % of 7S and 28 % of 6S pre-rRNA are present in the cytoplasmic fraction (Figure 14B, E) in contrary to the observation from the cell culture (Figure 13A, B).

S. lycopersicum and *O. sativa* are recently more in the focus when scientists explore ribosome biogenesis and probes for the detection of rRNA precursor have been successfully established. Northern hybridization for *S. lycopersicum* pre-rRNAs with p4, detected a 5´-5.8S precursor, which is equally distributed in the cytoplasmic and nuclear fractions (Figure 14C, F). Surprisingly, also 6S (p5) the very last 3´-extended precursor of 5.8S rRNA is comparably

on the same level as 5´-5.8S pre-rRNA (Figure 14F). While 7S pre-rRNA is most likely a nuclear precursor.

The monocot used in this study *O.sativa*, was also fractionated and the pre-rRNA was hybridized with a probe like *A. thaliana* and *S. lycopersicum* p4. Also, in *O. sativa* a precursor similar to 5´-5.8S pre-rRNA can be detected and moreover also in the cytoplasm (Figure 14D, G). However, the percentage distribution, shows that the 5´-5.8S pre-rRNA is not as abundant in the cytoplasm as in *A. thaliana* or *S. lycopersicum*. In *O. sativa* the 6S pre-rRNA is highly abundant in the cytoplasm but also the 7S pre-rRNA is very abundant in the cytoplasm in contrast to *A. thaliana* and *S. lycopersicum* (Figure 14D, G).This could indicate, that *O. sativa* as monocot might have evolved a unique way of rRNA processing than the two dicotyl plants.

Consequently, this analysis shows that the existence of an 5´-extended 5.8S precursor is a conserved feature in the plant kingdom.

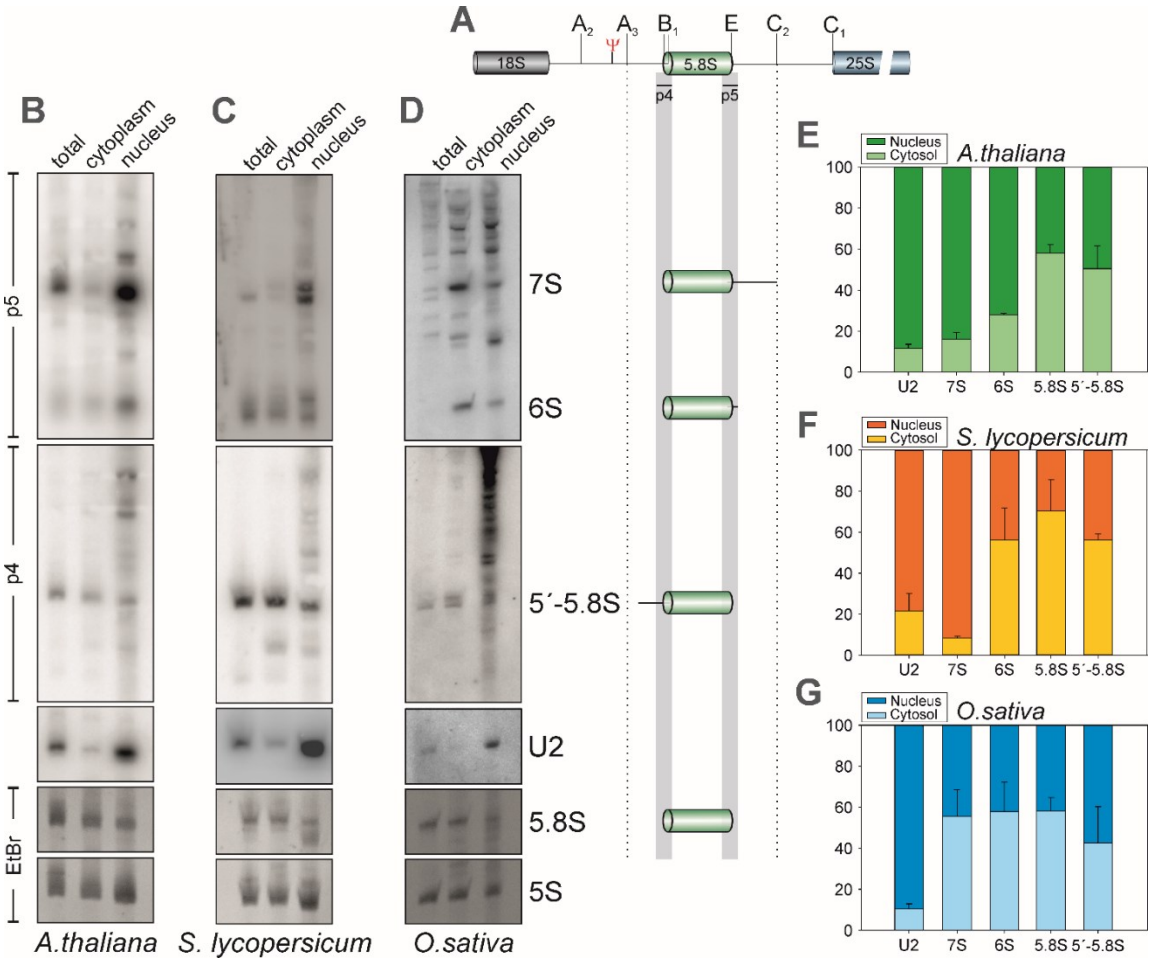

Figure 14. Analysis of 5´-5.8S pre-rRNA in different plant species.
Northern hybridization of total, cytoplasmic and nuclear RNA were performed for **A)** identification of 5.8S precursor of **B)** *Arabidopsis thaliana*, **C)** *Solanum lycopersicum* and **D)** *Oryza sativa* were performed. Plants were harvested 20 das. Probes used here are indicated in Table 1 and Table 3. The localization of the respective pre-rRNA, mature rRNAs and snRNAs given in percentages for **E)** *Arabidopsis thaliana,* **F)** *Solanum lycopersicum* and **G)** *Oryza sativa.* Calculations and standard deviations were performed from three biological replicates.

5.3 Factors involved in pre-rRNA processing

5.3.1 AtPRP24 and AtPCP2 are involved in pre-rRNA processing

The identification of new ribosome biogenesis factors is a challenging task. For that reason, a MS analysis was performed on nuclei, nucleoli and cytoplasmic fractions of Arabidopsis (Palm et al., 2016). To identify novel proteins, involved in pre-rRNA processing steps, northern hybridization was performed with T-DNA insertion mutants of AtPCP2 (At1g18850), AtPRP24 (At4g24270) and At1g29350 (RNA-Polymerase II degradation factor-like protein) based on their distribution in nucleoli (Figure 15). The membranes were hybridized with p1, p3, p4, p42 and p5 (Figure 15A, B). As p1 is binding to the 1083 nt insertion at the 5´-ETS, only the large precursor 35S* (Figure 8) is detectable. However, in none of the mutants such a precursor was found, indicating that processing of the first transcripts is not affected in the analyzed mutants (Figure 15B). The probe p3 binds in ITS1 close to 18S rRNA and detects 18S pre-rRNAs (Figure 15A). The protein AtPCP2 (Plant-specific component of the pre-rRNA processing complex 2) was found to be co-expressed with components of the pre-rRNA complex and co-localized with AtNuGWD1 and AtSWA1. AtNuGWD1 and AtSWA1 are most likely involved in 18S rRNA processing (Ishida et al., 2006). In the current study the heterozygous T-DNA line SAIL_35_C07 (Table 7) was used for northern blot detection as a homozygous line was not available. The *pcp2* mutant showed an accumulation of the large precursors 35S and 33/32S (Figure 15B, D). Even more dominant is the accumulation of the 27S-A_2 precursor (Figure 15B, D). Another precursor affected in *pcp2* is the 5´-5.8S precursor, that is accumulating as well although a high error bar implies a high variance in the measured values (Figure 15C, E). The gene At1g29350 encodes for an "RNA polymerase II degradation factor-like protein" and in the current study the Salk-line SALK_152117 was used for analysis of pre-rRNA processing defects (Figure 15). In comparison to wild-type only weak changes in abundance of large pre-rRNAs were observed (Figure 15B, D). However, a slight decrease of 18S-A_3 pre-rRNA was found (Figure 15D). The protein AtPRP24, a homologue of yeast/human Prp24/SART3(p110), was recently characterized to be involved in miRNA biogenesis and was renamed as "Serrate-Associated Protein 1" (SEAP1) (Li et al., 2021). In addition to AtPRP24s role in miRNA biogenesis, it is relevant for RNA splicing like its yeast and human counterpart. In this study, two T-DNA mutant alleles of *PRP24*, namely *prp24.1* and *prp24.2* were analyzed by northern blotting (Figure 15B, D). Probing reveals no dramatic change in pre-rRNA processing with slight differences of 33/32S pre-rRNA levels (Figure 15B, D). This accumulation is more prominent in *prp24.2* (Figure 15B, D). For the plant-specific precursor 5´-5.8S a two-fold increase is detected (Figure 15C, E). Moreover, *prp24.2* showed a higher increase, indicating that AtPRP24 is directly or indirectly involved in pre-rRNA processing.

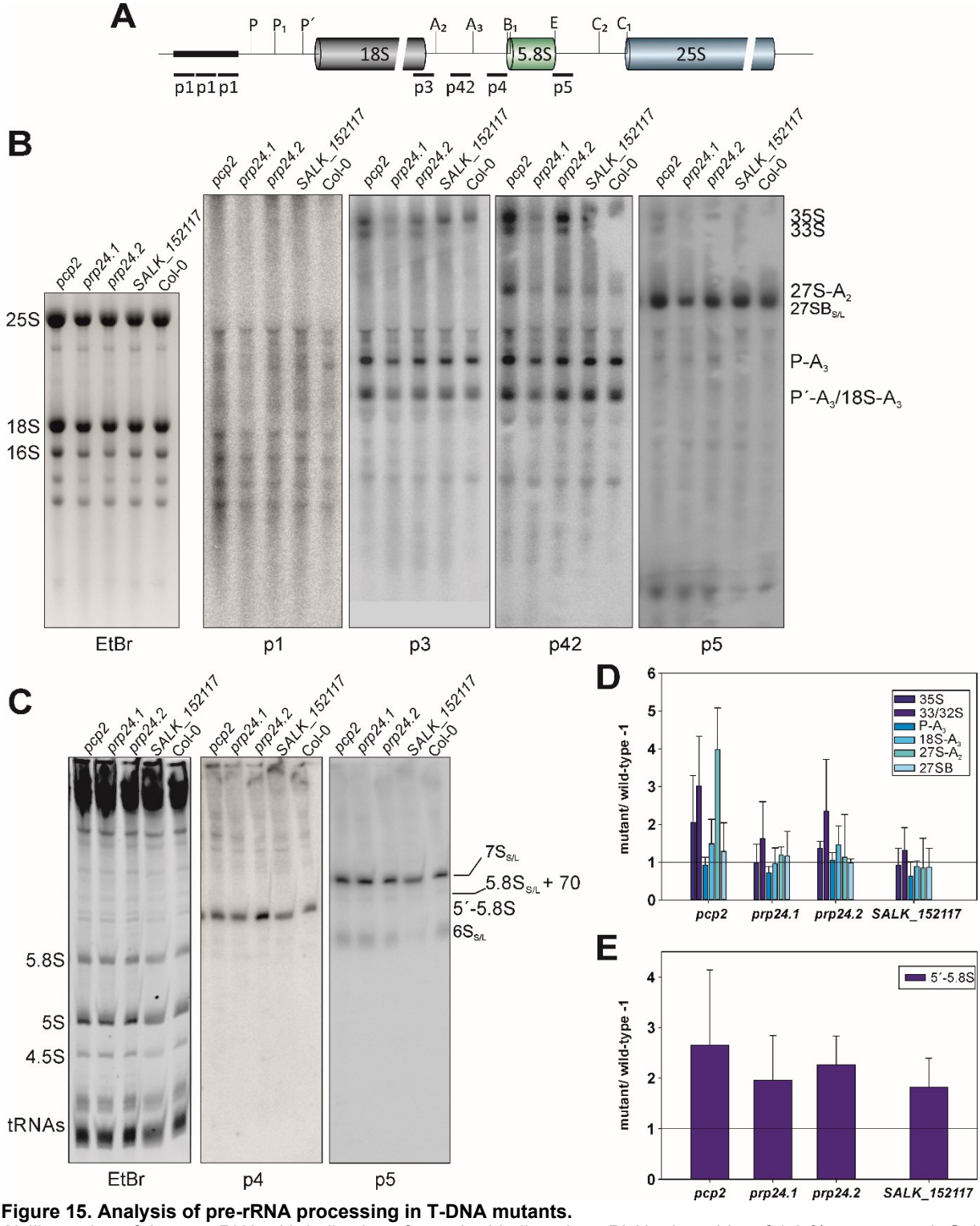

Figure 15. Analysis of pre-rRNA processing in T-DNA mutants.
A) Illustration of the pre-rRNA with indications for probe binding sites. **B)** Northern blot of 1.2 % agarose gel. Gel was stained with ethidium bromide (EtBr) for visualization of mature large rRNAs. The probes used for northern hybridization are indicated below (p1, p3, p42 and p5). Detected precursors are indicated on the right side. **C)** Northern blot of 16 % polyacrylamide gel (PAA-gel). The PAA gel was stained with EtBr for visualization of mature small rRNAs. Membrane was hybridized with p4 and p5 and precursors detected are indicated on the right site. **D)** Quantification of precursors detected in **A)**. For quantification, intensities of each precursor were normalized to EtBr stained mature 18S and 25S rRNA and to wild type (baseline at 1). Errors bars indicate standard deviation from three biological replicates. **E)** Quantification of 5´-5.8S pre-rRNA detected in **C)**. For quantification, intensities of the 5´-5.8S pre-rRNA were normalized to EtBr stained mature 5.8S and 5S rRNA and to wild type (baseline at 1). Error bars indicate standard deviation of at least three biological replicates.

5.3.2 *prp24.1* and *prp24.2* are homozygous lethal

Due to 5´-5.8S accumulation and larger 33/32S pre-rRNA, the protein AtPRP24 was explored further, for its role in processes other than as U4/U6 recruiting factor for the spliceosome and its unexpected role in miRNA biogenesis. The genomic region of Prp24 is contains by 16 exons and 16 introns (Figure 16. Analysis of T-DNA mutants. The mutant allele *prp24.1* has a single T-DNA insertion in intron 14 (Figure 16A, B). The mutant *prp24.2* has a double back-to-back insertion in exon 4 (Figure 16A, B). The positions form the T-DNAs were determined by sequencing (data not shown). For both mutants, a viable homozygous plant could not be recovered, due to the embryo-lethality. As shown for the SALK_043206, homozygous mutant seeds, were aborted and arrested in the globular stage (Li et al., 2021).

The AtPRP24 protein contains eight HAT-repeats (half-A-TPR), one RNA recognition motif (RRM) and one Lsm interaction motif. The HAT repeats are present in proteins, that are components of macromolecular complex for RNA processing and the Lsm interaction motif is required for interaction with Lsm proteins to promote U4/U6 formation. The RRM enables the protein binding to single-stranded RNA.

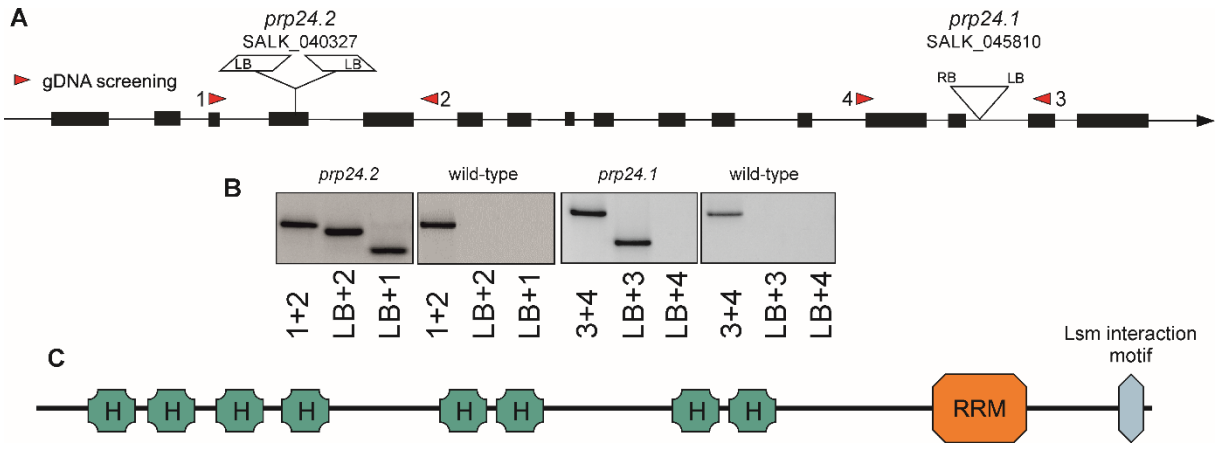

Figure 16. Analysis of T-DNA mutants.
A) T-DNA insertion of *prp24.1* and *prp24.2* are shown on the gene map. Exons are indicated as black boxes and introns as lines. Red arrows indicate positions of oligonucleotides used for PCR on gDNA. **B)** PCR of *prp24.2* and *prp24.1* with either genomic oligonucleotides (1+2 and 3+4) or in combination with T-DNA left-border (LB) oligo. **C)** Illustration of the protein AtPRP24 with eight HAT (half-A-TPR; H) repeats one RNA recognition motif (RRM) and one Lsm interaction motif close to the C-terminus.

5.3.3 AtPRP24 is involved in 5.8S pre-rRNA maturation

The observed accumulation of 5´-5.8S pre-rRNA in *prp24.2* was further analyzed by cytoplasmic and nucleoplasmic cellular fractionation analysis (Figure 17A). Besides, for better comparison the homozygous *rrpl6l2* mutant was used. AtRRP6L2 is known to be important among others for 6S pre-rRNA processing (Lange 2011; Weis, 2015; Thesis) and therefore the mutant is used as a factor accumulating 3´-extended 5.8S precursors (Figure 17A). Fractionated RNA according to chapter 4.2.2. were separated on a 16 % polyacrylamide gel prior to blotting. The first probe pU2 was used as control for the purity of the cytoplasmic fraction and only little contamination is observed in Col-0 and *prp24.2*, while *rrp6l2* cytoplasmic fraction was free of contamination (Figure 17A).

Upon p4 probing to determine 5´-extended 5.8S precursors, the Col-0 and *rrp6l2* showed lower levels of 5´-5.8S pre-rRNA in comparison to *prp24.2* showing higher accumulation in total and in the cytoplasmic fraction. Additionally, precursors larger than 5´-5.8S are highly abundant in *prp24.2* and *rrp6l2* mutants, indicating that accumulation of late-step 5.8S precursors, irrespective of the extended site, slows this precursor processing in a global manner. Next, the 3´-extended precursors were analyzed with p5. In here, *prp24.2* showed an accumulation of 6S and 7S pre-rRNA in the nucleoplasm with slight increase of 6S in the cytoplasmic fraction. In *rrp6l2*, the accumulation of 6S pre-rRNA was earlier observed (Lange 2011; Weis, 2015; Thesis) and the analysis shows accumulation of this precursor in all fractions and in total cells. Moreover, a second pre-RNA just below the 6S is emerging. Since p5 is binding overlapping at the 3´-end of 5.8S and ITS2, this additional RNA product might be a 5.8S precursor with shortened 5´-site, which is dominantly exported to the cytoplasm (Figure 17A).

Quantification of the signal intensities were normalized to EtBr stained 5S and to wild type and with baseline set to 1. For *prp24.2*, 5´-5.8S, 6S and 7S precursors are accumulating in the nucleoplasm (Figure 17B). Especially, 6S pre-rRNA levels are in increased in the nucleoplasm, while levels of 5´-5.8S pre-rRNA are comparably low. In the cytoplasm of *prp24.2* the precursor 5´-5.8S has the highest abundance. In *rrp6l2*, the cytoplasmic fraction shows a strong abundance for 6S precursors, while 5´-5.8S pre-rRNA is of the same levels as wild type (Figure 17B). In addition, the 6S pre-rRNA predominates the nucleoplasm in *rrp6l2* (Figure 17B).

Taken together, this analysis strengthens the observation that AtPRP24 is either directly or indirectly involved in the processing of 5.8S precursors. However, since precursors are affected originating from both sites of ITS1 and ITS2 in comparison to the *rrp6l2* mutant, it cannot be excluded that AtPRP24 is also involved in processing at the 3´-site. It is obvious that 5.8S rRNA processing in plants is way more complicated than expected and the identifications of these additional precursors might complete and extend the pre-rRNA processing scheme that is known so far.

Interestingly, the *rrp6l2* mutant is not only accumulating 6S, but has a second truncated form of 6S, that needs further investigations since it is dominantly transferred to the cytoplasm.

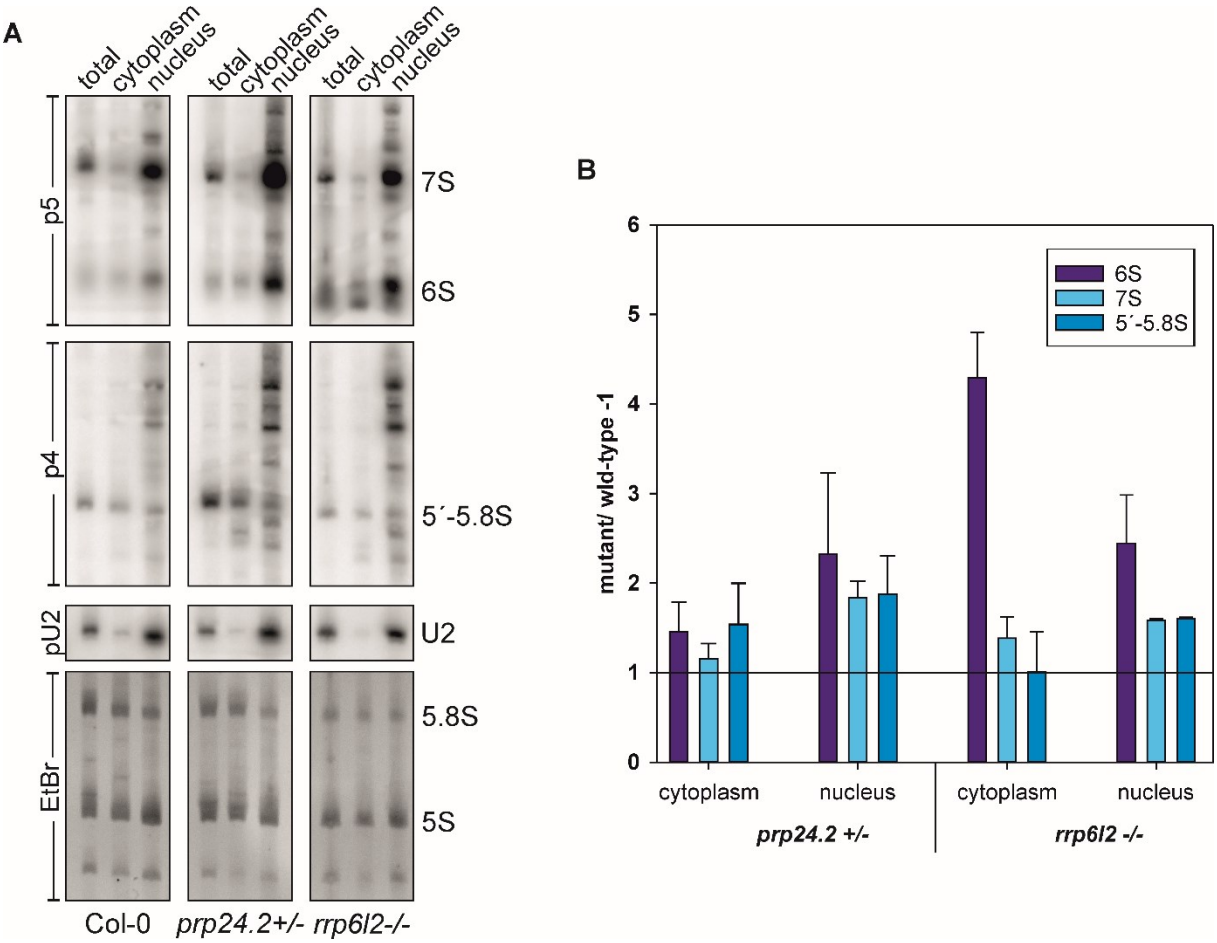

Figure 17. Analysis of 5.8S precursor processing defects in mutants.
A) RNA of fractionated wild-type (Col-0), *prp24*+/- and *rrp6l2*-/- mutants were separated on 16% polyacrylamide gel and electrophoretically blotted onto membranes. Membranes were hybridized with probes for U2 snRNA, p4 for 5´-extended 5.8S and p5 for 3´-extended 5.8S rRNA precursors. **B)** Quantification of signal intensities of 6S, 7S and 5´-5.8S rRNA in cytoplasm and nucleus of *prp24*+/- and *rrp6l2*-/- mutants. Values were normalized against EtBr stained 5S rRNA and are expressed as ratios to the intensities observed in wild type. Baseline is set to 1 and the standard deviation of two biological replicates is shown.

5.4 The role and identification of 5.8S precursors in *A. thaliana*

In order to identify additional precursors of 5.8S, the membranes from Figure 17A were additionally probed with p42, that binds downstream of A_2 and upstream of A_3 and re-probed with p43 that binds downstream of the A_3 cleavage site (Figure 18A). Furthermore, a probe binding upstream of C_2 cleavage site called p52 was used to confirm 3´ extremities of the precursors. Membranes from previous experiments of Col-0 and *prp24.2* (Figure 17A) are now depicted in full size to simplify direct comparisons of the precursors (Figure 18B).

5.4.1 *prp24.2* accumulates additional pre-5.8S precursors

Novel precursor observed on the membranes were numbered from 1 through 6 (Figure 18C). The precursor #1 is observed with p5 and p52 and is directly above 7S and sometimes even masked by 7S (*prp24.2*), indicating that the size is only ~10-20 nt longer than 7S pre-rRNA. However, precursor #1 is only faintly visible with probes binding upstream of the 5´-end of 5.8S rRNA. The precursor #2 is also above 7S and precursor #1 and observed with p5, p52 and with p4 and p43, indicating that this precursor is extended till C_2 and at least till A_3 cleavage sites. The precursor #3 appears with probes p4, p42 and p43, indicating that this pre-rRNA is extended till A_2 cleavage site (Figure 18A, C). However, it cannot be excluded that it is also extended to ITS2, since the high signal of 7S likely mask this precursor.

The precursors #4, #5 and #6 are the longest observed precursors and are more difficult to detect (Figure 18C). The precursor #4 is detected with p4, p42 and p43 but neither detected with p5 nor with p52, implying that this 5.8S precursor is only extended in the 5´-site. Precursor #5 is observed with p4, p5, p43 and p52 and likely span from at least A_3 in ITS1 till C_2 in ITS2. Probing with p42 does not show a distinct band and therefore it is not known if the precursor is extended till the A_2 cleavage site (Figure 18C). The largest precursor observed is #6, which is extended till A_2 as observed by probing with p42 and slightly also with p52, suggesting that this is the longest precursor. In order to find the exact 5´ and 3´ extremities of these 5.8S precursors, sequencing of these novel pre-rRNAs is required.

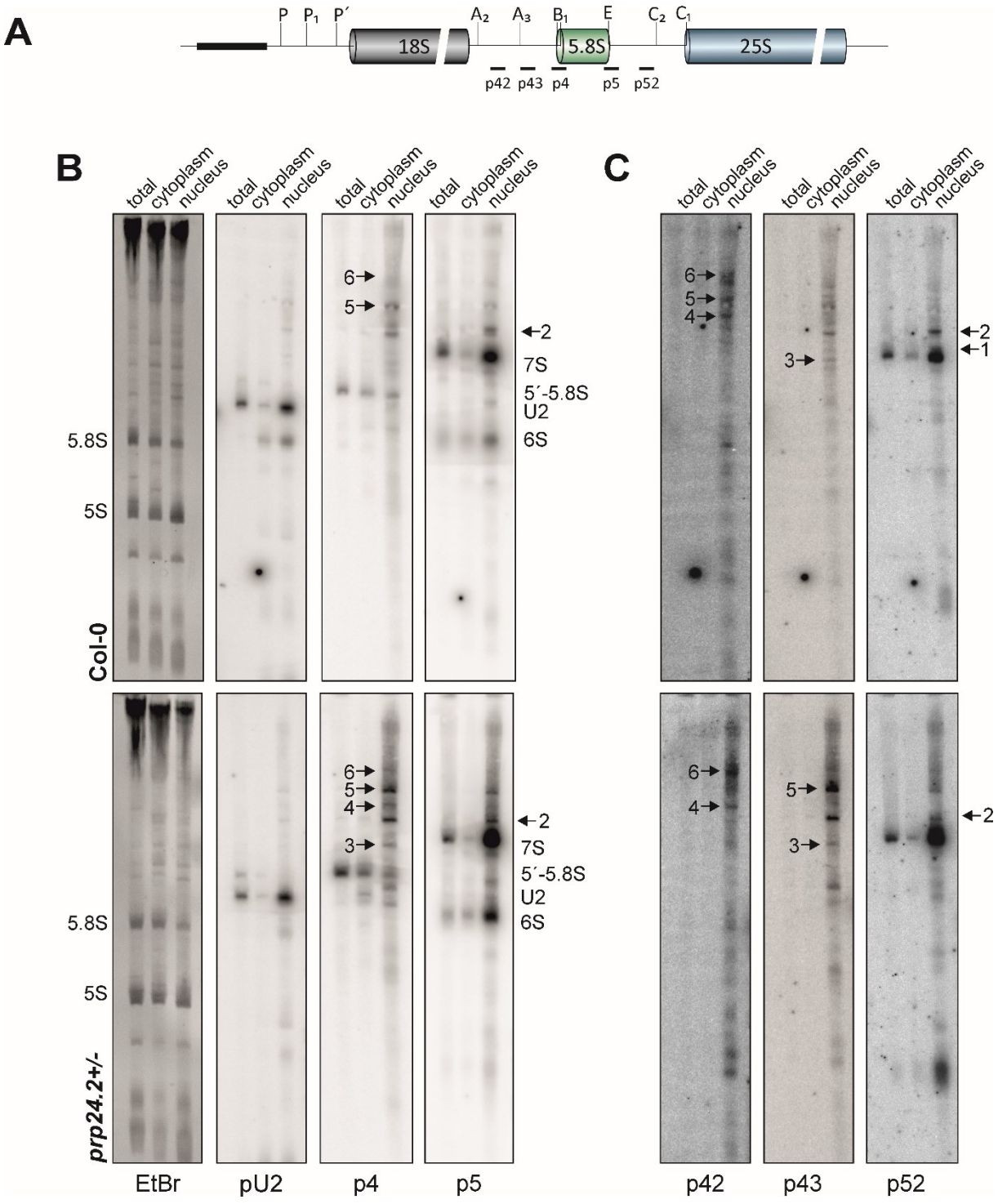

Figure 18. Analysis of 5.8S precursors in *prp24.2* and wild type.
A) The pre-rRNA scheme with binding sites for probes p4, p42, p43, p4, p5 and p52. **B)** and **C)** Membranes from Figure 17A of Col-0 and *prp24.2*+/- were further used for probing with additional probes binding upstream of the 5´-end of 5.8S (p42, p43 and p4) and downstream of the 3´-end of 5.8S (p5 and p52). Novel precursors were labeled with numbers.

5.4.2 Circular RT reveals the 3´ and 5´ extremities of the large 5.8S precursors

The 5.8S precursors in *A. thaliana* display high degree of heterogeneity. One simple method to investigate the extremities of RNAs is the circular RT-PCR in combination with Sanger sequencing (Palm et al., 2019; Shanmugam et al., 2021). To further understand 5.8S processing in general and to analyze if 5.8S processing is indeed affected in the *prp24.2* mutant, both wild type and *prp24.2* were used for the following experiment for better comparison. To determine the precise extremities of longer sized pre-5.8S precursors, cRT-PCR was performed on circularized total RNA of wild type and *prp24.2* mutant. The forward oligonucleotide (F1) chosen for cRT-PCR is binding 63 nt upstream of the 3´-end of 5.8S, the first reverse oligonucleotide (R1) is binding 16 nt downstream of 5´-end of 5.8S and the second reverse oligonucleotide (R2) is binding 19 nt downstream of the A_3 cleavage site (Figure 19A). With F1 and R1, one dominant PCR product of 160 bp (A1/WA1) in the nuclear fraction was selected for cloning (Figure 19B). For the oligo pair F1 and R2, five PCR products (B1-B5/WB1-WB5) in the nuclear fraction were selected for cloning into the pGEM-T vector. Sequencing revealed that the PCR product B5 is most likely a A_2-C_2 precursor and with that the largest precursor which solely carries 5.8S rRNA. It has a size of ~531 nt and was three-times more often observed in *prp24.2* (Figure 19C). The corresponding pre-rRNA is precursor #6 (Figure 18B,C; Figure 19D). The product B4/WB4 (Figure 18B) was sequenced as a A_2-C_2´, which is ~20 nt shorter than A_2-C_2 and ~502 nt long. This precursor is very faint and likely corresponds to precursor #5 (Figure 18B, C; Figure 19D). The products of B3/WB3 are heterogenous and includes precursors like A_2-5.8S-3´ (~454 nt), A_3´-C_2 (~428 nt) and A_2-5.8S (~412 nt) (Figure 19C). In *prp24.2* most of the sequenced products revealed the A_3´-C_2 precursor, while for wild type mostly the A_2-5.8S precursor was sequenced. The A_2-5.8S-3´ precursor was sequenced in both strains in very low number (Figure 19C). In combination of the sequenced products and the precursor detected with the different probes, mostly likely B3/WB3 corresponds to precursor #4 (Figure 18B,C; Figure 19D). For the products B2/WB2, a pre-rRNA with a large extension upstream of A_3 was observed for wild type and was named A_3´-5.8S (~389 nt) and a second dominant precursor from A_3 to C_2 (A_3-C_2) with a size of ~361 nt was observed in both *prp24.2* and wild type (Figure 19C). The latter precursor could correspond to precursor #2 (Figure 18B, C; Figure 19D). For B1/WB1 a precursor named A_3-5.8S-3´ (~269 nt) was observed and found exclusively in *prp24.2* (Figure 19C) and corresponds to precursor #3 (Figure 18B, C; Figure 19D). Finally, the 5´-5.8S pre-rRNA was sequenced and revealed a precursor that in the 5´-direction is extended by ~65 nt with a total size of 229 nt (Figure 18B; Figure 19C, D).

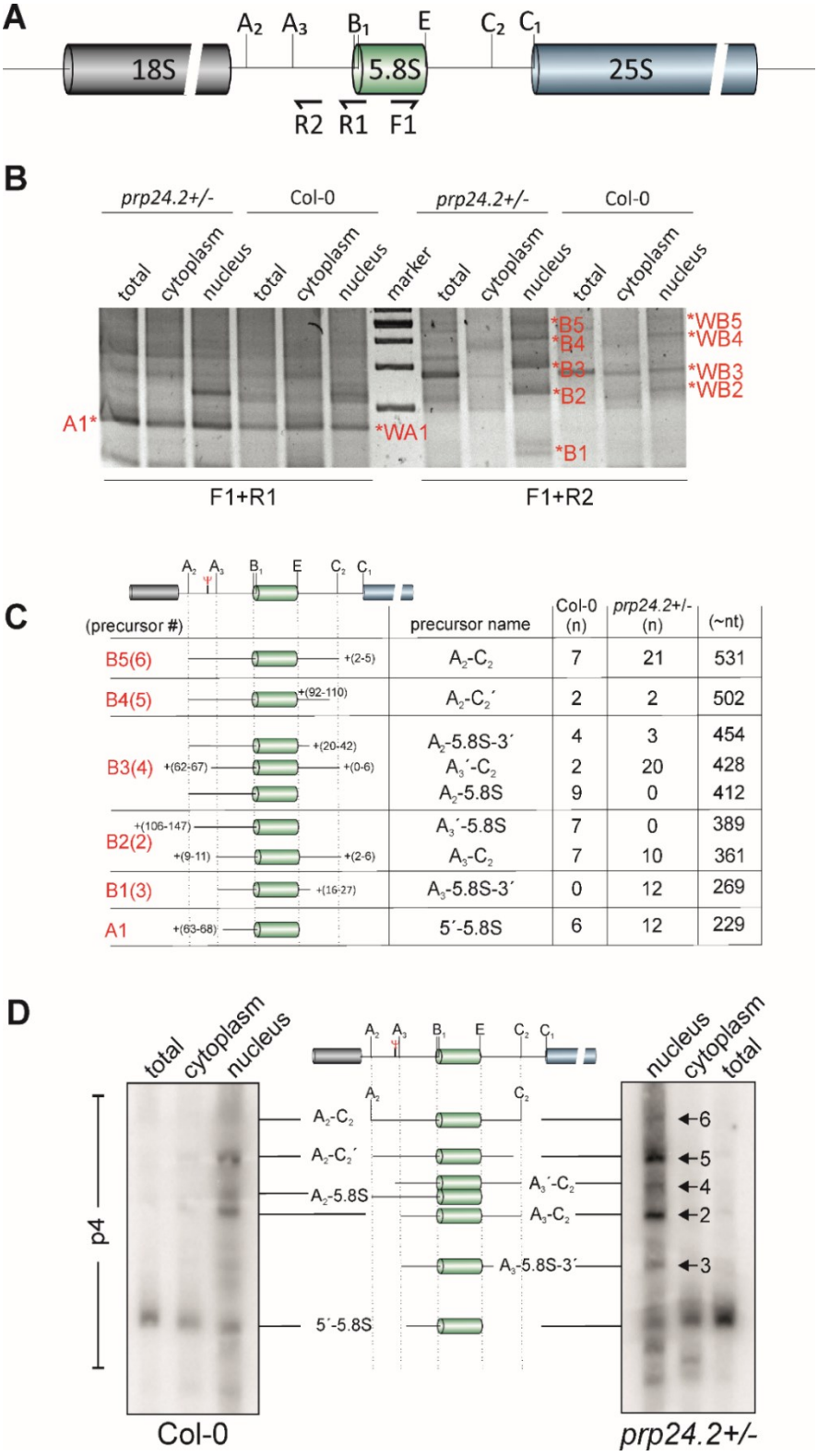

Figure 19. Circular-RT of 5.8S precursors in Col-0 and *prp24.2.*
A) schematic illustration of pre-rRNA with binding sites for cRT-PCR oligonucleotides. **B)** RT-PCR products of F1+R1 and F1+R2. PCR products with red labeling were analyzed with sequencing. **C)** Compilation of precursors found with sequencing of respective PCR products. The number of found precursors in Col-0 and *prp24+/-* are listed. Also, approximate size is given and a small scheme of the precursors. **D)** Membrane of Figure 17A probed with p4 was used for illustration of the found precursors.

In order to understand the processing of 5.8S pre-rRNAs, the double mutant *xrn2 xrn3* was used. In particular, this mutant shows several precursors of 5.8S rRNA that are extended in the 5´ region (Zakrzewska-Placzek et al., 2010; Figure 20). When this mutant was used for subcellular fractionation, it becomes obvious that most of the precursors are dominantly located in the nucleus and more interestingly, the 5´-5.8S pre-rRNA is only faintly detectable in the cytoplasm of the double mutant in comparison to Col-0. However, the 3´-extended 5.8S pre-rRNA 6S is still exported to the cytoplasm (Figure 20).

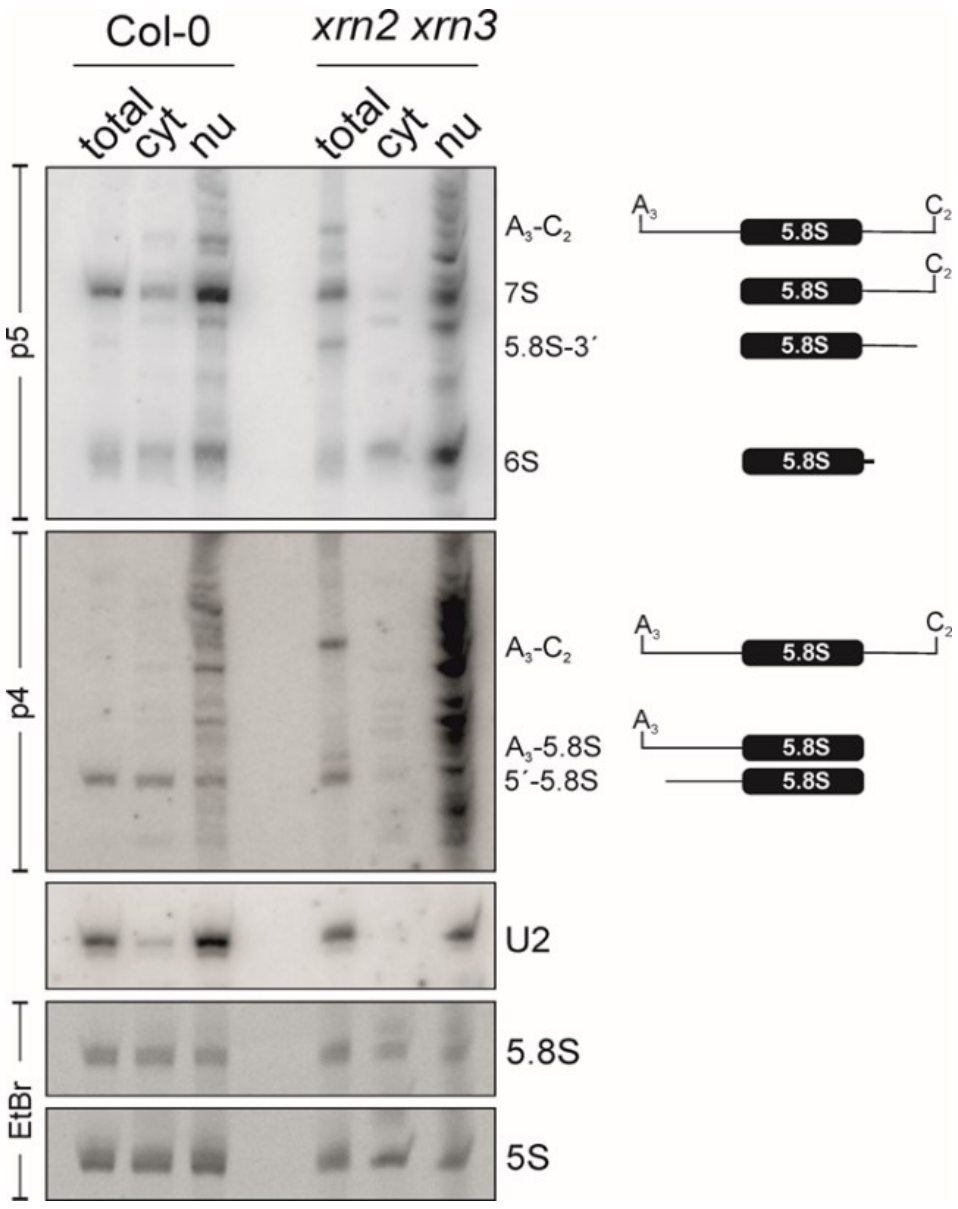

Figure 20. Subcellular fractionation of wild type and *xrn2 xrn3.*
Fractionation was performed with 14-day old seedlings as described in chapter 4.2.2. RNA of each fraction and total cells were loaded on a 16% polyacrylamide gel prior to northern blotting. Probes used here are listed in Table 1 and Table 3. The seeds of *xrn2 xrn3* were kindly provided by Joanna Kufel with permission form Allison Mallory.

5.4.3 The 5´-5.8S pre-rRNA is accumulating in polysomes of *prp24.2*

The next question aimed to understand, if the accumulation of the 5´-5.8S pre-rRNAs that is occurring in the cytoplasm are indeed associated to translating 80S ribosomes. The gradient fractionation was performed as described in section 4.1.6 and is based on a mixture of three protocols (Hsu et al., 2014; Weis et al., 2014; Firmino et al., 2020).

For sucrose density fractionation, 10 days old plants of Col-0 and *prp24.2* were lysed and poured onto a continuous 15 - 60% sucrose gradient before ultracentrifugation. The absorption profile was measured at 254 nm (Figure 21A). When profiles of both Col-0 and *prp24.2* are compared, no distinct differences are discernible. Nonetheless, minor differences in polysomal fractions of *prp24.2* were observed with slight increase in polysomal peaks (Figure 21A). RNA and proteins of the fractions were used for northern and western blotting (Figure 21B). The EtBr-stained polyacrylamide gel and agarose gel shows the position of mature 25S, 18S, 5.8S and 5S rRNA. Probing with p4 showed that 5´-5.8S is accumulating in 60S subunits but more distinctly in monosomes and actively translating ribosomes (polysomes) (Figure 21B, C). Interestingly, while 5´-5.8S is highly present in polysomes of *prp24.2*, the pre-rRNAs 7S and 6S are only moderately present in polysomes of *prp24.2* and Col-0 (Figure 21B).

For quantification of 5´-5.8S pre-rRNA levels in *prp24.2* and Col-0, intensities of 5´-5.8S signals were normalized to 5.8S rRNA levels in *prp24.2* and Col-0 individually. By that the high abundance of 5´-5.8S pre-rRNA in *prp24.2* stands out again and, in some fractions, even a two-fold increase can be recorded (Figure 21C).

Upon probing with α-AtRPL10, α-AtRPS10 and α-AtRPS3-2, the small subunits proteins AtRPS10 and AtRPS3-2 were detected in same levels in Col-0 and *prp24.2*, while for the LSU protein AtRPL10, slight differences are observed. It seems that especially in polysomal fractions and in 60S subunits AtRPL10 is to a lesser extent present in *prp24.2* than in comparison to Col-0 (Figure 21B). However, AtRPL10 is binding on the ribosome surface and has no direct contact with 5.8S rRNA, therefore it remains elusive why *prp24.2* displays lower levels of AtRPL10 in the 60S subunits but also in mature ribosomes.

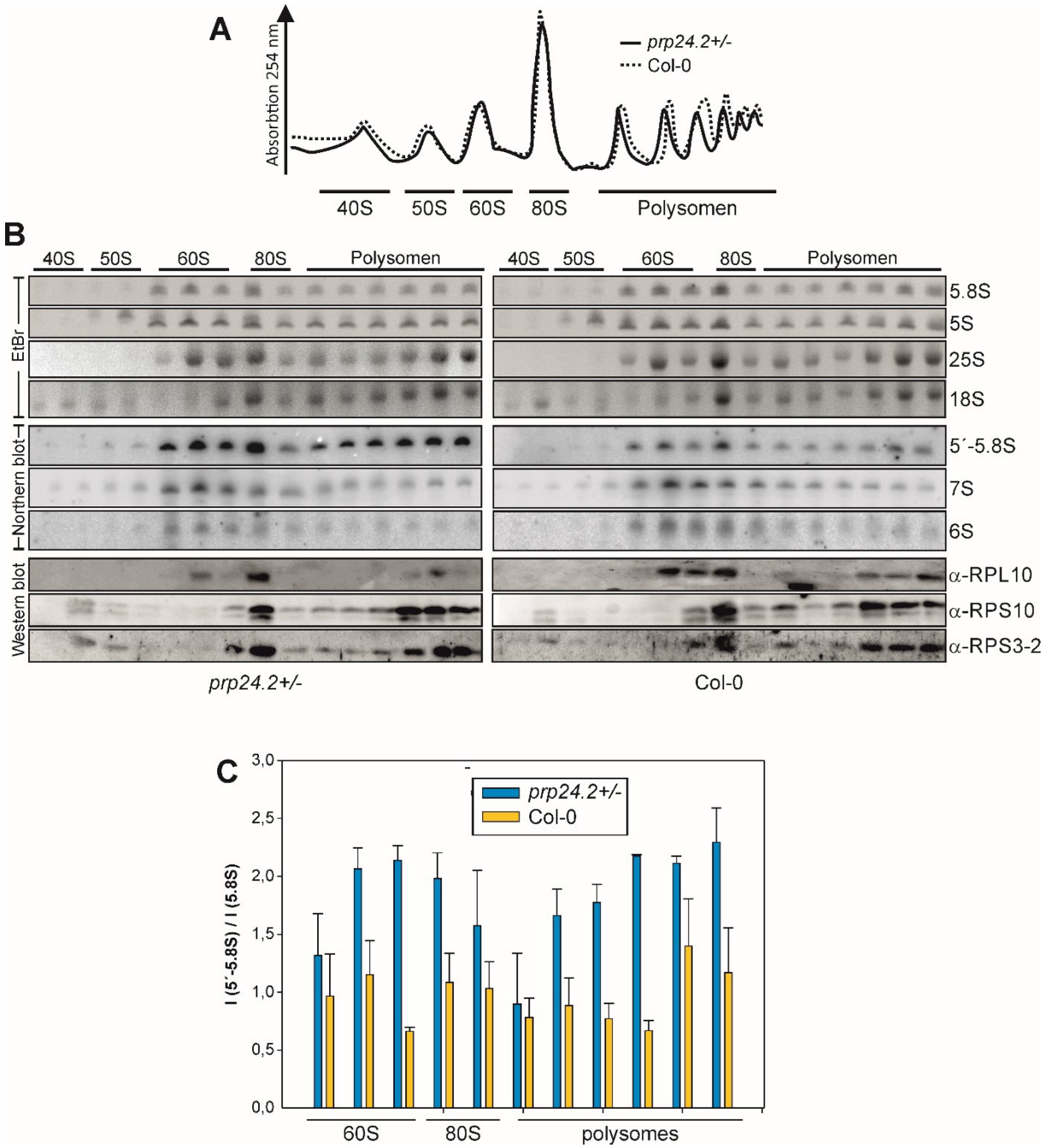

Figure 21. The 5´-5.8S pre-rRNA accumulates in monosomes and polysomes of *prp24.2*.
A) Lysates with an OD_{595} of 0.4 from 10 days old plants of Col-0 and *prp24.2* were loaded onto a continuous sucrose gradient and ultracentrifuged. The Absorption was measured at 254 nm and given as a profile. Subunits, monosomes (80S) and polysomes are indicated below the peaks. Col-0 is shown as line and *prp24.2* as dashed line. **B)** The fractions containing 40S, 60S, 80S and polysomes were used for RNA isolation using phenol-chloroform-isoamyl alcohol extractions and proteins were precipitated using methanol-chloroform. RNA was further used for northern blotting and proteins were subjected for western blotting. Polyacrylamide gel and agarose gel was stained with Ethidium bromide (EtBr) for visualization of mature rRNAs. Northern blot was hybridized with probes indicated on the right site and western blots incubated with antibodies indicated on the right site. **C)** Quantifications of the signal intensity of 5´-5.8S pre-rRNA normalized to 5.8S signal. Standard deviation was calculated based on two biological replicates.

In order to further test this hypothesis, western blotting of proteins from cytosolic and nuclear fractions of *prp24.2* and wild type was performed. The antibody for AtENP1 is used as marker for the nuclear fraction and AtNOB1 as a cytosolic marker. However, AtENP1 seems to be present also in the cytosolic fraction (Figure 22). The AtRPL10 antibody is raised to detect AtRPL10A and AtRPL10B. AtRPL10 was detected dominantly in the cytoplasmic fraction to almost same extent in *prp24.2* and wild type (Figure 22). In addition, the nuclear localization of AtRPL10 in Arabidopsis was often observed (Pendle et al., 2005; Palm et al., 2015). The discrepancies between AtRPL10 levels in *prp24.2* polysomes/monosomes and total protein extracts might be reasoned with limited amount of 5´extended 5.8S Ribosomes and thus changes in AtRPL10 levels are rarely detectable.

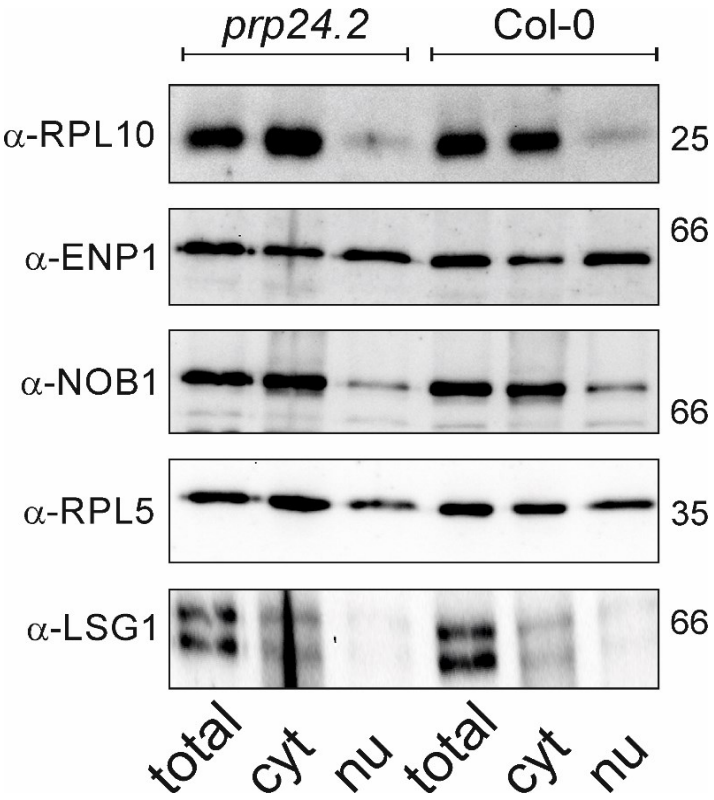

Figure 22. Western blotting of subcellular fractions of cytosolic and nuclear fraction.
Subcellular fractionation was performed as described in chapter 4.2.2. with 14-day old seedlings. Proteins were extracted from each fraction and total cells and 30 µg of extract was loaded onto 10% SDS gels for western blotting. Antibodies are indicated on the left side and protein marker size is indicated on the right site.

5.4.4 The *prp24.2* plants are less sensitive to cycloheximide

Defects in ribosome biogenesis are often connected to pronounced sensitivity against different antibiotics (Zhu et al., 2016). In here, the effect of cycloheximide were tested for their sensitivity on wild type and *prp24.2* seed germination (Figure 23). Cycloheximide is known as a translation elongation (translocation) inhibitor with a suggested binding site at the E-site of the 60S subunit (Schneider-Poetsch et al., 2010). As 5.8S rRNA is believed to be important for translocation (Elela and Nazar, 1997), the higher degree of polysomes with an extended 5.8S rRNA could influence the sensitivity of the mutant to cycloheximide. Different concentrations of CHX in the medium were tested. When MS medium was supplemented with 1µg/ml CHX, roots of *prp24.2* extended significantly in average almost 2-fold more than those of Col-0 (Figure 23). With 2µg/ml CHX, roots of *prp24.2* extended in average 0.5 mm shorter than with treatment of 1µg/ml CHX, the roots of Col-0 extended in average in the same way as under 1µg/ml CHX. With 3 µg/ml CHX the extension of roots of *prp24.2* is almost on the same level as Col-0, with an average size of about 0.3 mm (Figure 23). In conclusion, it can be hypothesized that the extension of 5.8S in polysomes might have a structural effect of the 60S subunit, by which CHX cannot bind any more efficiently on its site of action.

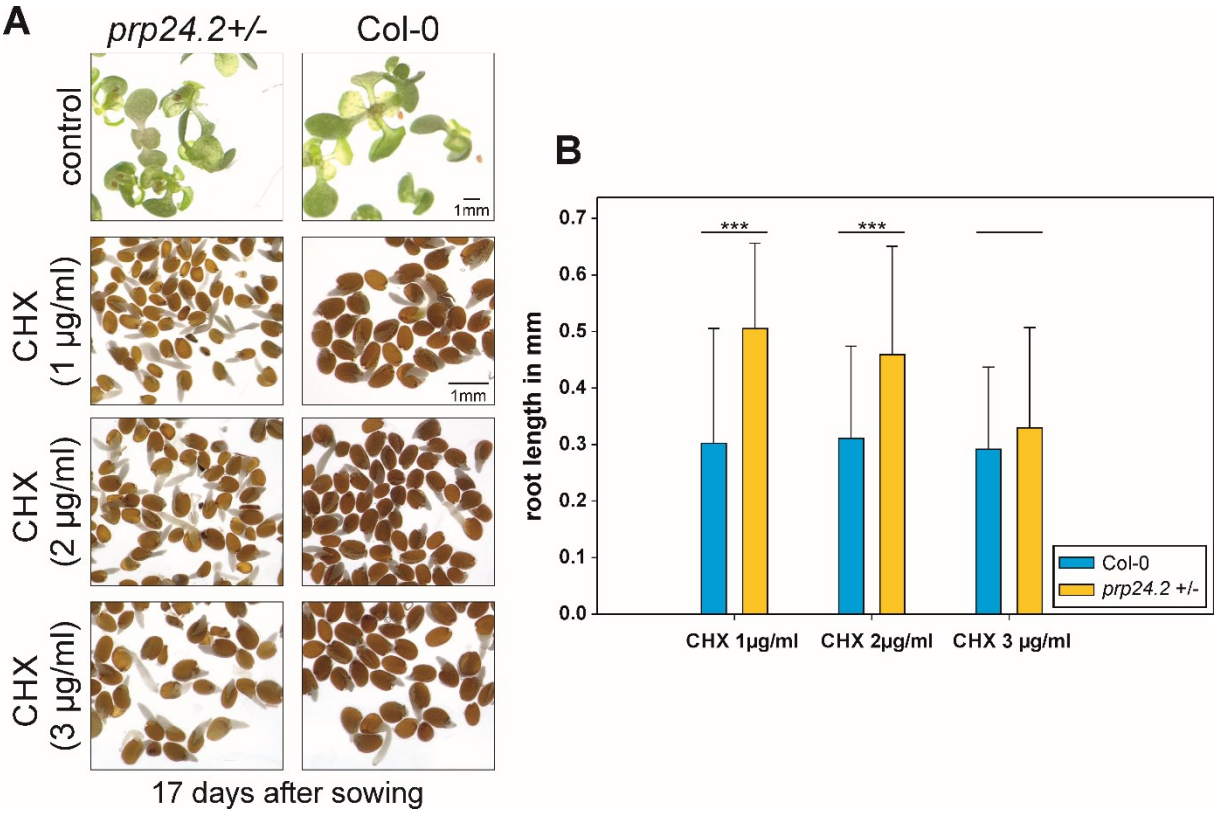

Figure 23. Analysis of cycloheximide sensitivity in seeds.
A) Seeds of Col-0 and *prp24.2+/-* were sown on ½ MS plates supplemented with either 1, 2 or 3 µg/µl cycloheximide (CHX). Plates were kept for 17 days in growth chambers under short-day conditions. After 17 days photographs were made with a stereo microscope. **B)** Root lengths are given in mm. Error bars were calculated from 47-76 roots lengths that were measured. Two-Way ANOVA was performed on genotype (*prp24*, WT) and treatment (CHX 1µg/ml; CHX 2µg/ml; CHX 3µg/ml) as variables and all pairwise multiple comparison procedure was performed using Holm-Sidak method to create adjusted p-values (*…<0.05;**…<0.01; ***…<0.001).

5.4.5 The production of 5.8S precursors is strictly regulated

For a better understanding of the role of the different 5.8S precursors and their processing, different stress treatments on Col-0 and *prp24.2* plants were performed. Since, Arabidopsis has all kinds of 3´- and 5´-extended precursors and moreover also with extensions in both 5´ and 3´ directions, the next experiment aimed to analyze if environmental stress conditions like heat and cold could influence specific precursors. Different conditions were tested beforehand for best treatment; thus, plants were selected to be treated for 1 h at 38°C and at 4°C for 24 hrs and sub-fractionated upon harvesting. The northern membranes were hybridized with p4, p5 and pU2 to ensure purity of the cytoplasmic fraction (Figure 24A). Under control growth conditions, the accumulation of 5´-5.8S is observable in total cells, cytoplasmic and nuclear fractions of *prp24.2* in comparison to Col-0. However, the same holds true under heat stress at 38°C for 1 h and under cold stress at 4°C. Noticeably, the accumulation is also observable in the nuclear fraction (Figure 24B). Mostly, the differences are dominant in the nuclear fractions. While Col-0 shows lower degree of the newly identified precursors A_3-5.8S-3´, A_3-C_2, A_3´-C_2, A_2-C_2´ and A_2-C_2 the *prp24.2* mutant is almost at control levels (Figure 24A).

However, 5´-5.8S pre-rRNA is more abundant under heat-stress in the mutant (Figure 24B), while under cold stress the opposite is happening. Under cold stress growth conditions, all newly identified precursors and mostly of the A_2-C_2 pre-rRNA is increased in Col-0, while only 5´-5.8S pre-rRNA is reduced in comparison to control conditions (Figure 24A, B). Just as in Col-0, *prp24.2* has also increased levels of the precursors in comparison to WT under control conditions, where also the A_2-C_2 pre-rRNA is highly abundant (Figure 24A, B).

In contrast, when membranes were hybridized with p5, a clear reduction of the 3´-extended precursors 6S, 5.8S+70 and 7S pre-rRNA is observed under heat stress conditions (Figure 24A, C). While Col-0 seems to be affected most, the 3´-extended precursors of 5.8S are to a lesser extent affected in *prp24.2* than Col-0 (Figure 24C). In contrast, when plants were treated with cold an accumulation for 5.8S+70 is observed, while 6S and 7S pre-rRNAs seem not to be affected as expected (Figure 24A, C).

In conclusion, the processing of the 5.8S precursors seems to be highly regulated upon changing environmental conditions. While higher temperature reduces the levels of precursors, lower temperature seems to have the contrary effect and enhanced level of precursors is observed. In conclusion, *prp24.2* seems not to be as affected as Col-0 under heat stress growth conditions and maintains 5.8S pre-rRNAs levels as almost under control conditions (Figure 24A, B, C).

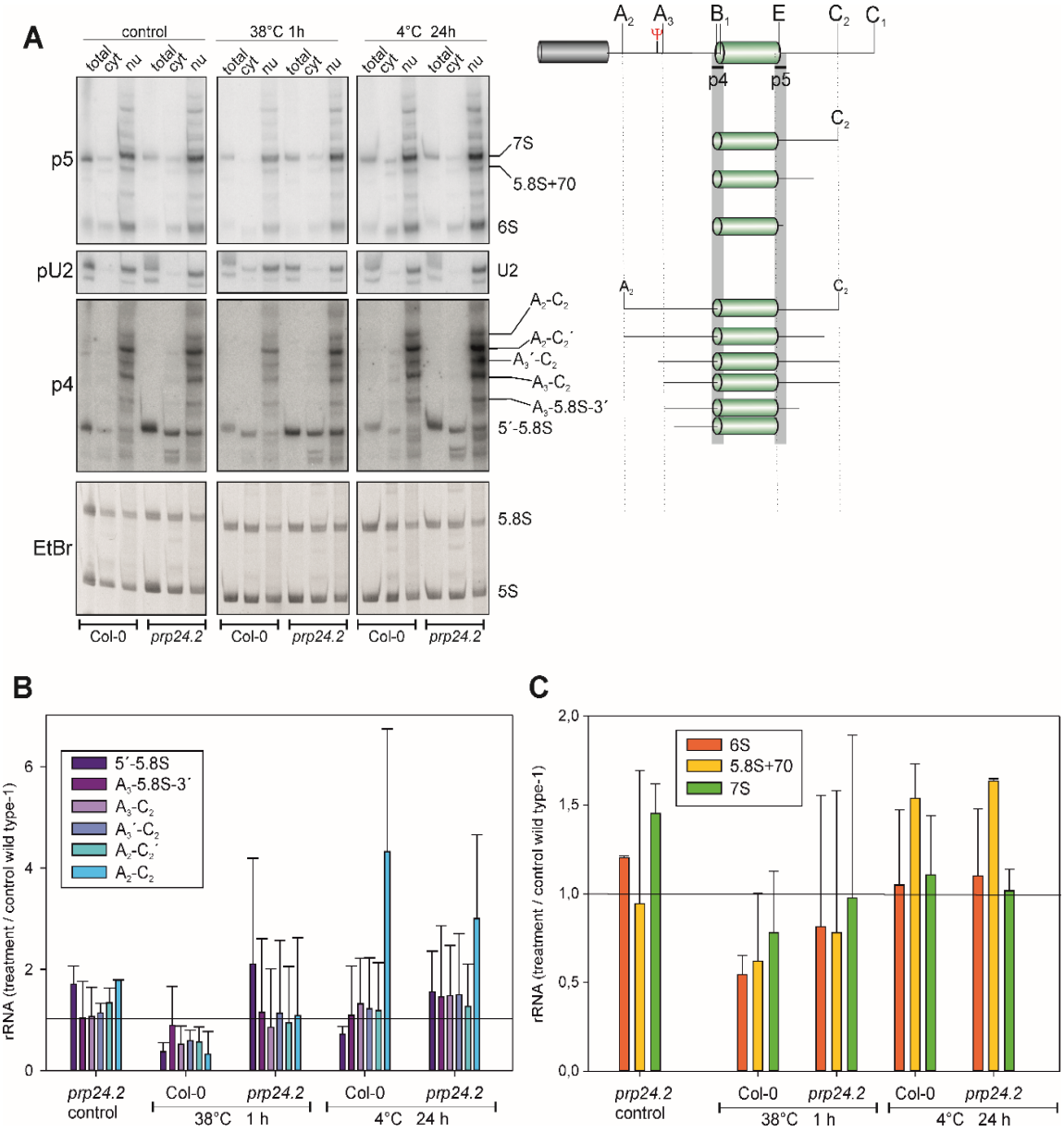

Figure 24. Analysis of 5.8S precursors upon stress in Col-0 and *prp24.2*.
A) 14-day old plants on ½ MS plates were treated for 1 h at 38°C or for 24 hrs at 4°C or kept untreated as controls. Subsequently after treatments plants were harvested, frozen un liquid nitrogen and fractionated. RNA was extracted from cytoplasmic and nuclear fraction and as a control from total cells. RNA was used for northern blotting using a 16 % polyacrylamide gel. Membrane was hybridized with pU2, p4 and p5. Quantifications of precursors found within nuclear fractions with probes p4 **(B)** and p5 **(C)** were normalized to U2 snRNA and Col-0 precursors under control conditions (Baseline at 1). Error bars are calculated based on two biological replicates.

6 Discussion

6.1 *A. thaliana* snoRNAs are showing high divergence in subcellular localization

Identification and characterization of snoRNAs is continually expanding due to their ubiquitous role in rRNA processing and thereby their implication in associated disease conditions. In plants, discovery of novel snoRNAs is focused mostly on the usage of genome sequences of certain model plant species and by that relying on homology-based computational predictions that must be validated by other experiments. Moreover, the cellular distribution of snoRNAs has not been adequately characterized. The in here performed analysis of *A. thaliana* cell suspension culture revealed the occurrence of 176 C/D box and 66 H/ACA box snoRNAs. 197 snoRNAs were previously described and deposited in databases, while 45 putative snoRNAs have been found in addition, including 24 C/D and 21 H/ACA box snoRNAs (Figure 9A). These new snoRNAs are located on not yet annotated chromosomal positions (Figure 9A). Moreover, for several snoRNAs multiple members of the family were detected, e.g., for U3 (Figure 10).

Plants contain versatile numbers of RBFs and RPs in comparison to other species (Ebersberger et al., 2014; Simm et al., 2015). Thus, it is reasonable to speculate that different snoRNPs are formed either during development of the plant or in a tissue specific manner. Hence, the different members of a snoRNA family might lead to distinct snoRNPs with different activity but comparable function.

Further, the nucleolar specific localization of snoRNAs has long been refuted e.g. based on snoRNAs trafficking between nucleus and cytoplasm upon oxidative stress in yeast (Holley et al., 2015; Li et al., 2017). This holds true for plant snoRNAs as well as SNORD72 and snoR106 are present in the cytoplasm as judged from northern hybridization (Figure 11J). However, the concentration is either low or the cytoplasm was contaminated with nuclear fraction, because FISH analyses yielded an exclusive nuclear signal of SNORD72 (Figure 11F).

In opposite, the 340 nt version of snoR106 stays within the nucleus, while the two smaller fragments (160 nt; Marker et al., 2002) are exported to the cytoplasm. Similarly, a long (260 nt) and short (170 nt) version of the H/ACA box snoRNA snoR100 exists (Marker et al., 2002), and the smaller fragment with 170 nt was detected in the cytoplasm (Figure 11L).

All analyzed C/D box snoRNAs U24-2, U33a, U27-1, SNORD72, snoR106, U49-1 and the U3-like snoRNAs have a size between 70 – 300 nt (Figure 10; Figure 11) as described for other known snoRNAs (Liang et al., 2019; Chen and Wu, 2009). Although, large size snoRNAs are an exception, the size of the U3-like snoRNAs from *A. thaliana* (ranging between 150 and 300

nt) is comparable to the U3 snoRNA of yeast (Egecioglu et al., 2006). In case of snoR135, FISH signal yielded a localization in cytoplasm and nucleus, however, a probe binding to snoR135 did not detect the RNA with northern hybridization in general. This might indicate that this snoRNA is low abundant although, a higher number of NGS reads were obtained in cytoplasm of RNA-seq analysis (Table S1) and a limited detection sensitivity makes it impossible to experimentally verify this snoRNA with northern hybridization. Furthermore, snoR135 is an orphan snoRNA with no known guiding site (Table S1). The H/ACA snoRNAs snoR100, snoR160 and snR77 ranges between 150 - 300 nt (Figure 11, Figure 12) and are thus comparable with H/ACA snoRNAs known from human (Marz et al., 2011).

Worth mentioning smaller fragments of snoRNAs could represent small RNA derived from snoRNAs (sdRNAs) that are known in yeast to regulate translation activity e.g., during heat shock (Mleczko et al., 2019). However, the smaller fragments in here were already observed under control conditions, indicating a different role for these sdRNAs in Arabidopsis. In future, such cytoplasmic snoRNAs and sdRNAs needs to be elucidated in detail.

The analysis of the snoRNA distribution in different tissues in the plant under control conditions depicts their functional divergence by which certain snoRNAs are used in a tissue specific manner. This experiment displayed that snoR160 is very low abundant in the shoot and highly abundant in the root of *A. thaliana* (Figure 12B, C). This might indicate that snoR160 is replaced in shoot cells by another snoRNA, because snoR160 is guiding the conversion of uridine to pseudouridine at U2855 (Sun et al., 2019; Table S2), which is a functionally crucial site of the PTC in the 60S subunit of *A. thaliana* (Figure 30). Moreover, the larger form of U24-2 is almost absent in shoot and flowers, whereas its smaller form is highly abundant in flowers (Figure 12B, C). The C/D box snoRNA U24-2 is known to guide 2´-O-methylation at three sites; Cm1439, Am1451 and Gm1452 (Brown et al., 2001; Azevedo-Favory et al., 2020), all three sites are in a region which is highly decorated with modifications and is therefore of significance (Figure 29).

For some of the newly identified snoRNAs, a complementary sequence on the rRNA was predicted (Figure 25). By this means it can be suggested that SNORD24 is guiding the ribosome methylation at position C1439 on the 25S rRNA (Figure 29), SNORD 33 ribosome methylation at position G3280 on the 25S rRNA (Figure 30) and SNORD72 the 2´-O-methylation at G1219 in the 18S rRNA (Table S3). The latter site is not yet experimentally determined (Table S3), which might indicate that the modification is regulated either by environmental cues or in a tissue specific manner. Thus, one can assume from distribution and localization experiments, that SNORD72 is more abundant in reproductive tissues like flowers (Figure 12). Further, the two U3-like snoRNAs U3.3 and U3.5 are targeting the same region in the 18S rRNA and guiding the 2´-O-methylation of A1087 and additionally U3.5 is also guiding

modification at G995 (Figure 25). Recently, the site U2855 in the 25S rRNA was found to be pseudouridylated (Sun et al., 2019) mediated by snoR160 (Figure 30).

Unfortunately, for snR77 another H/ACA snoRNA, the site of modification could not be identified. Hence, snR77 might be rather involved in guiding the modifications of other molecules like snRNAs (Figure 25).

Moreover, some snoRNAs accumulate in Cajal bodies (scaRNAs; Deryusheva and Gall, 2019) and are assumed to guide modifications of spliceosomal RNAs (Cao et al., 2018) or even of tRNAs (Nostramo and Hopper, 2019). Thus, it cannot be ruled out that some of the newly identified snoRNAs belong to this family.

Figure 25. Illustration of the complementary sites of newly discovered snoRNAs.
Depicted are the sequences of newly discovered snoRNAs and the binding sites on the 18S or 25S rRNA. The modification site is highlighted on the rRNA in bold and underlined. Blue and green letters indicate C and D boxes, respectively. ACA box is highlighted in magenta and yellow indicates putative duplex structures. Adapted from Streit et al. (2020).

6.2 The Arabidopsis modification landscape of the 5.8S and 25S rRNA

The number of modifications of rRNA is as extensive as the number of snoRNAs in Arabidopsis. Thus, it is very supportive to illustrate all modification sites in a secondary structure map, including the important and functional regions and next to it connecting all sites to the corresponding snoRNAs required for each modified site, summarized in the following chapter.

6.2.1 The modification sites of 5.8S

The 5.8S rRNA is part of the polycistronic unit that is transcribed as initiator of ribosome biogenesis. The secondary structure shows the proximity of 5.8S rRNA to 25S rRNA although through evolution, the 5.8S rRNA diverged to an independent rRNA and is not anymore part of the larger 25S rRNA (Nazar, 1980).

The 5.8S rRNA is characterized by 10 helices and two expansion segments (ES3 and ES4), that display additional rRNA parts that are missing in bacteria. Helices 2, 3, 4 and 10 (H2, 3, 4 and 10) are base pairing with the 25S rRNA (Figure 26). It possesses four modified sites, including two 2´-O-ribose methylation (Barneche et al., 2001; Brown et al., 2001; Qu et al., 2001) and two pseudouridylation sites (Sun et al., 2019) that are experimentally confirmed. The two pseudouridylation sites Ψ22 (between H2 and H3) and Ψ78 (H7) could not be assigned to a known snoRNA. A similar Ψ-site alike Ψ78 is also present in yeast at position Ψ73. In yeast, snR43 is responsible for guiding this modification (Piekna-Przybylska et al., 2007), whereas the counterpart could not be found in Arabidopsis.

In contrast, the two 2´-O-me sites Am47 (H5) and Gm79 (H7) are guided by snoR9-1/2 and 39BYa/b, respectively. Interestingly, H5-7 are surrounded by L24, L29, L37e and L39e (Armache et al., 2010a). One additional site, close to the 3´end of 5.8S at H10 in expansion segment 4 (ES4) at position Gm155 is predicted to be guided by snoR4a (Brown et al., 2001). However, radiographic labeling of wheat-embryo could not confirm the presence of this modification (Lau et al., 1974).

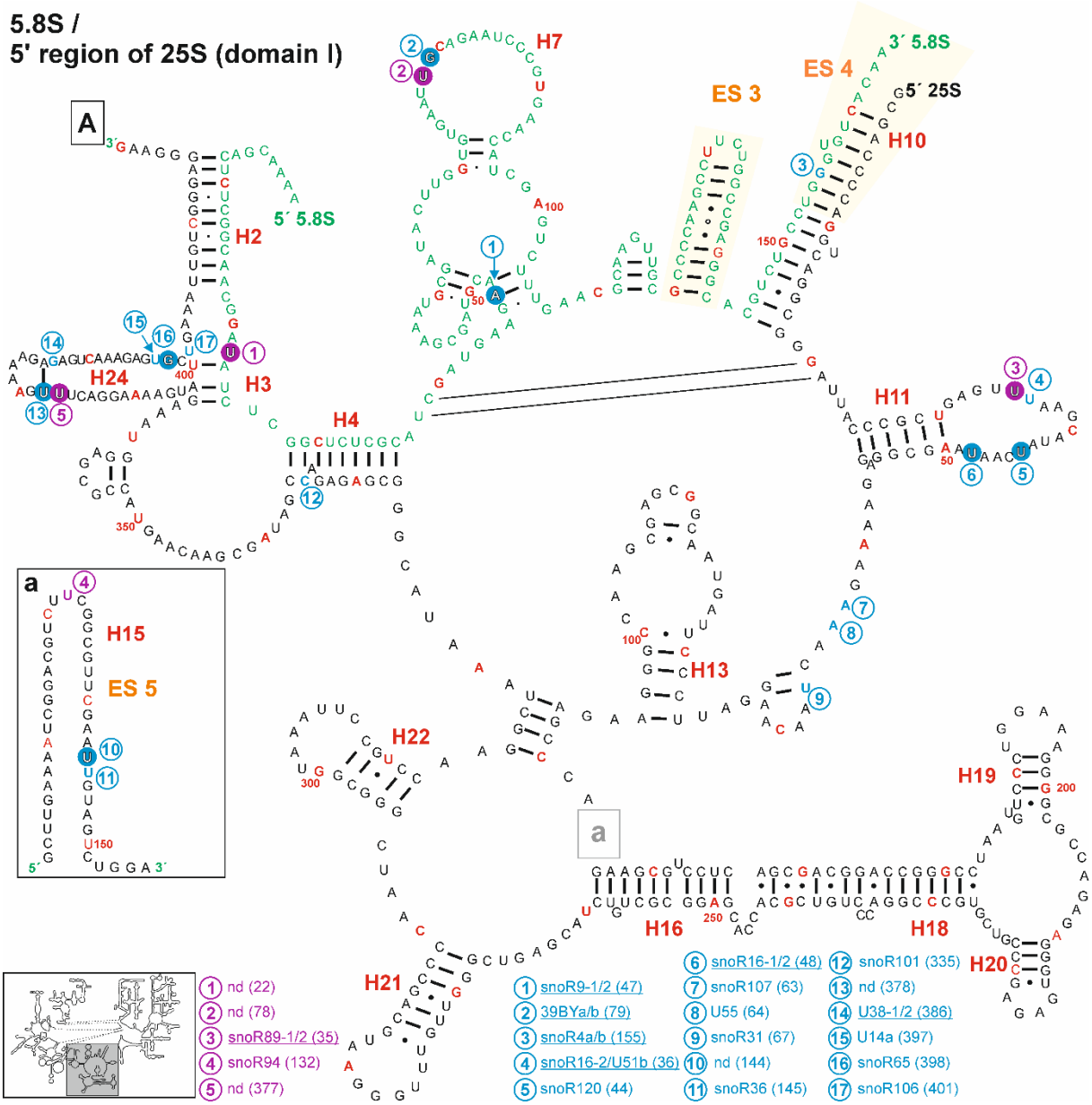

Figure 26. Secondary structure model of 5.8S and domain I of 25S rRNA of Arabidopsis.
The structure was created based on the RNAcentral database (The RNAcentral Consortium, 2019) and http://rna.icmb.utexas.edu. The 2´-O-methylation sites for predicted (blue letters) and verified positions (blue circle with white letters) and pseudouridylation sites for predicted (violet letters) and verified positions (violet circles with white letters) are shown. Next to modified positions, numbers in blue circles (C/D box) or violet circles (H/ACA box) indicate the snoRNA guiding the modification. Guiding snoRNAs were found using the snoRNA database snOPY (Yoshihama et al., 2013). If several snoRNAs are annotated to guide the modification, the name is underlined. Predicted and verified sites were obtained from Barneche et al. (2001), Brown et al. (2001), Qu et al. (20001), Sun et al. (2019) and Azevedo-Favory et al. (2020). Every tenth nucleotide is marked in red and every 50th nucleotide is labeled with the according number. Helices are labeled in red and the number (H1 etc.) A small illustration of the complete 60S rRNA in the lower left half is showing the position (grey) of the illustrated region. Adapted from Streit and Schleiff (2021).

6.2.2 The modifications of the 25S rRNA

The modifications of the 25S rRNA are numerous and due to the challenging secondary structure, the structure was dissected (Figure 26-30). The domains are characterized as

follows: domain I from bp 1-660 (Figure 26, 27), domain II from bp 660-1440 (Figure 28), domain III from bp 1440-1870 (Figure 27), domain IV from bp 1870-2370 (Figure 29) and domains V/VI from bp 2370-3375 (Figure 30; Paci and Fox, 2015).

Domain I contains 14 2´-O-me sites, from which five (Um44, Um48, Um144, Um378 and Gm398) have been mapped successively and nine are only predicted (Figure 26). For two sites (Um144 and Um378) the guiding snoRNA is unknown (Table S2, Figure 26). Overall, the verified methylations are concentrated in helix 11, 15 and 24. In contrast, two verified Ψ-sites are confirmed at H11 and H24 and one is predicted at H15 (Figure 26). The 3´ region of domain I of the 25S rRNA contains a recently mapped 2´-O-me site at Am660 (Azevedo-Favory et al., 2020), guided by U18-1/2. This region also contains the ES7, the largest expansion segment, localized on the ribosome surface (Ramos et al., 2016).

Domain III is characterized by the three expansion segments, ES19, ES26 and ES24 and helices 47-60 (H47- H60) (Figure 27). Especially H47/H50 and H59a/H60 are carrying many modifications (Figure 27). In yeast, it is believed that Nop4 is binding to H47, H32, H26, H33 and H60 and by that bringing domain II and III in close proximity (Granneman et al., 2011). Summing up, domain III contains 14 2´-O-me sites, from which nine were experimentally mapped and five predicted. Recently, two new Ψ-sites at positions Ψ1465 and Ψ1473 were mapped (Figure 27,Table S2).

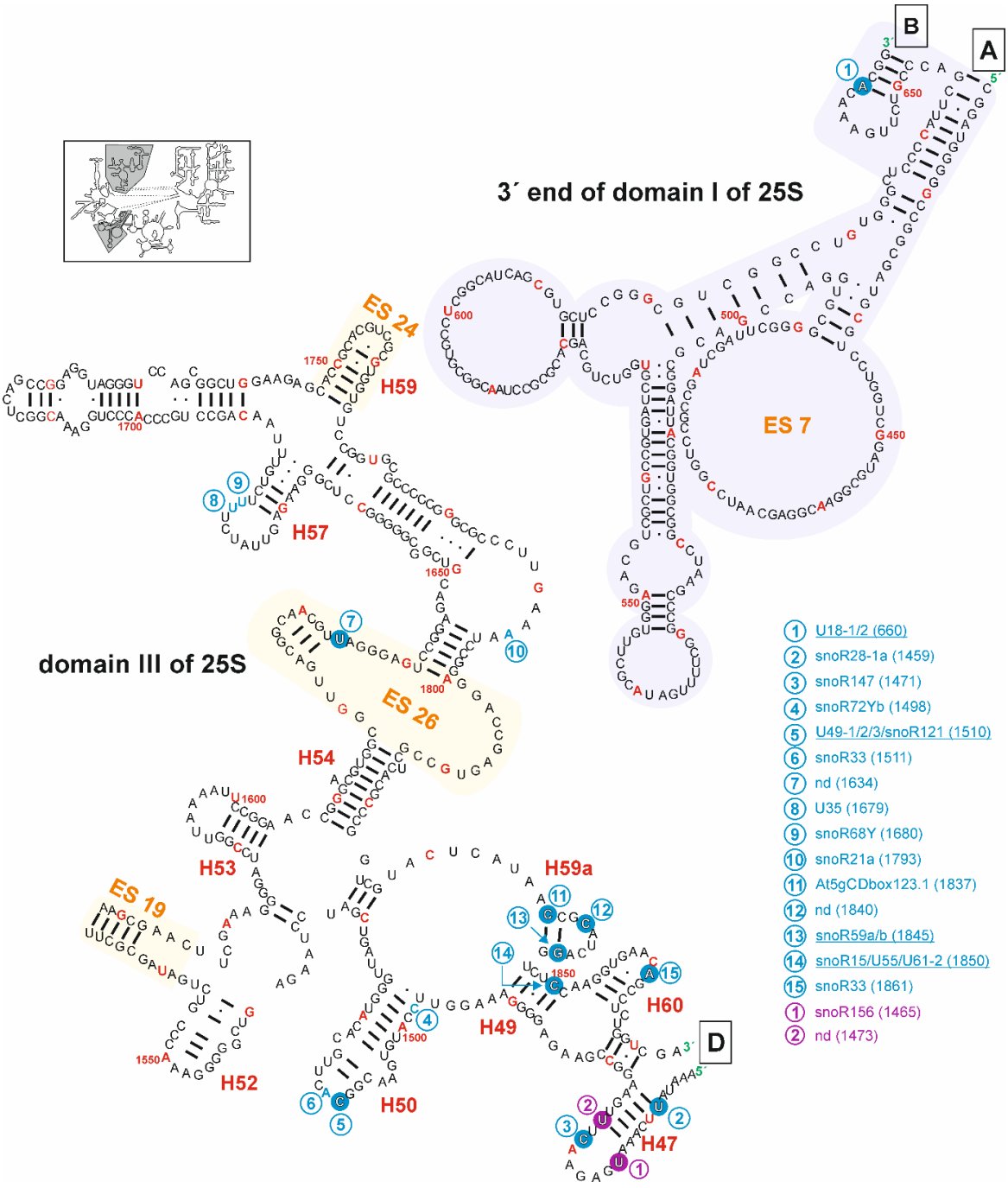

Figure 27. Secondary structure model of domain I and III of 25S rRNA of Arabidopsis.
The structure was created according to the legend of Figure 26. The framed large letters display connections to parts of 25S rRNA in subsequent figures. For A see Figure 26, for B and D see Figure 29. A small illustration of the complete 60S rRNA in the higher left half is showing the position (grey) of the illustrated regions. Adapted from Streit and Schleiff (2021).

Domain II of the 25S rRNA is extensively modified as it is one of the most important regions within this rRNA. The helices H43 and H44 are forming the GTPase center, a highly conserved region in ribosomes (Ryan and Draper, 1991). It could be shown in *Escherichia coli,* that this domain together with L10 and L11 is important for the regulation of GTP hydrolysis on the elongation factors EF-G and EF-TU (Egebjerg et al., 1990; Briones et al., 1998).

The GTPase center of Arabidopsis is highly modified (Figure 28). It contains two verified pseudouridylation sites at Ψ1246 guided by snoR96 and at Ψ1296 guided by an unknown snoRNA. In contrast, two verified 2´-O-me sites at Am1260 and Um1275 both guided by snoR22-2/3a/3b were confirmed (Figure 28). In total 29 predicted 2´-O-me sites were found from which 14 were experimentally confirmed (Figure 28). For pseudouridylation 13 out of 16 predicted sites were mapped.

Most of the modified sites are densely distributed in regions with stem structures. Thus, modifications affect primarily the helices H27, H31, H32, H35 and H38 (Figure 28). Helix 38 together with the inserted ES12, carries five confirmed modified sites, including three Ψ-sites and two 2´-O-me sites. For two Ψ-sites a matching guiding snoRNAs is known, but for the site Ψ1060, the corresponding snoRNA is not known (Figure 28). It has been found in yeast that helix 38 is involved in the intersubunit bridge and it contacts the A-site-bound tRNA (Spahn et al., 2001) and high degree of modifications likely leads to the structural stabilization of this region. Helix 31 in the ES9 carries one verified 2´-O-me and one verified Ψ-site, both sites are guided by known snoRNAs (Figure 28). Both, ES9 and ES12 are located at the back of the central protuberance (Spahn et al., 2001). Helix 35 carries one mapped 2´-O-me site and two Ψ-sites at Ψ892 and Ψ899, but the snoRNAs responsible for those sites have not identified (Figure 28). This could indicate that a stand-alone enzyme might be responsible for these modifications. Helix 33 carries another cluster of modifications, with two mapped 2´-O-me sites and one Ψ-site (Figure 28). In yeast, the protein Prp43 was found to bind amongst other to helix 34, where it is thought to be responsible for the release of a subset of snoRNAs binding to helices close to H34 (Bohnsack et al., 2009). However, the plant homolog remains to be identified.

Domain IV (Figure 29) and V (Figure 30) of the 25S rRNA shows a high degree of modifications. In Domain IV, a total of 30 sites for 2´-O-me were predicted, from which 20 are experimentally confirmed. For sites, Um1918 and Cm2283, the according snoRNAs are not determined (Figure 29). Among the regions with high density of modifications are the helices 68, 69 and 71, that are involved in the intersubunit bridge between the LSU and SSU (Spahn et al., 2001; Gigova et al., 2014). Helix 68 of yeast consists of two E-sites (exit sites) (Xie et al., 2012) and helix 69 interacts with tRNAs located in the A- and P-site, respectively (Ge and Yu, 2013). Additionally, this domain contains the flexible ES27, important for translational fidelity due to its function in preventing frameshift errors (Fujii et al., 2018) and as a scaffold for the enzyme methionine amino peptidase (MetAP), that removes the first methionine from the nascent polypeptide chain (Fujii et al., 2018; Knorr et al., 2019).

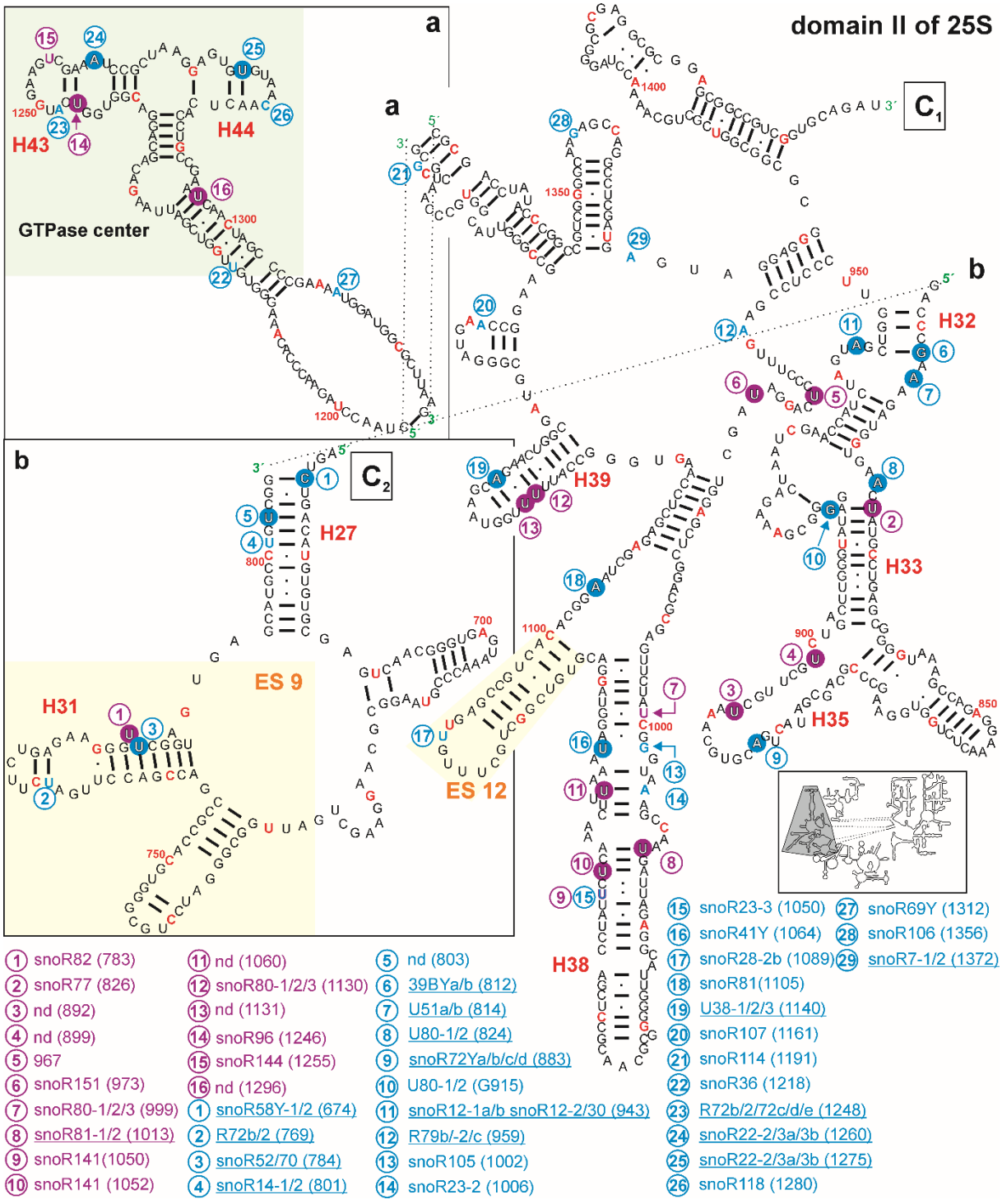

Figure 28. Secondary structure model of domain II of 25S rRNA of Arabidopsis.
The structure was created according to the legend of Figure 26 The framed large letters display connections to parts of 25S rRNA in subsequent figures. For **C** see Figure 29. A small illustration of the complete 60S rRNA in the lower right half is showing the position (grey) of the illustrated regions. Adapted from Streit and Schleiff (2021).

ES27 is not susceptible for modifications as shown for yeast and human (Piekna-Przybylska et al., 2007), but in Arabidopsis one pseudouridylation site at Ψ2028 (Figure 29) was recently identified without known snoRNA (Sun et al., 2019).

Domain V and VI (Figure 30) of the 25S rRNA carry the majority of modifications. In total 43 2´-O-me sites are predicted, from which 34 are verified and from 26 predicted pseudouridylation sites, 22 are confirmed (Figure 30). The most important and oldest region in this region is the peptidyl transferase center (PTC), responsible for the peptide bond formation and peptide release (Polacek and Mankin, 2005). The helices H73, H74, H75, H88, H89, H90, H91, H92 and H93 surrounding the PTC are particularly marked by high density of modified sites (Figure 30). In comparison to the human or yeast PTC regions, Arabidopsis shows the highest number of modified sites (Piekna-Przybylska et al., 2007). All together these findings support the fact, that modifications are required to maintain the structure of certain important regions like the PTC.

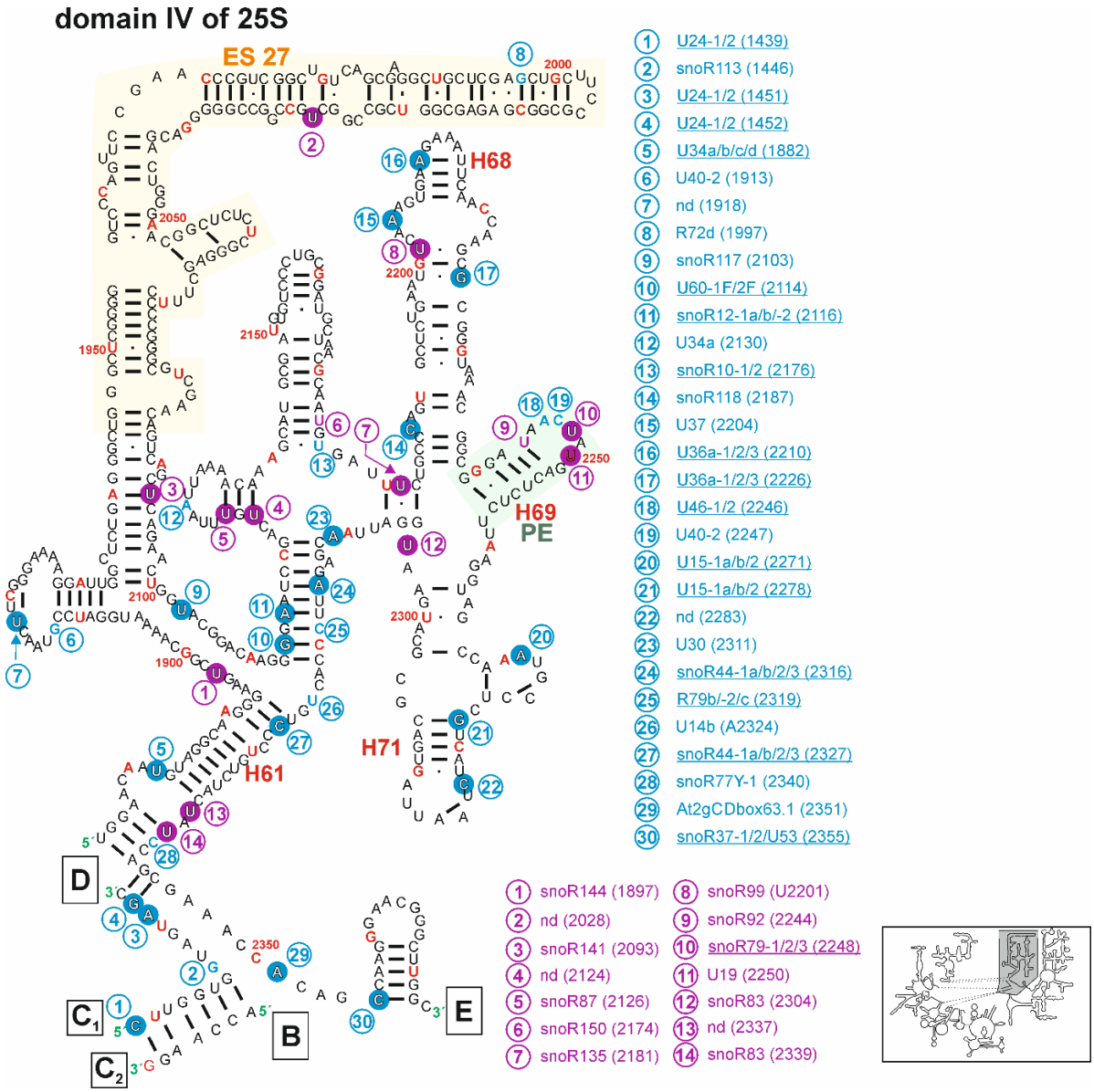

Figure 29. Secondary structure model of domain IV of 25S rRNA of Arabidopsis.
The structure was created according to the legend of Figure 26. The framed large letters display connections to parts of 25S rRNA in subsequent figures. For **C** see Figure 28, for **B and D** see Figure 27 and for E see Figure 30. **PE** annotates a pivoting element and ES expansion elements. A small illustration of the complete 60S rRNA in the lower right half is showing the position (grey) of the illustrated regions. Adapted from Streit and Schleiff (2021).

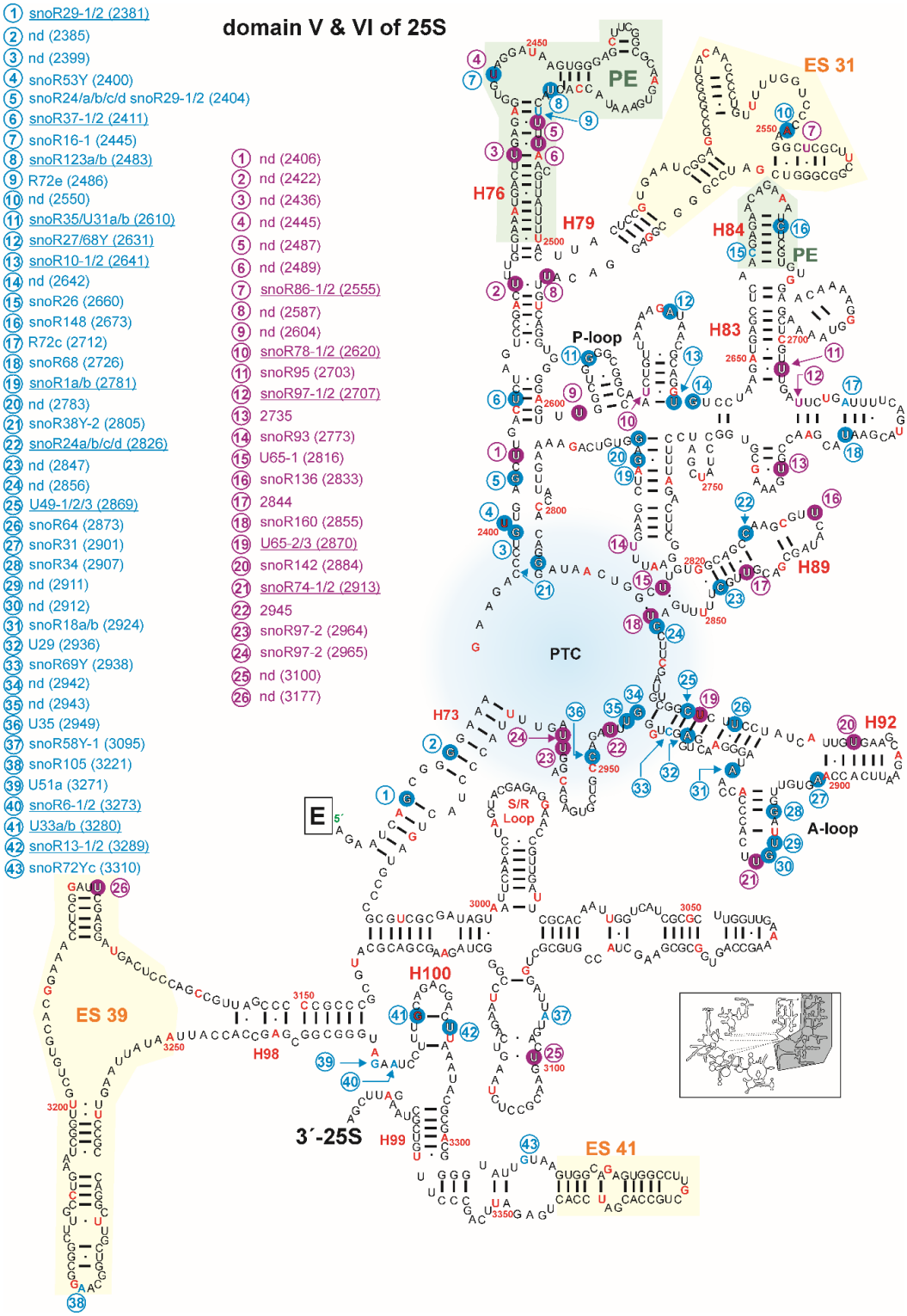

Figure 30. Secondary structure model of domain V and VI of 25S rRNA of Arabidopsis.
The structure was created according to the legend of Figure 26 The framed large letters display connections to parts of 25S rRNA in subsequent figures. For **E** see Figure 29. The region of the peptidyl transferase center (PTC) is indicated in blue. **ES**: expansion segment, **PE**: pivoting element. A small illustration of the complete 60S rRNA in the lower right half is showing the position (grey) of the illustrated regions. Adapted from Streit and Schleiff (2021).

Domain VI is close to the 3´-end of the 25S rRNA and contains the lowest degree of modifications (Figure 30). It harbors the conserved sarcin/ricin loop (S/R loop), which is prone for the attack of the two toxins, α-sarcin and ricin (Endo et al., 1988; Macbeth and Wool, 1999). One mapped pseudouridylation site is found in ES39, a segment without known function.

However, ES39 is located on the ribosome surface and might be an important region, since all eucaryotes possess this segment (Nygård et al., 2006).

Summarizing, the updated map presented here improves the overview and supports future analysis in this field. The majority of modifications can be found in important reactive sites such as the PTC or in the GTPase center. A comparison to yeast and human 60S subunit (Piekna-Przybylska et al., 2007), shows that the same regions are affected by modifications. Indicating that the rRNA modification landscape is evolved very similarly. So far 65 % of all predicted 2´-O-methylation sites were verified and 58 % of the predicted pseudouridylation sites were experimentally confirmed (Table S2). The 5.8S rRNA carries four verified sites, including two newly identified sites at Ψ22 and Ψ78 (Sun et al., 2019) and only one site at G155 could not be confirmed until now (Brown et al., 2001; Table S4). However, the snoRNA which might guide ribose methylation at site G155, was predicted to be snoR4a/4b due to the existing antisense elements (Brown et al., 2001). The helices near the PTC are crucial for the proper function of the ribosome. In human, H74 sustains the structure of the nascent polypeptide exit tunnel (NPET) (Wilson et al., 2020). Helix 89 interacts with the GTPase-associated center (Sergiev et al., 2005; Baxter-Roshek et al., 2007), Helix 93 is contacted by uL2 and induces

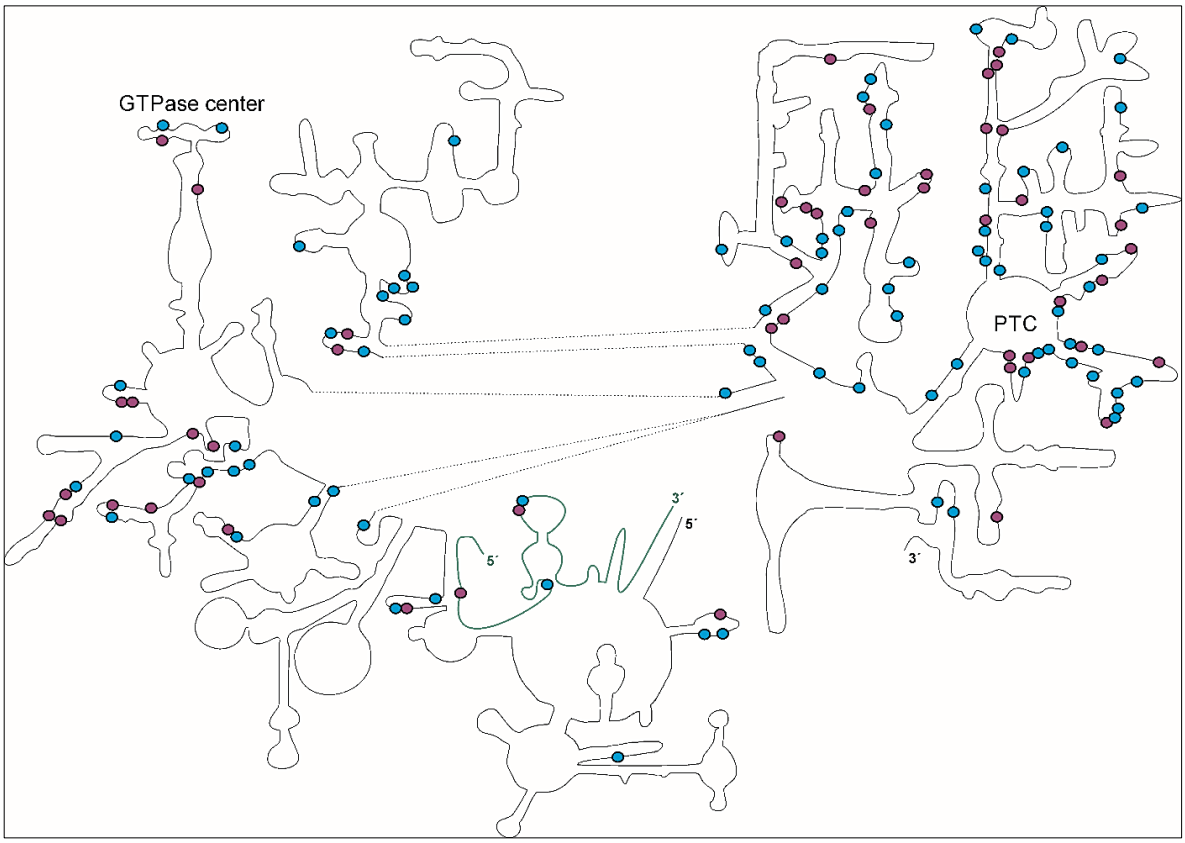

Figure 31. Secondary structure map of 60S rRNAs with verified modification sites.
All experimentally verified 2´-O-metyhaltion (blue circles) and pseudouridylation (violet circles) sites are depicted and an overview map of the 5.8S rRNA (green line) and 25S rRNA (black line). All modifications sites were collected from various publications (Barneche et al., 2001; Brown et al., 2001; Qu et al., 2001; Sun et al., 2019; Azevedo-Favory et al., 2020). Secondary structure map was created based on RNAcentral database (The RNAcentral Consortium, 2019) and http://www.rna.icmb.utexas.edu.

structural changes in the PTC (Yanshina et al., 2015) and Helix 92 is required for accurate folding of helices 90-92 in yeast (Baxter-Roshek et al., 2007). Other regions, including the P-loop (H80) and A-loop (H92) are important as binding sites for the A- and P-site tRNAs (Kim and Green, 1999).

6.2.3 The 18S rRNA modifications landscape

The 18S rRNA of Arabidopsis is encoded on two loci, one variant is on chromosome 3 and the other variant is located on chromosomes 2 and 4. The secondary structure map was created based on the sequence of chromosome 2 and 4 (Figure 32; Figure S1; Figure S2). The 40S subunit binds the mRNA in order to decode the genetic information in the "decoding center" formed by H18, 24, 31, 34 and 44 (Schluenzen et al., 2000; Liang et al., 2009). The 18S rRNA carries 44 confirmed 2´-O-methylation sites and 28 confirmed pseudouridylation sites (Figure 32; Figure S1; Figure S2; Table S3). Alike for 25S rRNA, the majority of modifications are found in functionally relevant sites of the decoding center and close to binding sites of RBFs (Figure 32; Figure S1; Figure S2). For yeast it is known that H44 contains a binding site for the helicase Prp43 required for maturation of 20S and 27S pre-rRNA, where it unwinds the pre-rRNA to enable the cleavage at site D by Nob1 (Bohnsack et al., 2009; Pertschy et al., 2009). Interestingly, *A. thaliana* carries a Am1754 modification close to this site, which is absent in yeast (Figure 32; Figure S1). This could indicate that *A. thaliana* requires that modification site for proper cleavage at site D in the final maturation step of 18S rRNA. Human and yeast rRNAs carry additionally to pseudouridylation and 2´-O-me sites also acetylated nucleotides, and hypermodified nucleotides, that have not been described so far in Arabidopsis. On the other site Arabidopsis is carrying modifications on sites that don’t have an equivalent in yeast or human. It also speculative if the modification landscape of Arabidopsis rRNA is now complete or if certain modifications are appearing only under specific circumstances like changes in environmental conditions. Therefore, future research should focus on different conditions and more importantly analyze different tissues of the plant.

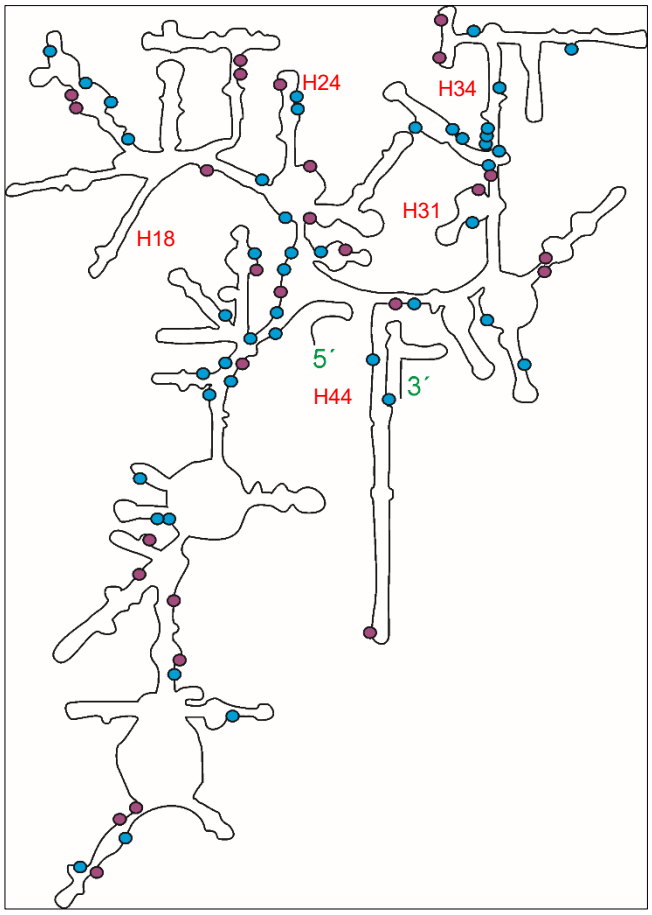

Figure 32. Secondary structure map of 40S subunit rRNA with verified modification sites.
All experimentally verified 2´-O-metyhaltion (blue circles) and pseudouridylation (violet circles) sites are depicted. All modifications sites were collected from various publications (Barneche et al., 2001; Brown et al., 2001; Qu et al., 2001; Sun et al., 2019; Azevedo-Favory et al., 2020). Secondary structure map was created based on RNAcentral database (The RNAcentral Consortium, 2019) and http://www.rna.icmb.utexas.edu.

6.3 Characterization of 5´-5.8S pre-rRNA in plants

6.3.1 The 5´-5.8S pre-rRNA is cytoplasmic in plants

The existence of yeast and vertebrate 5.8S pre-rRNA extended at the 3´-site was well described and cytoplasmic presence was experimentally validated (Ansel et al., 2008; Thomson and Tollervey, 2010; Henras et al., 2015; Pirouz et al., 2019). In turn the 5´-5.8S pre-rRNA appears to be important in Arabidopsis ribosome biogenesis (Zakrzewska-Placzek et al., 2010; Missbach et al., 2013; Palm et al., 2019). While for human such a 5´-extended 5.8S rRNA was not described, in yeast it was only found when factors like Rat1p, Xrn1p or Rrp17p were depleted (Henry et al., 1994; Oeffinger et al., 2009). Surprisingly, the plant specific 5´-5.8S pre-rRNA was found to be localized in the cytoplasm (Figure 13A, B). However, a clear

co-localization with RPS3-2, a marker of cytoplasmic 40S subunit, could not be confirmed (Figure 13E). Along with 5´-5.8S pre-rRNA, smaller fragments are also observed indicative for a 5´-5.8S degradation product (Figure 13. Analysis of 5´-5.8S pre-rRNA in Arabidopsis cell suspension culture.

A 5´-extended 5.8S precursor was observed in tomato (Frank Schroll, master thesis 2019) and in *Oryza sativa* rice (Hang et al., 2018) as well. Moreover, this precursor can be detected in the cytoplasm of both, the dicotyl and monocotyl plants (Figure 14), supporting again that 5´-5.8S is plant-specific and in contrast to yeast and vertebrates plays a major role for the maturation of 5.8S rRNA. Surprisingly, in contrast to Arabidopsis, rice and tomato 6S pre-rRNA is also cytoplasmic and resembles yeast and human 5.8S rRNA processing (Ansel et al., 2008; Henras et al., 2015; Pirouz et al., 2019).

6.3.2 Two factors related to 5.8S rRNA processing

AtPCP2 and AtPRP24 were discovered to participate in 5.8S processing. AtPCP2 was previously described to be relevant for 18S rRNA processing (Ishida et al., 2006). The heterozygous mutant *pcp2* uncovered a function in early steps of rRNA processing, due to accumulations of 35S but also 33/32S pre-rRNAs (Figure 15). Surprisingly, while 18S precursors are processed almost at normal levels in comparison to wild type, 27S-A_2 pre-rRNA, a precursor of pathway 1, is strongly accumulated (Figure 15B, D). The accumulation of the 5´-5.8S pre-rRNA in the mutant indicates that this precursor is a product of pathway 1, and the impact of AtPCP2 on 5´-5.8S is likely associated with an upstream processing defect.

AtPRP24 is the plant homologue of the human spliceosome associated factor 3 (SART3) and the yeast pre-mRNA processing 24 factor (PRP24) (Raghunathan & Guthrie, 1998; Bae et al., 2007; Bell et al., 2002). Furthermore, AtPRP24 is either directly or indirectly involved in the processing of a subset of pre-rRNAs like 33/32S and 5´-5.8S pre-rRNA (Figure 15). The Arabidopsis *PRP24* gene consists of 16 exons and the AtPRP24 protein harbors eight HAT motifs (Half-a-TPR), one RRM and a Lsm interaction motif (Figure 16). A T-DNA insertion mutant (SALK_043206), with an insertion in the fourth intron of *PRP24* gene was shown to be homozygous lethal due to embryo lethality (Li et al., 2021). Most probably AtPRP24 is required for embryo development, for gametophyte transmission and for pollen development (Li et al., 2021). Worth mentioning, in here distinct mutant lines were used namely the T-DNA line *prp24.1* (SALK_045810) and *prp24.2* (SALK_040327) (Figure 16). As described before homozygous plants were not viable (data not shown). The mutant allele *prp24.2*, contains a double T-DNA insertion in exon four, while *prp24.1* has a single insertion in intron 14. However, in *prp24.1* the phenotype is only marginally reliable due to varying results in rRNA processing defects (Figure 15). This phenomenon is probably due to the intronic insertion by which

differences in intron splicing efficacy can cause those varying effects (Ulker et al., 2008). Moreover, it is very likely that in *prp24.1*, due to the late T-DNA insertion, a truncated mRNA could be produced that at the end would lead to a truncated protein. Thus, to overcome all these possibilities, *prp24.2* has been chosen for all upcoming experiments.

6.3.3 AtPRP24 is involved in 5´-5.8S processing

The mutant *prp24.2* shows strong accumulation of 5´-5.8S pre-rRNA especially in the cytoplasm (Figure 17). Recently AtPRP24 (SEAP1) was discovered to be involved in promoting the biogenesis of miRNAs (Li et al., 2021). MicroRNAs are a class of non-coding RNAs of about 21 nt that are involved in the regulation of gene expression in plants and animals by binding to ARGONAUTE1 (AGO1) (Xie et al., 2005; Wang et al., 2004). In the *amiR*^{SEAP1} mutant, for some miRNA the abundance was reduced, and the transcript levels of target transcripts were slightly increased (Li et al., 2021). Recent studies in human showed that miRNAs can affect ribosome biogenesis by repressing or activating RPs and RBFs (McCool et al., 2020). In Arabidopsis, for AtFIERY1 and AtXRN2 and AtXRN3 mutants, a high number of rRNA-derived siRNAs (risiRNAs) are observed, which in turn leads to the loading of risiRNAs into AGO1 instead of miRNAs and by that causing rRNA processing defects (You et al., 2019). Interestingly, *fry1-6* exhibits reduced levels of miR156 and miR166 and higher abundance of miR395 (You et al., 2019), that was also observed for *amiR*^{SEAP1} (Li et al., 2021). In *fry1-6*, several pre-rRNAs like 35S*, 27S and pre-5.8S precursors are accumulating. Similar accumulations were observed for *xrn2 xrn3* mutants (Zakrzewska-Placzek et al., 2010). However, the pre-rRNAs accumulating in *prp24.2* slightly differ from those of *fry1-6* and *xrn2 xrn3* indicating that dissimilar mechanisms are involved. FIERY is indirectly involved in activation of XRN 2/3/4 function by degrading 3´-phosphoadensine 5´-phosphate (PAP), that if not degraded in turn reduces XRN activity (You et al., 2019).

Nevertheless, the cause of rRNA accumulation in *prp24.2* remains unclear. For comparisons, a factor involved in 3´-end maturation of 5.8S rRNA was used. The mutant *rrp6l2* shows strong accumulation of 6S and 20S pre-rRNA (Lange 2011; Sikorski et al., 2015; Weis, 2015; Thesis) and is therefore a good candidate to analyze and compare 3´ defective processing products of 5.8S precursors with those obtained from 5´ defective 5.8S processing mutants. Fractionation experiments revealed that 6S is dominantly exported to the cytoplasm in pre-60S subunits (Figure 17). While on the other hand, 5´-5.8S pre-rRNA levels in the cytoplasm are on the same levels as in wild-type. Most interestingly, a shorter form of 6S is dominantly exported, that however, indicates a 5´-truncated 5.8S precursor (Figure 14). A similar precursor was already identified in mouse cells, where depletion of L17/uL22 enhanced the production of a 5´-cropped 5.8S rRNA (Wang et al., 2015). For the case of *rrp6l2* the presence of this cropped 5.8S precursor could so far not be shown to be associated with functional

ribosomes. According to the size, with 6S having a size of 174 nt, the smaller fragment could also be due to ITS2 fragments, which are accumulating in the mutant. RRP6L2 is part of the exosome, that is involved in 3´ processing but also in degradation of rRNA processing by-products like the 5´ETS (Lange et al., 2008). In this direction it is possible that ITS1 or ITS2 fragments are also targets of the exosome complex.

6.3.4 Insertion of newly discovered 5.8S precursors into pre-rRNA processing scheme

Very intriguingly, northern blotting of sub fractionated pre-rRNAs in wild type and *prp24.2* unveiled many precursors of 5.8S rRNA that remained undetectable at total RNA hybridization analysis (Figure 18B). Probing with different probes within ITS1 and ITS2 further supported the findings (Figure 18C). The existence of additional 5.8S precursors apart from those that are known and the accumulation of the plant-specific 5´-5.8S pre-rRNA was often detected when mutants of factors involved in ribosome biogenesis were examined. Among these mutants are *rrp5.1* and *rrp5.2* (Missbach et al., 2013), *xrn2 xrn3* (Zakrzewska-Placzek et al., 2010) and *brx1-2* (Weis et al., 2015b). In order to identify the exact 5´ and 3´ sites of those novel precursors, circular RT-PCR with subsequent sequencing was performed (Figure 19). This yielded many putative precursors and based on the number of identified sequences a revised model for pre-rRNA processing is proposed (Figure 33).

Starting point for 5.8S maturation for both *prp24.2* and wild type is the A_2-C_2 pre-rRNA with a size of 531 nt, that usually is barely visible with northern blotting. An A_2-C_2 pre-rRNA was already described for yeast, when exosome mutants were analyzed (Allmang et al., 2000). Since 5´-5.8S pre-rRNA accumulations often occur along with pre-rRNAs from the minor pathway 1 (5´-ETS-first) like observed for *brx1-2* (33/32S and 27SA_2 pre-rRNAs) and *xrn2 xrn3* (27SA_2) (Weis et al., 2015b; Zakrzewska-Placzek et al., 2010) it can be hypothesized that 5´-5.8S pre-rRNAs are produced in pathway 1, while 3´ extended precursors like 7S and 6S are products of the major pathway 2 (Palm et al., 2019). This fact assumes that the newly identified precursors are also majorly produced in pathway 1 and therefore a new proposed rRNA processing model was created, which only focused on pathway 1 (Figure 33). However, it cannot be excluded that e.g. A_2-C_2, A_3´-C_2 and A_3-C_2 are also precursors of 7S and therefore part of pathway 2. Nonetheless, for reasons of simplification pathway 2 was left out. Overall, the newly discovered precursors can be grouped into a minor and major 5.8S processing pathway (Figure 33). Starting from A_2-C_2, the *prp24.2* mutant is suggested to have a major 5´ 5.8S pre-rRNA processing way initiated by an 5´-3´ exoribonucleolytic digestion of A_2-C_2 to A_3´-C_2, which is subsequently cleaved at site A_3 to produce a A_3-C_2 precursors that is further cleaved or digested at the 3´ site to produce A_3-5.8S-3´ (Figure 33). In the minor way, processing is initiated at the 3´site. The A_2-C_2 precursor is likely digested by an 3´-5´

exoribonuclease to A_2-C_2´, further digestion produces the A_2-5.8S-3´ pre-rRNA, which is probably the precursor for A_3-5.8S-3´ (Figure 33). The A_3-5.8S-3´ could result from both ways and further processing of it could lead to 5´-5.8S pre-rRNA, which is then exported to the cytoplasm, where it might be further processed. Interestingly, for *prp24.2*, a few precursors were not detected at all, but were found instead in wild type (Figure 19C). These precursors include the A_2-5.8S and A_3´-5.8S pre-rRNAs, which might indicate that 3´ processing is defective in *prp24.2*. Also, that the majority of the precursors found still contained the C_2 cleavage site, indicates that the 3´ site in ITS2 is defective in processing. However, one could argue that due to the high abundance of major pathway precursors probably caused by accumulations due to delay in processing, that the minor pathway is the main way that is in use for 5.8S processing (Figure 33). In wild type, the major proposed 5.8S processing way starts with the A_2-C_2 precursor, and unlike *prp24.2*, processing is driven at the 3´ site in ITS2 (Figure 33). This leads to an A_2-C_2´ precursor, that might be digested to the A_2-5.8S-3´ precursor, followed by an E cleavage that produces the A_2-5.8S pre-rRNA and then the 5´ site seems to be processed by exoribonucleolytic digestion to the A_3´-5.8S precursor (Figure 33). In contrast, the minor way, uses a processing scheme that starts at the 5´site in ITS1. The minor way is proposed to generate the A_3´-C_2 precursor and digestion could lead to the A_3-C_2 precursor, which could be subsequently cleaved or digested on both extremities to produce the 5´-5.8S pre-rRNA (Figure 33). For any way, whether A_3´-5.8S or A_3-C_2 the downstream precursor could be the 5´-5.8S pre-rRNA, that is further processed before or after cytoplasmic export of the pre-60S subunit. Furthermore, the sequencing of each of these precursors revealed a variety of different precursors (Figure S3). This could indicate that maturation of 5.8S is a multi-step process, by which the formation of every precursor has its own role and might indicate the tight coupling between processing and quality control mechanisms that actively play a crucial role during ribosome biogenesis. It needs to be considered that ITS1 and ITS2 regions can also be targets for post-transcriptional modifications. Hence, it was found that 61 nt upstream of the A_3 cleavage site a pseudouridylation site was detected (Sun et al., 2019; Figure 19D).

Surprisingly, *prp24.2* strongly accumulates the precursor A_3´-C_2 that harbors this site (Figure 19C). In fact, the production of these particular precursors might function as a quality control, by which the presence or absence of the modification leads to the altered production of individual precursors. Unfortunately, this mechanism is not described at all since analysis about modifications are always focused on the rRNA instead of the external/internal transcribed spacers.

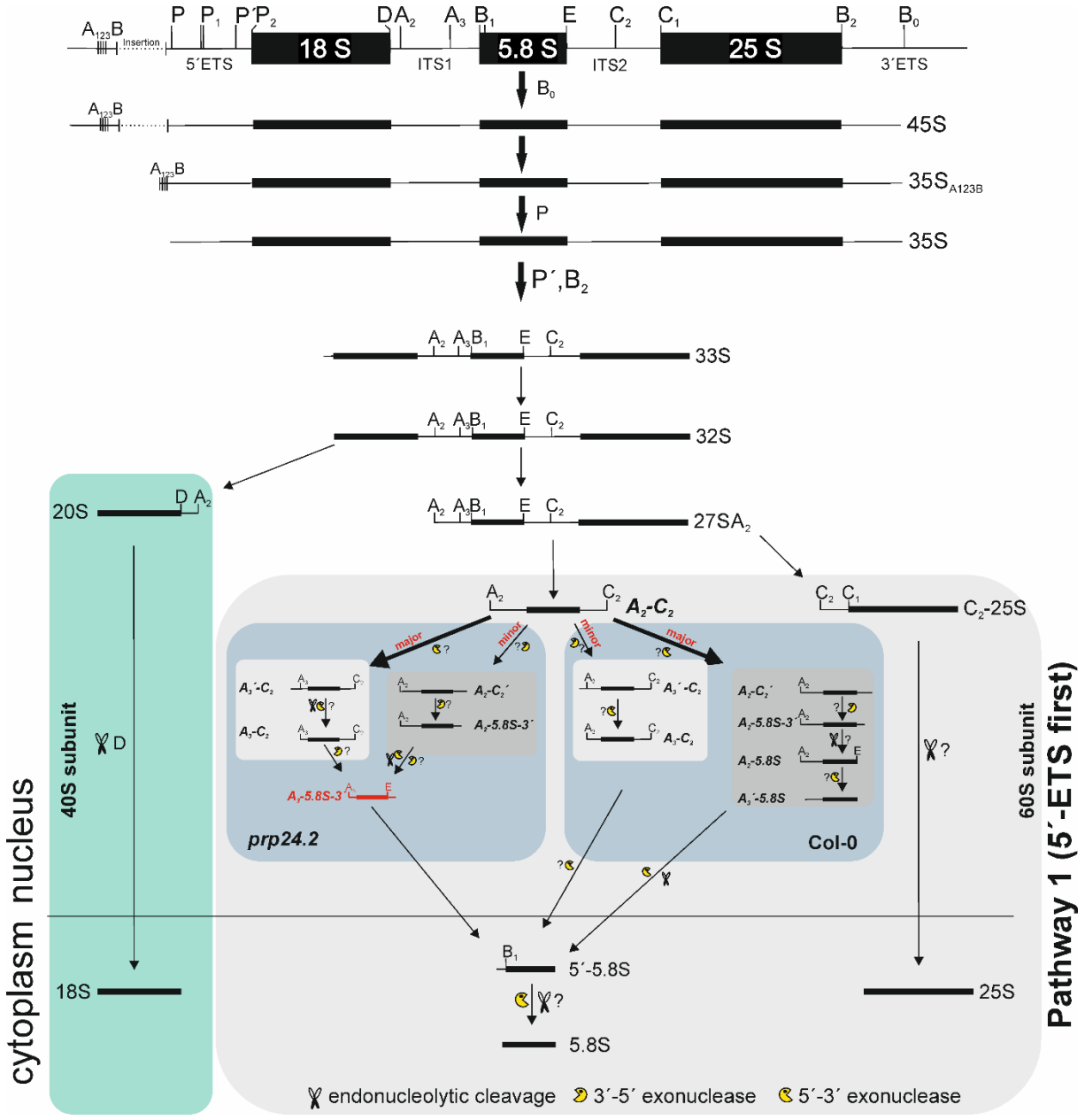

Figure 33. Proposed model for rRNA processing scheme for *prp24.2* and Col-0.
The analysis of *prp24.2* highlighted the way for the identification of novel 5.8S precursors that were not in focus in the past. For wild type novel 5.8S precursors were identified by sequencing. The 5´-5.8S pre-rRNA is suggested to evolve from the minor pathway 1. Newly identified precursors labeled in bold and italics were obtained from Figure 19C. For each processing step suggested cleavage by endoribonucleases or exoribonucleases is given. The prevailing rRNA processing scheme were adapted and modified from Weis et al, (2015b). Based on the abundance of individual precursors that were sequenced, the processing pathway was separated in a major (dark grey, bold arrow) and minor (light grey, thin arrow) way.

The sequencing illustrates the complexity and intertwining mechanisms behind the processing and maturation of 5.8S rRNA in Arabidopsis especially considering that most likely not all existing precursors were experimentally determined. The comparison of Col-0 and *prp24*.2 has led to a hypothesis for the minor and major pathway for the processing of 5.8S. In Col-0, the major way is primarily characterized by precursors that are processed in ITS2. This leads to the hypothesis that complexes that are usually formed around cleavage or digestion sites are

sterically hindering other proteins from binding at cleavage and digestion sites on the 5´ end of 5.8S like A_3 in ITS1 (Figure 34). Vice versa, in Col-0 the minor pathway shows precursors that are processed only in ITS1 but are not processed in ITS2. The mutant *prp24.2* has a major pathway characterized by precursors processed in ITS1 and the minor pathway characterized by ITS2 only processing. One could assume that AtPRP24 has a role in the activation of proteins responsible for the processing especially in the ITS2 region. The largest portion of accumulated precursors in *prp24.2* is constituted of 3´-extended 5.8S precursors. It might be possible that indirect or direct contribution of AtPRP24 is leading to a well-balanced processing mechanism between the ITS1 and ITS2 cleavage and digestion sites.

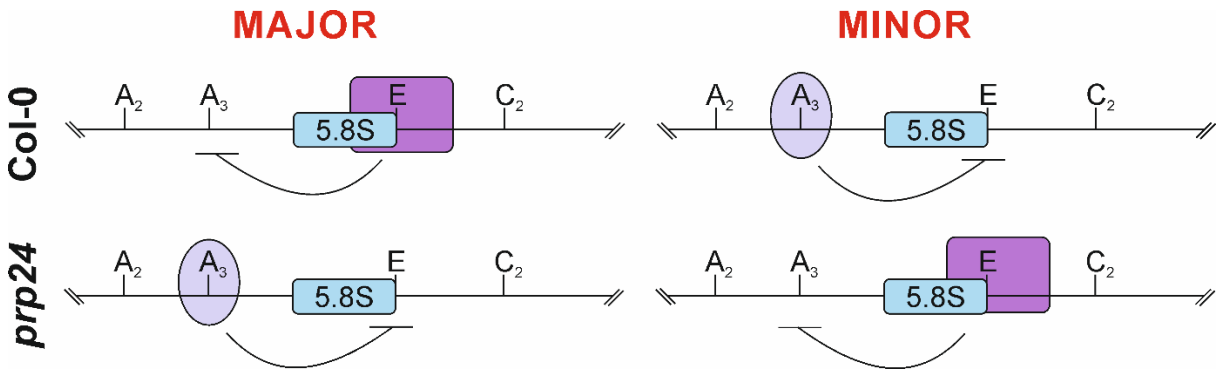

Figure 34. Proposed model of the mechanisms behind the minor and major 5.8S processing pathways. Sequencing of novel 5.8S rRNA precursors revealed a possible structure-dependent processing preference. In the major 5.8S processing scheme of Col-0, the complex formation around E-site is hindering further processing in ITS1 at site A_3, while in the minor pathway complex formation around A_3 is hindering proper processing at site E. For *prp24* the major pathway is possibly characterized by a complex formation around site A_3, hindering processing at site E and the minor pathway is characterized by a complex formation at site E, hindering cleavages and/or digestions at site A_3.

Interestingly, the 5.8S processing was not disturbed in *xrn2* and *xrn3* single mutants, the double *xrn2 xrn3* mutant displayed several precursors like the A_3-5.8S and 5.8S-3´ pre-rRNAs that were not found whether in wild type nor in the *prp24.2* (Zakrzewska-Placzek et al., 2010; Figure 20). The 5.8S-3´ pre-rRNA was not detected in the sequencing experiments due to the position of the R1 oligonucleotide on the pre-rRNA (Figure 19A). Interestingly, it is very obvious that 5´ processing is heavily altered in the double mutant since many precursors with 5´ extensions are accumulating in the nuclear fraction (Figure 20). The A_3-5.8S pre-rRNA, which was detected in the total cells of *xrn2 xrn3* is only faintly visible in the nuclear fraction. This is contradictory since it could be expected that this particular precursor is enriched in one of the fractions. In contrast the A_3-C_2 pre-rRNA is enriched in the nuclear fraction. Furthermore, the 5´-5.8S pre-rRNA is almost not detected in the cytoplasmic fraction, while on the other site 6S is exported more dominantly suggesting that due to defects in 5´-3´ exoribonucleolytic cleavages, 60S subunits with a 3´-extended 5.8S precursor is more favored for export.

However, it requires sucrose density fractionation, followed by northern hybridization for pre-rRNAs and rRNAs, that could reveal the composition of monosomes and polysomes in the *xrn2 xrn3* mutant.

6.3.5 Polysomes of *prp24.2* contained 5´-5.8S pre-rRNA

In the *prp24.2* mutant, apparently there were no differences in the ratios between 40S to 60S when compared to wild type (Figure 21). The comparison of the polysomal fractions on the other hand, appears to show higher peaks for the heavy polysomal fractions in the mutant. This suggests a high number of ribosomes attached to a single mRNA (Gandin et al., 2014). Remarkably, 5´-5.8S pre-rRNA accumulated in the 60S subunit, in the 80S monosomes and in the polysomes (Figure 21B, C). Furthermore, AtRPL10 is to a lesser extent associated with the heavy polysomes in *prp24.2,* while the levels of small subunit proteins AtRPS3-2 and AtRPS10 are not affected (Figure 21B). This led to the suggestion that the RP composition especially of the large subunit of the *prp24.2* ribosomes might be different.

The high abundance of 5´-5.8S pre-rRNA in polysomal fractions (Figure 21) suggests that ribosomes with a 5´ extended 5.8S rRNA are involved in translation. This trend is similar to observations in the eukaryote *Trypanosoma brucei*, where a 5´ extended 5.8S pre-rRNA was similarly observed in 60S, 80S and polysomes upon depletion of the 5´ - 3´ exoribonuclease XRNE, the functional homologue of yeast Rat1 (Sakyiama et al., 2013).
Similar results were discovered for the RNA helicase mutant *dob1-1* in yeast, where 7S pre-rRNA accumulated in the cytoplasm and moreover it was found that 7S was incorporated into translating ribosomes (Rodríguez-Galán et al., 2015). In any way such an extension at the 5´ or 3´ site of 5.8S rRNA in the 60S subunit may possibly have a structural affect, by which the structure especially in the areas where the extension begins is altered. A hypothetical model of the 60S subunit and of the 80S ribosome was created based on PDB ID: 5TGM (Melnikov et al., 2016), highlighting the 5´-extension of 5.8S (Figure 35A). The extension begins already within the 60S subunit, since the 5´-end of 5.8S is buried in the structure of 60S subunit (Martinez-Seidel et al., 2020). A secondary RNA structure prediction revealed that the extension forms a stem-loop structure and due to an internal bulge, it possibly deviates to the 60S surface forming tertiary structures with the 25S rRNA.

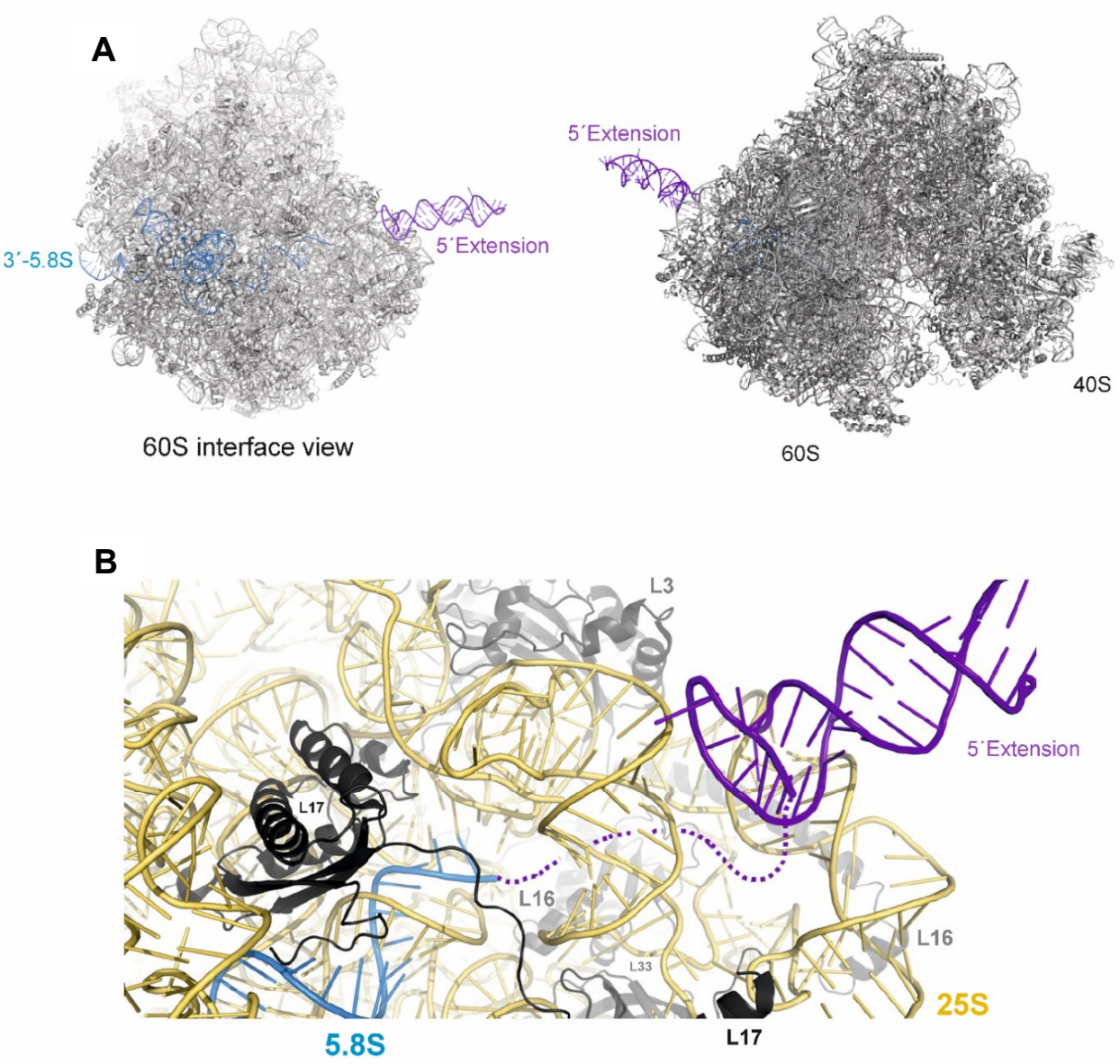

Figure 35. Hypothetical model of the 5.8S 5´ extension in the structures of 60S subunit and 80S ribosome. **A)** Left, the 60S subunit from the interface view, highlighting the 5´ extension and the 3´-end of 5.8S rRNA. The RNA was folded with RNAfold and a structural model created with RNAcomposer (Popenda et al., 2012; Hofacker, 2003). Right, the same shown in context of the corresponding 80S ribosome as adapted from PDB ID: 5TGM (Melnikov et al., 2016). **B)** Zoom-in of the Structure at the 5´-end of the 5.8S rRNA in close proximity to RPs and the 64 nt extension. 5.8S rRNA is colored in blue, the extension in violet, 25S in gold, RpL17 in black and L16 and L33 in dark and light grey, respectively. The structure model was kindly created and provided by Dr. Andreas Schlundt, Goethe University.

It is very likely that the extension at the 5´-end of 5.8S rRNA in the 60S subunit is not fully solvent-exposed but is lying on the 60S surface, where different ribosomal proteins of the large subunit but also the 25S rRNA itself might be sterically influenced. To this end, manual optical inspection of the modified 60S subunit has been carried out to reveal the ribosomal proteins that are theoretically in the vicinity of the extension or directly in contact with 5.8S rRNA (Figure 36). The proteins were highlighted in the structure model with different colors depending on if they are in a) direct vicinity/surface, b) in more distal vicinity or c) adjacent to the 5.8S rRNA core (Figure 36A, B).

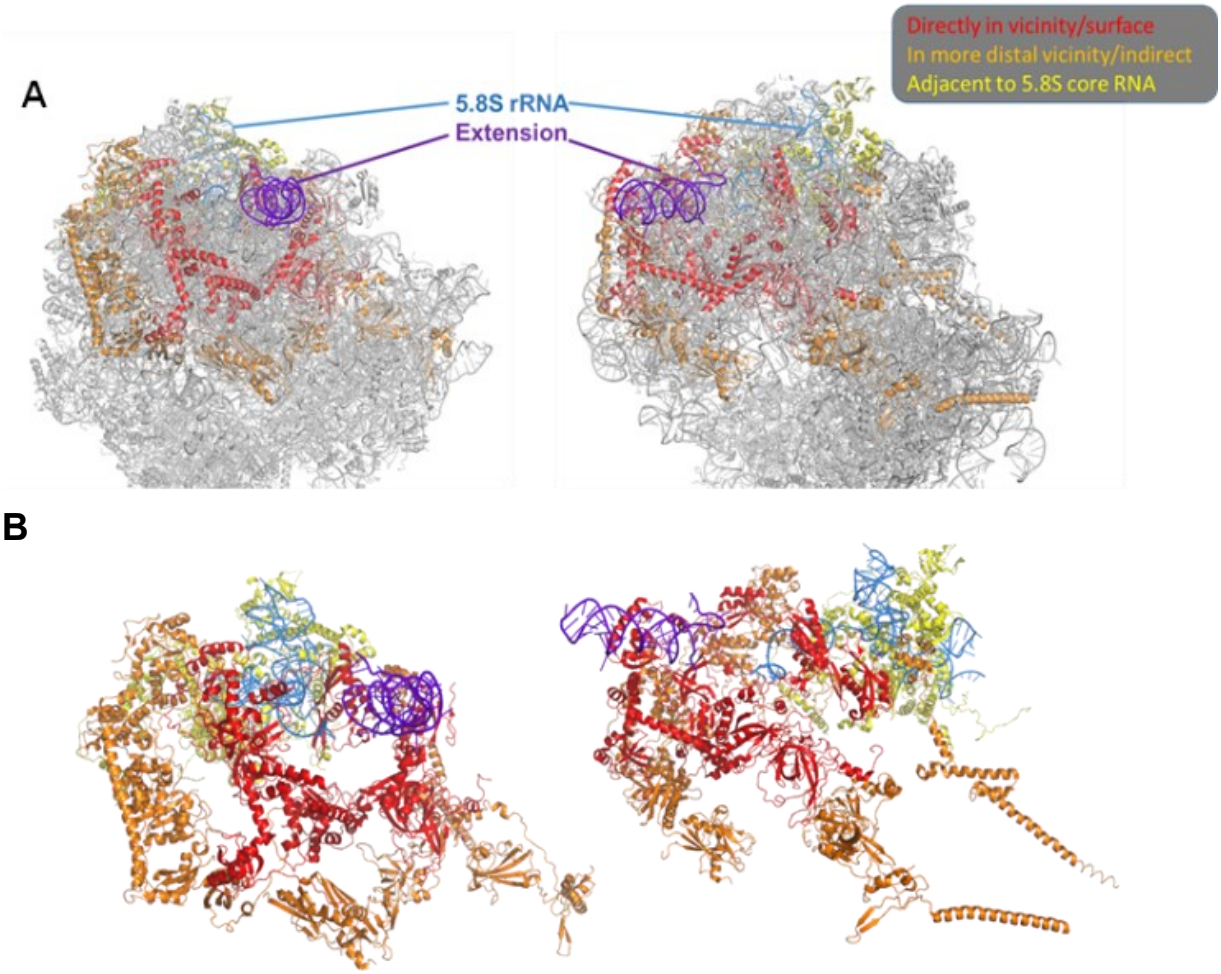

Figure 36. Structure of the 60S subunit.
A) Structure of the 60S subunit with the 5´extension (violet) of 5.8S rRNA (light blue). **B)** Proteins that could be affected by the extension or by structural rearrangements of the 5.8S inside the ribosome. The color code indicates the distance of the proteins to 5.8S. Red (direct vicinity), orange (more distal vicinity) and yellow (adjacent to the 5.8S core). Note that all other ribosomal components are hidden for clarity. For structure modeling information see legend of Figure 35. The structure model was kindly created and provided by Dr. Andreas Schlundt, Goethe University.

The ribosomal proteins, which are predicted to be in close proximity to the extension and of 5.8S rRNA based on suggested model are L3, L6, L14, L16, L17, L31, L32 and L33 (Figure 37A). Previously it was described that Rpl17 depletion in mouse led to the production of a 5´ shortened 5.8S species that nevertheless was also found in polysomal fractions (Wang et al., 2015). Proteins that are in more distal vicinity (orange) to the extension are L4, L7, L9, L18, L19, L20, L23, L24, L40 and S6 (Figure 37B). Also, the core region of 5.8S is in direct contact to proteins like L8, L13, L15, L25, L26, L35, L37 and L39 (Figure 37C). Interestingly in yeast, it could be shown that depletion of L3, L4, L7, L8, L16, L18, L20, L32 and L33 has led to a deviated 5´end processing of the 5.8S pre-rRNA, promoting the idea that those proteins are supporting the structural interactions between the 25S and 5.8S rRNA and that these interactions are required for correct processing of the 5´ end of 5.8S (Pöll et al., 2009).

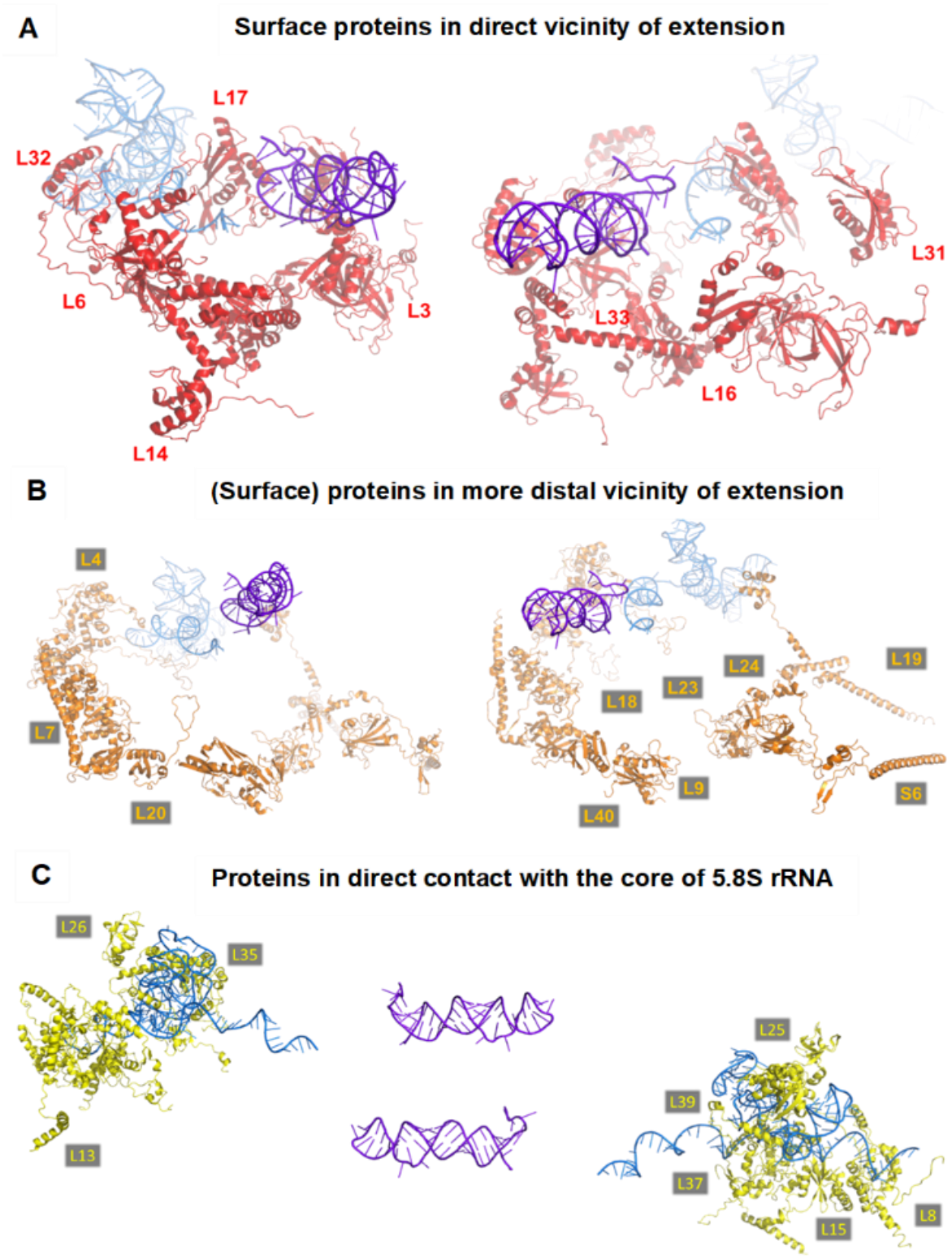

Figure 37. Analysis of proteins in close proximity to 5.8S rRNA.
A) Proteins that are in direct vicinity to 5.8S or to the extension. **B)** Proteins that are in more distal vicinity of the extension. **C)** Proteins that are in direct contact to the 5.8S rRNA core region. For structure modeling information see legend of Figure 35. The underlying structure model was kindly created and pictures provided by Dr. Andreas Schlundt, Goethe University.

6.4 Future perspectives

The variety of snoRNAs for the post-transcriptional modification of rRNAs represents the toolbox for divergence of ribosome function and this requires additional investigations especially in plants in order to find those snoRNAs for the many modified sites in Arabidopsis rRNA that were not described yet (Brown et al., 2001; Streit et al., 2020). In this study, the first part focused on finding novel snoRNAs and while we found some new ones, still many are missing for the experimentally verified modification sites on rRNA. Therefore, future research should focus on different environmental conditions. While under control conditions only a certain subset of snoRNAs is required or sufficient for rRNA modifications, it is very likely that different tissues or even different stress conditions could expose snoRNAs that usually, when a plant is growing under normal circumstances, are not expressed (Figure 12). Also in this study, we analyzed the cellular distribution of some snoRNAs and found that certain snoRNAs are exported to the cytoplasm as observed for yeast under stress conditions (Mleczko et al., 2019). In the future it needs to be elucidated how, when and why these snoRNAs are actually acting in the cytoplasm. In the past, only one publication was found that mutated snoRNAs in Arabidopsis in order to analyze its function (Zhu et al., 2016). Unfortunately, while T-DNA mutants for several coding regions of Arabidopsis are established and available, for snoRNAs it seems to be more difficult. In order to analyze the function of certain snoRNAs, the CRISPR-Cas9 mutagenesis could be employed (Filippova et al., 2019).

Secondly the identification of new ribosome biogenesis factors is one of the major foci for plant ribosome biogenesis (Palm et al., 2016; Palm et al., 2019). Especially the plant specific 5´-5.8S pre-rRNA increasingly comes into focus (Zakrzewska-Placzek et al., 2010; Weis et al., 2015b; Missbach et al. 2013; Palm et al., 2019). In this study, two new candidates were identified, namely AtPCP2 and AtRPR24, and mutants of both showed an accumulation of the 5´-5.8S precursor (Figure 15). Further experiments revealed that 5´-5.8S pre-rRNA is also present in translating ribosomes. This led to determining how theoretically such a long extension might influence the structure of the 60S subunit (Figure 35; Figure 36; Figure 37). However, in order to correlate with experimental evidence for a real hindrance in the structure would require the isolation of these specialized ribosomes. In fact, preliminary results showed that capturing of these ribosomes is not as trivial as expected. A pull-down experiment with magnetic-beads coupled to a 50 nt long antisense oligo was not able to efficiently pull-out the 5´-5.8S ribosomes as judged by native polyacrylamide gel analysis (data not shown). A different approach utilizes RiboTag, thereby the ribosomes contain a hemagglutinin-tag (HA) on one ribosomal protein and by using an HA-antibody the ribosomes and even polysomes can be isolated (Sanz et al., 2019).

It was discovered that 5.8S is actually required for ribosome translocation (Elela and Nazar, 1997. However, when cell free extracts with mutated 5.8S rRNA were treated with CHX, ribosomes showed enhanced sensitivity, by which translocation was affected. In *prp24.2* it could be shown that seeds showed lesser sensitivity against CHX in different concentrations. This in particular may be due to the extension that somehow might affect the structure within the 60S subunit so that binding of CHX is hampered. Based on yeast analysis, CHX is binding in a pocket in the E-site on the 60S subunit with involvement of eL42(de Loubresse et al., 2014). However, eL42 (Arabidopsis L36a) is not speculated to be affected by the extension (Figure 35; Figure 36; Figure 37). For analyzing the exact reason why *prp24.2* shows slightly lesser sensitivity against CHX, the isolation of the ribosomes with extension would be required as explained above.

7 References

Abou Elela, S., & Nazar, R. N. (1997). Role of the 5.8S rRNA in ribosome translocation. *Nucleic acids research*, *25*(9), 1788–1794.

Alharbi, A., Iyer, N., Al Qaryoute, A., Raman, R., Burks, D. J., Azad, R. K., & Jagadeeswaran, P. (2021). Role of ribosomal RNA released from red cells in blood coagulation in zebrafish and humans. *Blood advances*, *5*(22), 4634–4647.

Allmang, C., Kufel, J., Chanfreau, G., Mitchell, P., Petfalski, E., & Tollervey, D. (1999). Functions of the exosome in rRNA, snoRNA and snRNA synthesis. *The EMBO journal*, *18*(19), 5399–5410.

Allmang, C., Mitchell, P., Petfalski, E., & Tollervey, D. (2000). Degradation of ribosomal RNA precursors by the exosome. *Nucleic acids research*, *28*(8), 1684–1691.

Anders, S., Pyl, P. T., & Huber, W. (2015). HTSeq--a Python framework to work with high-throughput sequencing data. *Bioinformatics (Oxford, England)*, *31*(2), 166–169.

Ansel, K. M., Pastor, W. A., Rath, N., Lapan, A. D., Glasmacher, E., Wolf, C., Smith, L. C., Papadopoulou, N., Lamperti, E. D., Tahiliani, M., Ellwart, J. W., Shi, Y., Kremmer, E., Rao, A., & Heissmeyer, V. (2008). Mouse Eri1 interacts with the ribosome and catalyzes 5.8S rRNA processing. *Nature structural & molecular biology*, *15*(5), 523–530.

Armache, J. P., Jarasch, A., Anger, A. M., Villa, E., Becker, T., Bhushan, S., Jossinet, F., Habeck, M., Dindar, G., Franckenberg, S., Marquez, V., Mielke, T., Thomm, M., Berninghausen, O., Beatrix, B., Söding, J., Westhof, E., Wilson, D. N., & Beckmann, R. (2010). Cryo-EM structure and rRNA model of a translating eukaryotic 80S ribosome at 5.5-A resolution. *Proceedings of the National Academy of Sciences of the United States of America*, *107*(46), 19748–19753.

Asha, S., & Soniya, E. V. (2017). The sRNAome mining revealed existence of unique signature small RNAs derived from 5.8SrRNA from Piper nigrum and other plant lineages. *Scientific reports*, *7*, 41052.

Azevedo-Favory, J., Gaspin, C., Ayadi, L., Montacié, C., Marchand, V., Jobet, E., Rompais, M., Carapito, C., Motorin, Y., & Sáez-Vásquez, J. (2021). Mapping rRNA 2'-O-methylations and identification of C/D snoRNAs in Arabidopsis thaliana plants. *RNA biology*, *18*(11), 1760–1777.

Bae, E., Reiter, N. J., Bingman, C. A., Kwan, S. S., Lee, D., Phillips, G. N., Jr, Butcher, S. E., & Brow, D. A. (2007). Structure and interactions of the first three RNA recognition motifs of splicing factor prp24. *Journal of molecular biology*, *367*(5), 1447–1458.

Barneche, F., Gaspin, C., Guyot, R., & Echeverría, M. (2001). Identification of 66 box C/D snoRNAs in Arabidopsis thaliana: extensive gene duplications generated multiple isoforms predicting new ribosomal RNA 2'-O-methylation sites. *Journal of molecular biology*, *311*(1), 57–73.

Baudin-Baillieu, A., & Namy, O. (2021). *Saccharomyces cerevisiae*, a Powerful Model for Studying rRNA Modifications and Their Effects on Translation Fidelity. *International journal of molecular sciences*, *22*(14), 7419.

Baxter-Roshek, J. L., Petrov, A. N., & Dinman, J. D. (2007). Optimization of ribosome structure and function by rRNA base modification. *PloS one*, *2*(1), e174.

Behrmann, E., Loerke, J., Budkevich, T. V., Yamamoto, K., Schmidt, A., Penczek, P. A., Vos, M. R., Bürger, J., Mielke, T., Scheerer, P., & Spahn, C. M. (2015). Structural snapshots of actively translating human ribosomes. *Cell*, *161*(4), 845–857.

Belardinelli, R., Sharma, H., Peske, F., Wintermeyer, W., & Rodnina, M. V. (2016). Translocation as continuous movement through the ribosome. *RNA biology*, *13*(12), 1197–1203.

Bell, M., Schreiner, S., Damianov, A., Reddy, R., & Bindereif, A. (2002). p110, a novel human U6 snRNP protein and U4/U6 snRNP recycling factor. *The EMBO journal*, *21*(11), 2724–2735.

Berardini, T. Z., Reiser, L., Li, D., Mezheritsky, Y., Muller, R., Strait, E., & Huala, E. (2015). The Arabidopsis information resource: Making and mining the "gold standard" annotated reference plant genome. *Genesis (New York, N.Y. : 2000)*, *53*(8), 474–485.

Beringer, M., & Rodnina, M. V. (2007). The ribosomal peptidyl transferase. *Molecular cell*, *26*(3), 311–321.

Bohnsack, M. T., Martin, R., Granneman, S., Ruprecht, M., Schleiff, E., & Tollervey, D. (2009). Prp43 bound at different sites on the pre-rRNA performs distinct functions in ribosome synthesis. *Molecular cell*, *36*(4), 583–592.

Bradford M. M. (1976). A rapid and sensitive method for the quantitation of microgram quantities of protein utilizing the principle of protein-dye binding. *Analytical biochemistry*, *72*, 248–254.

Briggs, M. W., Burkard, K. T., & Butler, J. S. (1998). Rrp6p, the yeast homologue of the human PM-Scl 100-kDa autoantigen, is essential for efficient 5.8 S rRNA 3' end formation. *The Journal of biological chemistry*, *273*(21), 13255–13263.

Briones, E., Briones, C., Remacha, M., & Ballesta, J. P. (1998). The GTPase center protein L12 is required for correct ribosomal stalk assembly but not for Saccharomyces cerevisiae viability. *The Journal of biological chemistry*, *273*(48), 31956–31961.

Brown, J. W., Clark, G. P., Leader, D. J., Simpson, C. G., & Lowe, T. (2001). Multiple snoRNA gene clusters from Arabidopsis. *RNA (New York, N.Y.)*, *7*(12), 1817–1832.

Brown, J. W., Echeverria, M., & Qu, L. H. (2003). Plant snoRNAs: functional evolution and new modes of gene expression. *Trends in plant science*, *8*(1), 42–49.

Cao, T., Rajasingh, S., Samanta, S., Dawn, B., Bittel, D. C., & Rajasingh, J. (2018). Biology and clinical relevance of noncoding sno/scaRNAs. *Trends in cardiovascular medicine*, *28*(2), 81–90.

Carroll, A. J., Heazlewood, J. L., Ito, J., & Millar, A. H. (2008). Analysis of the Arabidopsis cytosolic ribosome proteome provides detailed insights into its components and their post-translational modification. *Molecular & cellular proteomics : MCP*, *7*(2), 347–369.

Castle, C. D., Cassimere, E. K., Lee, J., and Denicourt, C. (2010). Las1L is a nucleolar protein required for cell proliferation and ribosome biogenesis. *Molecular and cellular biology*, *30*(18), 4404–4414.

Chang, I. F., Szick-Miranda, K., Pan, S., & Bailey-Serres, J. (2005). Proteomic characterization of evolutionarily conserved and variable proteins of Arabidopsis cytosolic ribosomes. *Plant physiology*, *137*(3), 848–862.

Chen, H. M., & Wu, S. H. (2009). Mining small RNA sequencing data: a new approach to identify small nucleolar RNAs in Arabidopsis. *Nucleic acids research*, *37*(9), e69.

Chomczynski, P., & Sacchi, N. (1987). Single-step method of RNA isolation by acid guanidinium thiocyanate-phenol-chloroform extraction. *Analytical biochemistry*, *162*(1), 156–159.

Cloix, C., Tutois, S., Yukawa, Y., Mathieu, O., Cuvillier, C., Espagnol, M. C., Picard, G., & Tourmente, S. (2002). Analysis of the 5S RNA pool in Arabidopsis thaliana: RNAs are heterogeneous and only two of the genomic 5S loci produce mature 5S RNA. *Genome research*, *12*(1), 132–144.

Cognat, V., Pawlak, G., Duchêne, A. M., Daujat, M., Gigant, A., Salinas, T., Michaud, M., Gutmann, B., Giegé, P., Gobert, A., & Maréchal-Drouard, L. (2013). PlantRNA, a database for tRNAs of photosynthetic eukaryotes. *Nucleic acids research*, *41*(Database issue), D273–D279.

Comella, P., Pontvianne, F., Lahmy, S., Vignols, F., Barbezier, N., Debures, A., Jobet, E., Brugidou, E., Echeverria, M., & Sáez-Vásquez, J. (2008). Characterization of a ribonuclease III-like protein required for cleavage of the pre-rRNA in the 3'ETS in Arabidopsis. *Nucleic acids research*, *36*(4), 1163–1175.

Copenhaver, G. P., & Pikaard, C. S. (1996). RFLP and physical mapping with an rDNA-specific endonuclease reveals that nucleolus organizer regions of Arabidopsis thaliana adjoin the telomeres on chromosomes 2 and 4. *The Plant journal: for cell and molecular biology*, *9*(2), 259–272.

Coute, Y., Kindbeiter, K., Belin, S., Dieckmann, R., Duret, L., Bezin, L., Sanchez, J..C and Diaz J.J. (2008) ISG20L2, a novel vertebrate nucleolar exoribonuclease involved in ribosome biogenesis. Mol Cell Proteomics 7, 546– 559.

Decatur, W. A., & Fournier, M. J. (2002). rRNA modifications and ribosome function. *Trends in biochemical sciences*, *27*(7), 344–351.

Deryusheva, S., & Gall, J. G. (2019). scaRNAs and snoRNAs: Are they limited to specific classes of substrate RNAs? *RNA (New York, N.Y.)*, *25*(1), 17–22.

Dieci, G., Preti, M., & Montanini, B. (2009). Eukaryotic snoRNAs: a paradigm for gene expression flexibility. *Genomics*, *94*(2), 83–88.

Dimitrova, D. G., Teysset, L., & Carré, C. (2019). RNA 2'-O-Methylation (Nm) Modification in Human Diseases. *Genes*, *10*(2), 117.

Dragon, F., Lemay, V., and Trahan, C. (2006). snoRNAs: biogenesis, structure and function. *Encycl. Life Sci*. 2006, 1–7.

Duncan, S., Olsson, T., Hartley, M., Dean, C., & Rosa, S. (2017). Single Molecule RNA FISH in *Arabidopsis* Root Cells. *Bio-protocol*, *7*(8), e2240.

Ebersberger, I., Simm, S., Leisegang, M. S., Schmitzberger, P., Mirus, O., von Haeseler, A., Bohnsack, M. T., & Schleiff, E. (2014). The evolution of the ribosome biogenesis pathway from a yeast perspective. *Nucleic acids research*, *42*(3), 1509–1523.

Edwards, K., Johnstone, C., & Thompson, C. (1991). A simple and rapid method for the preparation of plant genomic DNA for PCR analysis. *Nucleic acids research*, *19*(6), 1349.

Egebjerg, J., Douthwaite, S. R., Liljas, A., & Garrett, R. A. (1990). Characterization of the binding sites of protein L11 and the L10 (L12)4 pentameric complex in the GTPase domain of 23 S ribosomal RNA from Escherichia coli. *Journal of molecular biology*, *213*(2), 275–288.

Egecioglu, D. E., Henras, A. K., & Chanfreau, G. F. (2006). Contributions of Trf4p- and Trf5p-dependent polyadenylation to the processing and degradative functions of the yeast nuclear exosome. *RNA (New York, N.Y.)*, *12*(1), 26–32.

Endo, Y., Chan, Y. L., Lin, A., Tsurugi, K., & Wool, I. G. (1988). The cytotoxins alpha-sarcin and ricin retain their specificity when tested on a synthetic oligoribonucleotide (35-mer) that mimics a region of 28 S ribosomal ribonucleic acid. *The Journal of biological chemistry*, *263*(17), 7917–7920.

Erales, J., Marchand, V., Panthu, B., Gillot, S., Belin, S., Ghayad, S. E., Garcia, M., Laforêts, F., Marcel, V., Baudin-Baillieu, A., Bertin, P., Couté, Y., Adrait, A., Meyer, M., Therizols, G., Yusupov, M., Namy, O., Ohlmann, T., Motorin, Y., Catez, F., & Diaz, J. J. (2017). Evidence for rRNA 2'-O-methylation plasticity: Control of intrinsic translational capabilities of human ribosomes. *Proceedings of the National Academy of Sciences of the United States of America*, *114*(49), 12934–12939.

Faber, A. W., Vos, H. R., Vos, J. C., & Raué, H. A. (2006). 5'-end formation of yeast 5.8SL rRNA is an endonucleolytic event. *Biochemical and biophysical research communications*, *345*(2), 796–802.

Fafard-Couture, É., Bergeron, D., Couture, S., Abou-Elela, S., & Scott, M. S. (2021). Annotation of snoRNA abundance across human tissues reveals complex snoRNA-host gene relationships. *Genome biology*, *22*(1), 172.

Filippova, J. A., Matveeva, A. M., Zhuravlev, E. S., Balakhonova, E. A., Prokhorova, D. V., Malanin, S. J., Shah Mahmud, R., Grigoryeva, T. V., Anufrieva, K. S., Semenov, D. V., Vlassov, V. V., & Stepanov, G. A. (2019). Are Small Nucleolar RNAs "CRISPRable"? A Report on Box C/D Small Nucleolar RNA Editing in Human Cells. *Frontiers in pharmacology*, *10*, 1246.

Firmino, A., Gorka, M., Graf, A., Skirycz, A., Martinez-Seidel, F., Zander, K., Kopka, J., & Beine-Golovchuk, O. (2020). Separation and Paired Proteome Profiling of Plant Chloroplast and Cytoplasmic Ribosomes. *Plants (Basel, Switzerland)*, *9*(7), 892.

Fujii, K., Susanto, T. T., Saurabh, S., & Barna, M. (2018). Decoding the Function of Expansion Segments in Ribosomes. *Molecular cell*, *72*(6), 1013–1020.e6.

Gandin, V., Sikström, K., Alain, T., Morita, M., McLaughlan, S., Larsson, O., & Topisirovic, I. (2014). Polysome fractionation and analysis of mammalian translatomes on a genome-wide scale. *Journal of visualized experiments: JoVE*, (87), 51455.

Garreau de Loubresse, N., Prokhorova, I., Holtkamp, W., Rodnina, M. V., Yusupova, G., & Yusupov, M. (2014). Structural basis for the inhibition of the eukaryotic ribosome. *Nature*, *513*(7519), 517–522.

Gasse, L., Flemming, D., & Hurt, E. (2015). Coordinated Ribosomal ITS2 RNA Processing by the Las1 Complex Integrating Endonuclease, Polynucleotide Kinase, and Exonuclease Activities. *Molecular cell*, *60*(5), 808–815.

Ge, J., & Yu, Y. T. (2013). RNA pseudouridylation: new insights into an old modification. *Trends in biochemical sciences*, *38*(4), 210–218.

Gigova, A., Duggimpudi, S., Pollex, T., Schaefer, M., & Koš, M. (2014). A cluster of methylations in the domain IV of 25S rRNA is required for ribosome stability. *RNA (New York, N.Y.)*, *20*(10), 1632–1644.

Gómez Ramos, L. M., Smeekens, J. M., Kovacs, N. A., Bowman, J. C., Wartell, R. M., Wu, R., & Williams, L. D. (2016). Yeast rRNA Expansion Segments: Folding and Function. *Journal of molecular biology*, *428*(20), 4048–4059.

Granneman, S., Petfalski, E., & Tollervey, D. (2011). A cluster of ribosome synthesis factors regulate pre-rRNA folding and 5.8S rRNA maturation by the Rat1 exonuclease. *The EMBO journal*, *30*(19), 4006–4019.

Gregory, B., Rahman, N., Bommakanti, A., Shamsuzzaman, M., Thapa, M., Lescure, A., Zengel, J. M., & Lindahl, L. (2019). The small and large ribosomal subunits depend on each other for stability and accumulation. *Life science alliance*, *2*(4), e201900508.

Gy, I., Gasciolli, V., Lauressergues, D., Morel, J. B., Gombert, J., Proux, F., Proux, C., Vaucheret, H., & Mallory, A. C. (2007). Arabidopsis FIERY1, XRN2, and XRN3 are endogenous RNA silencing suppressors. *The Plant cell*, *19*(11), 3451–3461.

Hang, R., Wang, Z., Deng, X., Liu, C., Yan, B., Yang, C., Song, X., Mo, B., & Cao, X. (2018). Ribosomal RNA Biogenesis and Its Response to Chilling Stress in *Oryza sativa*. *Plant physiology*, *177*(1), 381–397.

Haruehanroengra, P., Zheng, Y. Y., Zhou, Y., Huang, Y., & Sheng, J. (2020). RNA modifications and cancer. *RNA biology*, *17*(11), 1560–1575.

Heerklotz, D., Döring, P., Bonzelius, F., Winkelhaus, S., & Nover, L. (2001). The balance of nuclear import and export determines the intracellular distribution and function of tomato heat stress transcription factor HsfA2. *Molecular and cellular biology*, *21*(5), 1759–1768.

Henras, A. K., Plisson-Chastang, C., O'Donohue, M. F., Chakraborty, A., & Gleizes, P. E. (2015). An overview of pre-ribosomal RNA processing in eukaryotes. *Wiley interdisciplinary reviews. RNA*, *6*(2), 225–242.

Henry, Y., Wood, H., Morrissey, J. P., Petfalski, E., Kearsey, S., & Tollervey, D. (1994). The 5' end of yeast 5.8S rRNA is generated by exonucleases from an upstream cleavage site. *The EMBO journal*, *13*(10), 2452–2463.

Hofacker I. L. (2003). Vienna RNA secondary structure server. *Nucleic acids research*, *31*(13), 3429–3431.

Holley, C. L., Li, M. W., Scruggs, B. S., Matkovich, S. J., Ory, D. S., & Schaffer, J. E. (2015). Cytosolic accumulation of small nucleolar RNAs (snoRNAs) is dynamically regulated by NADPH oxidase. *The Journal of biological chemistry*, *290*(18), 11741–11748.

Hsu, Y. F., Chen, Y. C., Hsiao, Y. C., Wang, B. J., Lin, S. Y., Cheng, W. H., Jauh, G. Y., Harada, J. J., & Wang, C. S. (2014). AtRH57, a DEAD-box RNA helicase, is involved in feedback inhibition of glucose-mediated abscisic acid accumulation during seedling development and additively affects pre-ribosomal RNA processing with high glucose. *The Plant journal: for cell and molecular biology*, *77*(1), 119–135.

Huang, H., & Karbstein, K. (2021). Assembly factors chaperone ribosomal RNA folding by isolating helical junctions that are prone to misfolding. *Proceedings of the National Academy of Sciences of the United States of America*, *118*(25), e2101164118.

Ishida, T., Maekawa, S., & Yanagisawa, S. (2016). The Pre-rRNA Processing Complex in Arabidopsis Includes Two WD40-Domain-Containing Proteins Encoded by Glucose-Inducible Genes and Plant-Specific Proteins. *Molecular plant*, *9*(2), 312–315.

Ito, S., Akamatsu, Y., Noma, A., Kimura, S., Miyauchi, K., Ikeuchi, Y., Suzuki, T., & Suzuki, T. (2014). A single acetylation of 18 S rRNA is essential for biogenesis of the small ribosomal subunit in Saccharomyces cerevisiae. *The Journal of biological chemistry*, *289*(38), 26201–26212.

Jorjani, H., Kehr, S., Jedlinski, D. J., Gumienny, R., Hertel, J., Stadler, P. F., Zavolan, M., & Gruber, A. R. (2016). An updated human snoRNAome. *Nucleic acids research*, *44*(11), 5068–5082.

Kalvari, I., Argasinska, J., Quinones-Olvera, N., Nawrocki, E. P., Rivas, E., Eddy, S. R., Bateman, A., Finn, R. D., & Petrov, A. I. (2018). Rfam 13.0: shifting to a genome-centric resource for non-coding RNA families. *Nucleic acids research*, *46*(D1), D335–D342.

Kerpedjiev, P., Hammer, S., & Hofacker, I. L. (2015). Forna (force-directed RNA): Simple and effective online RNA secondary structure diagrams. *Bioinformatics (Oxford, England)*, *31*(20), 3377–3379.

Khatter, H., Myasnikov, A. G., Natchiar, S. K., & Klaholz, B. P. (2015). Structure of the human 80S ribosome. *Nature*, *520*(7549), 640–645.

Kim, D. F., & Green, R. (1999). Base-pairing between 23S rRNA and tRNA in the ribosomal A site. *Molecular cell*, *4*(5), 859–864.

Kim, S. H., Spensley, M., Choi, S. K., Calixto, C. P., Pendle, A. F., Koroleva, O., Shaw, P. J., & Brown, J. W. (2010). Plant U13 orthologues and orphan snoRNAs identified by RNomics of RNA from Arabidopsis nucleoli. *Nucleic acids research*, *38*(9), 3054–3067.

Kiss T. (2001). Small nucleolar RNA-guided post-transcriptional modification of cellular RNAs. *The EMBO journal*, *20*(14), 3617–3622.

Knorr, A. G., Schmidt, C., Tesina, P., Berninghausen, O., Becker, T., Beatrix, B., & Beckmann, R. (2019). Ribosome-NatA architecture reveals that rRNA expansion segments coordinate N-terminal acetylation. *Nature structural & molecular biology*, *26*(1), 35–39.

Konikkat, S., & Woolford, J. L., Jr (2017). Principles of 60S ribosomal subunit assembly emerging from recent studies in yeast. *The Biochemical journal*, *474*(2), 195–214.

Kressler, D., Linder, P., & de La Cruz, J. (1999). Protein trans-acting factors involved in ribosome biogenesis in Saccharomyces cerevisiae. *Molecular and cellular biology*, *19*(12), 7897–7912.

Kruszka, K., Barneche, F., Guyot, R., Ailhas, J., Meneau, I., Schiffer, S., Marchfelder, A., & Echeverría, M. (2003). Plant dicistronic tRNA-snoRNA genes: a new mode of expression of the small nucleolar RNAs processed by RNase Z. *The EMBO journal*, *22*(3), 621–632.

Kumakura, N., Otsuki, H., Tsuzuki, M., Takeda, A., and Watanabe, Y. (2013). Arabidopsis AtRRP44A is the functional homolog of Rrp44/Dis3, an exosome component, is essential for viability and is required for RNA processing and degradation. *PloS one*, *8*(11), e79219.

Laemmli U. K. (1970). Cleavage of structural proteins during the assembly of the head of bacteriophage T4. *Nature*, *227*(5259), 680–685.

Lafontaine D. L. (2015). Noncoding RNAs in eukaryotic ribosome biogenesis and function. *Nature structural & molecular biology*, *22*(1), 11–19.

Lange, H., Holec, S., Cognat, V., Pieuchot, L., Le Ret, M., Canaday, J., & Gagliardi, D. (2008). Degradation of a polyadenylated rRNA maturation by-product involves one of the three RRP6-like proteins in Arabidopsis thaliana. *Molecular and cellular biology*, *28*(9), 3038–3044.

Lange, H., Sement, F. M., & Gagliardi, D. (2011). MTR4, a putative RNA helicase and exosome co-factor, is required for proper rRNA biogenesis and development in Arabidopsis thaliana. *The Plant journal: for cell and molecular biology*, *68*(1), 51–63.

Lau, R. Y., Kennedy, T. D., & Lane, B. G. (1974). Wheat-embryo ribonucleates. III. Modified nucleotide constituents in each of the 5.8S, 18S and 26S ribonucleates. *Canadian journal of biochemistry*, *52*(12), 1110–1123.

Layat, E., Sáez-Vásquez, J., & Tourmente, S. (2012). Regulation of Pol I-transcribed 45S rDNA and Pol III-transcribed 5S rDNA in Arabidopsis. *Plant & cell physiology*, *53*(2), 267–276.

Leader, D. J., Clark, G. P., Watters, J., Beven, A. F., Shaw, P. J., & Brown, J. W. (1997). Clusters of multiple different small nucleolar RNA genes in plants are expressed as and processed from polycistronic pre-snoRNAs. *The EMBO journal*, *16*(18), 5742–5751.

Li, M. W., Sletten, A. C., Lee, J., Pyles, K. D., Matkovich, S. J., Ory, D. S., & Schaffer, J. E. (2017). Nuclear export factor 3 regulates localization of small nucleolar RNAs. *The Journal of biological chemistry*, *292*(49), 20228–20239.

Li, M., Yu, H., Liu, K., Yang, W., Zhou, B., Gan, L., Li, S., Zhang, C., & Yu, B. (2021). Serrate-Associated Protein 1, a splicing-related protein, promotes miRNA biogenesis in Arabidopsis. *The New phytologist*, *232*(5), 1959–1973.

Liang, J., Wen, J., Huang, Z., Chen, X. P., Zhang, B. X., & Chu, L. (2019). Small Nucleolar RNAs: Insight Into Their Function in Cancer. *Frontiers in oncology*, *9*, 587.

Liang, X. H., & Crooke, S. T. (2011). Depletion of key protein components of the RISC pathway impairs pre-ribosomal RNA processing. *Nucleic acids research*, *39*(11), 4875–4889.

Liang, X. H., Liu, Q., & Fournier, M. J. (2009). Loss of rRNA modifications in the decoding center of the ribosome impairs translation and strongly delays pre-rRNA processing. *RNA (New York, N.Y.)*, *15*(9), 1716–1728.

Lo, A. C., & Nazar, R. N. (1982). Topography of 5.8 S rRNA in rat liver ribosomes. Identification of diethyl pyrocarbonate-reactive sites. *The Journal of biological chemistry*, *257*(7), 3516–3524.

Locati, M. D., Pagano, J., Girard, G., Ensink, W. A., van Olst, M., van Leeuwen, S., Nehrdich, U., Spaink, H. P., Rauwerda, H., Jonker, M. J., Dekker, R. J., & Breit, T. M. (2017). Expression of distinct maternal and somatic 5.8S, 18S, and 28S rRNA types during zebrafish development. *RNA (New York, N.Y.)*, *23*(8), 1188–1199.

Lui, L., & Lowe, T. (2013). Small nucleolar RNAs and RNA-guided post-transcriptional modification. *Essays in biochemistry*, *54*, 53–77.

Macbeth, M. R., & Wool, I. G. (1999). The phenotype of mutations of G2655 in the sarcin/ricin domain of 23 S ribosomal RNA. *Journal of molecular biology*, *285*(3), 965–975.

Marcel, V., Ghayad, S. E., Belin, S., Therizols, G., Morel, A. P., Solano-Gonzàlez, E., Vendrell, J. A., Hacot, S., Mertani, H. C., Albaret, M. A., Bourdon, J. C., Jordan, L., Thompson, A., Tafer, Y., Cong, R., Bouvet, P., Saurin, J. C., Catez, F., Prats, A. C., Puisieux, A., & Diaz, J. J. (2013). p53 acts as a safeguard of translational control by regulating fibrillarin and rRNA methylation in cancer. *Cancer cell*, *24*(3), 318–330.

Marker, C., Zemann, A., Terhörst, T., Kiefmann, M., Kastenmayer, J. P., Green, P., Bachellerie, J. P., Brosius, J., & Hüttenhofer, A. (2002). Experimental RNomics: identification of 140 candidates for small non-messenger RNAs in the plant Arabidopsis thaliana. *Current biology: CB*, *12*(23), 2002–2013.

Marz, M., Gruber, A. R., Höner Zu Siederdissen, C., Amman, F., Badelt, S., Bartschat, S., Bernhart, S. H., Beyer, W., Kehr, S., Lorenz, R., Tanzer, A., Yusuf, D., Tafer, H., Hofacker, I. L., & Stadler, P. F. (2011). Animal snoRNAs and scaRNAs with exceptional structures. *RNA biology*, *8*(6), 938–946.

Martinez-Seidel, F., Beine-Golovchuk, O., Hsieh, Y. C., & Kopka, J. (2020). Systematic Review of Plant Ribosome Heterogeneity and Specialization. *Frontiers in plant science*, *11*, 948.

Mathias, A. P., Williamson, R., Huxley, H. E., & Page, S. (1964). Occurrence And Function of Polysomes In Rabbit Reticulocytes. *Journal Of Molecular Biology*, *9*, 154–167.

McCool, M. A., Bryant, C. J., & Baserga, S. J. (2020). MicroRNAs and long non-coding RNAs as novel regulators of ribosome biogenesis. *Biochemical Society transactions*, *48*(2), 595–612.

McKeown, P., Pendle, A. F., & Shaw, P. J. (2008). Preparation of Arabidopsis nuclei and nucleoli. *Methods in molecular biology (Clifton, N.J.)*, *463*, 67–75.

Melnikov, S., Mailliot, J., Rigger, L., Neuner, S., Shin, B. S., Yusupova, G., Dever, T. E., Micura, R., & Yusupov, M. (2016). Molecular insights into protein synthesis with proline residues. *EMBO reports*, *17*(12), 1776–1784.

Micol-Ponce, R., Sarmiento-Mañús, R., Fontcuberta-Cervera, S., Cabezas-Fuster, A., de Bures, A., Sáez-Vásquez, J., & Ponce, M. R. (2020). SMALL ORGAN4 Is a Ribosome Biogenesis Factor Involved in 5.8S Ribosomal RNA Maturation. *Plant physiology*, *184*(4), 2022–2039.

Missbach, S., Weis, B. L., Martin, R., Simm, S., Bohnsack, M. T., & Schleiff, E. (2013). 40S ribosome biogenesis co-factors are essential for gametophyte and embryo development. *PloS one*, *8*(1), e54084.

Mleczko, A. M., Machtel, P., Walkowiak, M., Wasilewska, A., Pietras, P. J., & Bąkowska-Żywicka, K. (2019). Levels of sdRNAs in cytoplasm and their association with ribosomes are dependent upon stress conditions but independent from snoRNA expression. *Scientific reports*, *9*(1), 18397.

Motorin, Y., Quinternet, M., Rhalloussi, W., & Marchand, V. (2021). Constitutive and variable 2'-O-methylation (Nm) in human ribosomal RNA. *RNA biology*, *18*(sup1), 88–97.

Munro, A. J., Jackson, R. J., & Korner, A. (1964). Studies on the nature of polysomes. *The Biochemical journal*, *92*(2), 289–299.

Nawrocki, E. P., & Eddy, S. R. (2013). Infernal 1.1: 100-fold faster RNA homology searches. *Bioinformatics (Oxford, England)*, *29*(22), 2933–2935.

Nazar R. N. (1980). A 5.8 S rRNA-like sequence in prokaryotic 23 S rRNA. *FEBS letters*, *119*(2), 212–214.

Nazar, R. N. (1984). The ribosomal 5.8S RNA: eukaryotic adaptation or processing variant? *Canadian journal of biochemistry and cell biology = Revue canadienne de biochimie et biologie cellulaire*, *62*(6), 311–320.

Nazar, R. N., Sitz, T. O., & Busch, H. (1975). Structural analyses of mammalian ribosomal ribonucleic acid and its precursors. Nucleotide sequence of ribosomal 5.8 S ribonucleic acid. *The Journal of biological chemistry*, *250*(22), 8591–8597.

Norris, K., Hopes, T., & Aspden, J. L. (2021). Ribosome heterogeneity and specialization in development. *Wiley interdisciplinary reviews. RNA*, *12*(4), e1644.

Nostramo, R. T., & Hopper, A. K. (2019). Beyond rRNA and snRNA: tRNA as a 2'-O-methylation target for nucleolar and Cajal body box C/D RNPs. *Genes & development*, *33*(13-14), 739–740.

Nygård, O., Alkemar, G., & Larsson, S. L. (2006). Analysis of the secondary structure of expansion segment 39 in ribosomes from fungi, plants and mammals. *Journal of molecular biology*, *357*(3), 904–916.

Ojha, S., Malla, S., & Lyons, S. M. (2020). snoRNPs: Functions in Ribosome Biogenesis. *Biomolecules*, *10*(5), 783.

Paci, M., & Fox, G. E. (2015). Major centers of motion in the large ribosomal RNAs. *Nucleic acids research*, *43*(9), 4640–4649.

Palm, D., Simm, S., Darm, K., Weis, B. L., Ruprecht, M., Schleiff, E., & Scharf, C. (2016). Proteome distribution between nucleoplasm and nucleolus and its relation to ribosome biogenesis in Arabidopsis thaliana. *RNA biology*, *13*(4), 441–454.

Palm, D., Streit, D., Ruprecht, M., Simm, S., Scharf, C., & Schleiff, E. (2018). Late ribosomal protein localization in *Arabidopsis thaliana* differs to that in *Saccharomyces cerevisiae*. *FEBS open bio*, *8*(9), 1437–1444.

Palm, D., Streit, D., Shanmugam, T., Weis, B. L., Ruprecht, M., Simm, S., & Schleiff, E. (2019). Plant-specific ribosome biogenesis factors in Arabidopsis thaliana with essential function in rRNA processing. *Nucleic acids research*, *47*(4), 1880–1895.

Pendle, A. F., Clark, G. P., Boon, R., Lewandowska, D., Lam, Y. W., Andersen, J., Mann, M., Lamond, A. I., Brown, J. W., & Shaw, P. J. (2005). Proteomic analysis of the Arabidopsis nucleolus suggests novel nucleolar functions. *Molecular biology of the cell*, *16*(1), 260–269.

Penzo, M., Casoli, L., Ceccarelli, C., Treré, D., Ludovini, V., Crinò, L., & Montanaro, L. (2013). DKC1 gene mutations in human sporadic cancer. *Histology and histopathology*, *28*(3), 365–372.

Penzo, M., Galbiati, A., Treré, D., & Montanaro, L. (2016). The importance of being (slightly) modified: The role of rRNA editing on gene expression control and its connections with cancer. *Biochimica et biophysica acta*, *1866*(2), 330–338.

Pertschy, B., Schneider, C., Gnädig, M., Schäfer, T., Tollervey, D., & Hurt, E. (2009). RNA helicase Prp43 and its co-factor Pfa1 promote 20 to 18 S rRNA processing catalyzed by the endonuclease Nob1. *The Journal of biological chemistry*, *284*(50), 35079–35091.

Pestov, D. G., Stockelman, M. G., Strezoska, Z., & Lau, L. F. (2001). ERB1, the yeast homolog of mammalian Bop1, is an essential gene required for maturation of the 25S and 5.8S ribosomal RNAs. *Nucleic acids research*, *29*(17), 3621–3630.

Piekna-Przybylska, D., Decatur, W. A., & Fournier, M. J. (2008). The 3D rRNA modification maps database: with interactive tools for ribosome analysis. *Nucleic acids research*, *36*(Database issue), D178–D183.

Pilla, S. P., Thomas, A., & Bahadur, R. P. (2019). Dissecting macromolecular recognition sites in ribosome: implication to its self-assembly. *RNA biology*, *16*(9), 1300–1312.

Pillet, B., Mitterer, V., Kressler, D., & Pertschy, B. (2017). Hold on to your friends: Dedicated chaperones of ribosomal proteins: Dedicated chaperones mediate the safe transfer of ribosomal proteins to their site of pre-ribosome incorporation. *BioEssays : news and reviews in molecular, cellular and developmental biology*, *39*(1), 1–12.

Pirouz, M., Munafò, M., Ebrahimi, A. G., Choe, J., & Gregory, R. I. (2019). Exonuclease requirements for mammalian ribosomal RNA biogenesis and surveillance. *Nature structural & molecular biology*, *26*(6), 490–500.

Polacek, N., & Mankin, A. S. (2005). The ribosomal peptidyl transferase center: structure, function, evolution, inhibition. *Critical reviews in biochemistry and molecular biology*, *40*(5), 285–311.

Popenda, M., Szachniuk, M., Antczak, M., Purzycka, K. J., Lukasiak, P., Bartol, N., Blazewicz, J., & Adamiak, R. W. (2012). Automated 3D structure composition for large RNAs. *Nucleic acids research*, *40*(14), e112.

Pöll, G., Braun, T., Jakovljevic, J., Neueder, A., Jakob, S., Woolford, J. L., Jr, Tschochner, H., & Milkereit, P. (2009). rRNA maturation in yeast cells depleted of large ribosomal subunit proteins. *PloS one*, *4*(12), e8249.

Preti, M., O'Donohue, M. F., Montel-Lehry, N., Bortolin-Cavaillé, M. L., Choesmel, V., & Gleizes, P. E. (2013). Gradual processing of the ITS1 from the nucleolus to the

cytoplasm during synthesis of the human 18S rRNA. *Nucleic acids research*, *41*(8), 4709–4723.

Qu, G., Kruszka, K., Plewka, P., Yang, S. Y., Chiou, T. J., Jarmolowski, A., Szweykowska-Kulinska, Z., Echeverria, M., & Karlowski, W. M. (2015). Promoter-based identification of novel non-coding RNAs reveals the presence of dicistronic snoRNA-miRNA genes in Arabidopsis thaliana. *BMC genomics*, *16*, 1009.

Qu, L. H., Meng, Q., Zhou, H., & Chen, Y. Q. (2001). Identification of 10 novel snoRNA gene clusters from Arabidopsis thaliana. *Nucleic acids research*, *29*(7), 1623–1630.

Quast, C., Pruesse, E., Yilmaz, P., Gerken, J., Schweer, T., Yarza, P., Peplies, J., & Glöckner, F. O. (2013). The SILVA ribosomal RNA gene database project: improved data processing and web-based tools. *Nucleic acids research*, *41*(Database issue), D590–D596.

Raghunathan, P. L., & Guthrie, C. (1998). A spliceosomal recycling factor that reanneals U4 and U6 small nuclear ribonucleoprotein particles. *Science (New York, N.Y.)*, *279*(5352), 857–860.

Rodor, J., Jobet, E., Bizarro, J., Vignols, F., Carles, C., Suzuki, T., Nakamura, K., & Echeverría, M. (2011). AtNUFIP, an essential protein for plant development, reveals the impact of snoRNA gene organisation on the assembly of snoRNPs and rRNA methylation in Arabidopsis thaliana. *The Plant journal: for cell and molecular biology*, *65*(5), 807–819.

Rodríguez-Galán, O., García-Gómez, J. J., Kressler, D., & de la Cruz, J. (2015). Immature large ribosomal subunits containing the 7S pre-rRNA can engage in translation in Saccharomyces cerevisiae. *RNA biology*, *12*(8), 838–846.

Rostom, A. A., Fucini, P., Benjamin, D. R., Juenemann, R., Nierhaus, K. H., Hartl, F. U., Dobson, C. M., & Robinson, C. V. (2000). Detection and selective dissociation of intact ribosomes in a mass spectrometer. *Proceedings of the National Academy of Sciences of the United States of America*, *97*(10), 5185–5190.

Runte, M., Hüttenhofer, A., Gross, S., Kiefmann, M., Horsthemke, B., & Buiting, K. (2001). The IC-SNURF-SNRPN transcript serves as a host for multiple small nucleolar RNA species and as an antisense RNA for UBE3A. *Human molecular genetics*, *10*(23), 2687–2700.

Ryan, P. C., & Draper, D. E. (1991). Detection of a key tertiary interaction in the highly conserved GTPase center of large subunit ribosomal RNA. *Proceedings of the National Academy of Sciences of the United States of America*, *88*(14), 6308–6312.

Sáez-Vásquez, J., & Delseny, M. (2019). Ribosome Biogenesis in Plants: From Functional 45S Ribosomal DNA Organization to Ribosome Assembly Factors. *The Plant cell*, *31*(9), 1945–1967.

Sakyiama, J., Zimmer, S. L., Ciganda, M., Williams, N., & Read, L. K. (2013). Ribosome biogenesis requires a highly diverged XRN family 5'->3' exoribonuclease for rRNA processing in Trypanosoma brucei. *RNA (New York, N.Y.)*, *19*(10), 1419–1431.

Sambrook, J., and Russell, D.W. (2001). Molecular Cloning: A Laboratory Manual 3rd Edition. (Cold Spring Harbor: Cold Spring Harbor Laboratory Press).

Sanz, E., Bean, J. C., Carey, D. P., Quintana, A., & McKnight, G. S. (2019). RiboTag: Ribosomal Tagging Strategy to Analyze Cell-Type-Specific mRNA Expression In Vivo. *Current protocols in neuroscience*, *88*(1), e77.

Schilders, G., van Dijk, E., & Pruijn, G. J. (2007). C1D and hMtr4p associate with the human exosome subunit PM/Scl-100 and are involved in pre-rRNA processing. *Nucleic acids research*, *35*(8), 2564–2572.

Schillewaert, S., Wacheul, L., Lhomme, F., & Lafontaine, D. L. (2012). The evolutionarily conserved protein Las1 is required for pre-rRNA processing at both ends of ITS2. *Molecular and cellular biology*, *32*(2), 430–444.

Schluenzen, F., Tocilj, A., Zarivach, R., Harms, J., Gluehmann, M., Janell, D., Bashan, A., Bartels, H., Agmon, I., Franceschi, F., & Yonath, A. (2000). Structure of functionally activated small ribosomal subunit at 3.3 angstroms resolution. *Cell*, *102*(5), 615–623.

Schneider, C. A., Rasband, W. S., & Eliceiri, K. W. (2012). NIH Image to ImageJ: 25 years of image analysis. *Nature methods*, *9*(7), 671–675.

Schneider-Poetsch, T., Ju, J., Eyler, D. E., Dang, Y., Bhat, S., Merrick, W. C., Green, R., Shen, B., & Liu, J. O. (2010). Inhibition of eukaryotic translation elongation by cycloheximide and lactimidomycin. *Nature chemical biology*, *6*(3), 209–217.

Schwartz, S., Bernstein, D. A., Mumbach, M. R., Jovanovic, M., Herbst, R. H., León-Ricardo, B. X., Engreitz, J. M., Guttman, M., Satija, R., Lander, E. S., Fink, G., & Regev, A. (2014). Transcriptome-wide mapping reveals widespread dynamic-regulated pseudouridylation of ncRNA and mRNA. *Cell*, *159*(1), 148–162.

Sedlazeck, F. J., Rescheneder, P., & von Haeseler, A. (2013). NextGenMap: fast and accurate read mapping in highly polymorphic genomes. *Bioinformatics (Oxford, England)*, *29*(21), 2790–2791.

Sergiev, P. V., Lesnyak, D. V., Burakovsky, D. E., Kiparisov, S. V., Leonov, A. A., Bogdanov, A. A., Brimacombe, R., & Dontsova, O. A. (2005). Alteration in location of a conserved GTPase-associated center of the ribosome induced by mutagenesis influences the structure of peptidyltransferase center and activity of elongation factor G. *The Journal of biological chemistry*, *280*(36), 31882–31889.

Shanmugam, T., Abbasi, N., Kim, H. S., Kim, H. B., Park, N. I., Park, G. T., Oh, S. A., Park, S. K., Muench, D. G., Choi, Y., Park, Y. I., & Choi, S. B. (2017). An Arabidopsis divergent pumilio protein, APUM24, is essential for embryogenesis and required for faithful pre-rRNA processing. *The Plant journal: for cell and molecular biology*, *92*(6), 1092–1105.

Shanmugam, T., Streit, D., Schroll, F., Kovacevic, J., & Schleiff, E. (2021). Dynamics and thermal sensitivity of ribosomal RNA maturation paths in plants. *Journal of experimental botany*, erab434. Advance online publication.

Sharma, S., & Lafontaine, D. (2015). 'View From A Bridge': A New Perspective on Eukaryotic rRNA Base Modification. *Trends in biochemical sciences*, *40*(10), 560–575.

Sharma, S., Yang, J., van Nues, R., Watzinger, P., Kötter, P., Lafontaine, D., Granneman, S., & Entian, K. D. (2017b). Specialized box C/D snoRNPs act as antisense guides to target RNA base acetylation. *PLoS genetics*, *13*(5), e1006804.

Shi, Z., Fujii, K., Kovary, K. M., Genuth, N. R., Röst, H. L., Teruel, M. N., & Barna, M. (2017). Heterogeneous Ribosomes Preferentially Translate Distinct Subpools of mRNAs Genome-wide. *Molecular cell*, *67*(1), 71–83.e7.

Sikorski, P. J., Zuber, H., Philippe, L., Sement, F. M., Canaday, J., Kufel, J., Gagliardi, D., & Lange, H. (2015). Distinct 18S rRNA precursors are targets of the exosome complex, the exoribonuclease RRP6L2 and the terminal nucleotidyltransferase TRL in Arabidopsis thaliana. *The Plant journal : for cell and molecular biology*, *83*(6), 991–1004.

Simm, S., Fragkostefanakis, S., Paul, P., Keller, M., Einloft, J., Scharf, K. D., & Schleiff, E. (2015). Identification and Expression Analysis of Ribosome Biogenesis Factor Co-orthologs in Solanum lycopersicum. *Bioinformatics and biology insights*, *9*, 1–17.

Sloan, K. E., Mattijssen, S., Lebaron, S., Tollervey, D., Pruijn, G. J., & Watkins, N. J. (2013). Both endonucleolytic and exonucleolytic cleavage mediate ITS1 removal during human ribosomal RNA processing. *The Journal of cell biology*, *200*(5), 577–588.

Sloan, K. E., Warda, A. S., Sharma, S., Entian, K. D., Lafontaine, D., & Bohnsack, M. T. (2017). Tuning the ribosome: The influence of rRNA modification on eukaryotic ribosome biogenesis and function. *RNA biology*, *14*(9), 1138–1152.

Spahn, C. M., Beckmann, R., Eswar, N., Penczek, P. A., Sali, A., Blobel, G., & Frank, J. (2001). Structure of the 80S ribosome from Saccharomyces cerevisiae--tRNA-ribosome and subunit-subunit interactions. *Cell*, *107*(3), 373–386.

Sridhar, P., Gan, H. H., & Schlick, T. (2008). A computational screen for C/D box snoRNAs in the human genomic region associated with Prader-Willi and Angelman syndromes. *Journal of biomedical science*, *15*(6), 697–705.

Streit, D., & Schleiff, E. (2021). The Arabidopsis 2'-O-Ribose-Methylation and Pseudouridylation Landscape of rRNA in Comparison to Human and Yeast. *Frontiers in plant science*, *12*, 684626.

Streit, D., Shanmugam, T., Garbelyanski, A., Simm, S., & Schleiff, E. (2020). The Existence and Localization of Nuclear snoRNAs in *Arabidopsis thaliana* Revisited. *Plants (Basel, Switzerland)*, *9*(8), 1016.

Sun, L., Xu, Y., Bai, S., Bai, X., Zhu, H., Dong, H., Wang, W., Zhu, X., Hao, F., & Song, C. P. (2019). Transcriptome-wide analysis of pseudouridylation of mRNA and non-coding RNAs in Arabidopsis. *Journal of experimental botany*, *70*(19), 5089–5600.

Sun, L., Xu, Y., Bai, S., Bai, X., Zhu, H., Dong, H., Wang, W., Zhu, X., Hao, F., & Song, C. P. (2019). Transcriptome-wide analysis of pseudouridylation of mRNA and non-coding RNAs in Arabidopsis. *Journal of experimental botany*, *70*(19), 5089–5600.

Taoka, M., Nobe, Y., Yamaki, Y., Sato, K., Ishikawa, H., Izumikawa, K., Yamauchi, Y., Hirota, K., Nakayama, H., Takahashi, N., & Isobe, T. (2018). Landscape of the complete RNA chemical modifications in the human 80S ribosome. *Nucleic acids research*, *46*(18), 9289–9298.

The RNAcentral Consortium (2019). RNAcentral: a hub of information for non-coding RNA sequences. *Nucleic acids research*, *47*(D1), D221–D229.

Thomson, E., & Tollervey, D. (2010). The final step in 5.8S rRNA processing is cytoplasmic in Saccharomyces cerevisiae. *Molecular and cellular biology*, *30*(4), 976–984.

Tomecki, R., Sikorski, P. J., & Zakrzewska-Placzek, M. (2017). Comparison of preribosomal RNA processing pathways in yeast, plant and human cells - focus on coordinated action of endo- and exoribonucleases. *FEBS letters*, *591*(13), 1801–1850.

Toots, I., Metspalu, A., Lind, A., Saarma, M., & Villems, R. (1979). Immobilized eukaryotic 5.8 S RNA binds Escherichia coli and rat liver ribosomal proteins. *FEBS letters*, *104*(1), 193–196.

Tsang, C. K., Bertram, P. G., Ai, W., Drenan, R., & Zheng, X. F. (2003). Chromatin-mediated regulation of nucleolar structure and RNA Pol I localization by TOR. *The EMBO journal*, *22*(22), 6045–6056.

Ulker, B., Peiter, E., Dixon, D. P., Moffat, C., Capper, R., Bouché, N., Edwards, R., Sanders, D., Knight, H., & Knight, M. R. (2008). Getting the most out of publicly available T-DNA insertion lines. *The Plant journal : for cell and molecular biology*, *56*(4), 665–677.

Venturi, G., Zacchini, F., Vaccari, C. L., Trerè, D., & Montanaro, L. (2021). Primer extension coupled with fragment analysis for rapid and quantitative evaluation of 5.8S rRNA isoforms. *PloS one*, *16*(12), e0261476.

Wang, M., Parshin, A. V., Shcherbik, N., & Pestov, D. G. (2015). Reduced expression of the mouse ribosomal protein Rpl17 alters the diversity of mature ribosomes by enhancing production of shortened 5.8S rRNA. *RNA (New York, N.Y.)*, *21*(7), 1240–1248.

Wang, X. J., Reyes, J. L., Chua, N. H., & Gaasterland, T. (2004). Prediction and identification of Arabidopsis thaliana microRNAs and their mRNA targets. *Genome biology*, *5*(9), R65.

Weis, B. L., Kovacevic, J., Missbach, S., & Schleiff, E. (2015a). Plant-Specific Features of Ribosome Biogenesis. *Trends in plant science*, *20*(11), 729–740.

Weis, B. L., Missbach, S., Marzi, J., Bohnsack, M. T., & Schleiff, E. (2014). The 60S associated ribosome biogenesis factor LSG1-2 is required for 40S maturation in Arabidopsis thaliana. *The Plant journal: for cell and molecular biology*, *80*(6), 1043–1056.

Weis, B. L., Palm, D., Missbach, S., Bohnsack, M. T., & Schleiff, E. (2015b). atBRX1-1 and atBRX1-2 are involved in an alternative rRNA processing pathway in Arabidopsis thaliana. *RNA (New York, N.Y.)*, *21*(3), 415–425.

Weis, B.L. (2015). Pre-rRNA processing in A. thaliana and the role of 60S ribosome biogenesis factors. [Doctoral dissertation, Goethe University].

Wilson, D. M., Li, Y., LaPeruta, A., Gamalinda, M., Gao, N., & Woolford, J. L., Jr (2020). Structural insights into assembly of the ribosomal nascent polypeptide exit tunnel. *Nature communications*, *11*(1), 5111.

Woolford, J. L., Jr, & Baserga, S. J. (2013). Ribosome biogenesis in the yeast Saccharomyces cerevisiae. *Genetics*, *195*(3), 643–681.

Wu, S., Wang, Y., Wang, J., Li, X., Li, J., & Ye, K. (2021). Profiling of RNA ribose methylation in Arabidopsis thaliana. *Nucleic acids research*, *49*(7), 4104–4119.

Xie, Z., Allen, E., Fahlgren, N., Calamar, A., Givan, S. A., & Carrington, J. C. (2005). Expression of Arabidopsis MIRNA genes. *Plant physiology*, *138*(4), 2145–2154.

Yanshina, D. D., Bulygin, K. N., Malygin, A. A., & Karpova, G. G. (2015). Hydroxylated histidine of human ribosomal protein uL2 is involved in maintaining the local structure of 28S rRNA in the ribosomal peptidyl transferase center. *The FEBS journal*, *282*(8), 1554–1566.

You, C., He, W., Hang, R., Zhang, C., Cao, X., Guo, H., Chen, X., Cui, J., & Mo, B. (2019). FIERY1 promotes microRNA accumulation by suppressing rRNA-derived small interfering RNAs in Arabidopsis. *Nature communications*, *10*(1), 4424.

Yoshihama, M., Nakao, A., & Kenmochi, N. (2013). snOPY: a small nucleolar RNA orthological gene database. *BMC research notes*, *6*, 426.

Zakrzewska-Placzek, M., Souret, F. F., Sobczyk, G. J., Green, P. J., & Kufel, J. (2010). Arabidopsis thaliana XRN2 is required for primary cleavage in the pre-ribosomal RNA. *Nucleic acids research*, *38*(13), 4487–4502.

Zhang, L., Lin, J., & Ye, K. (2013). Structural and functional analysis of the U3 snoRNA binding protein Rrp9. *RNA (New York, N.Y.)*, *19*(5), 701–711.

Zhang, Y. J., Yang, J. H., Shi, Q. S., Zheng, L. L., Liu, J., Zhou, H., Zhang, H., & Qu, L. H. (2014). Rapid birth-and-death evolution of imprinted snoRNAs in the Prader-Willi syndrome locus: implications for neural development in Euarchontoglires. *PloS one*, *9*(6), e100329.

Zhu, P., Wang, Y., Qin, N., Wang, F., Wang, J., Deng, X. W., & Zhu, D. (2016). Arabidopsis small nucleolar RNA monitors the efficient pre-rRNA processing during ribosome biogenesis. *Proceedings of the National Academy of Sciences of the United States of America*, *113*(42), 11967–11972.

Zywicki, M., Bakowska-Zywicka, K., & Polacek, N. (2012). Revealing stable processing products from ribosome-associated small RNAs by deep-sequencing data analysis. *Nucleic acids research*, *40*(9), 4013–4024.

8 Appendix

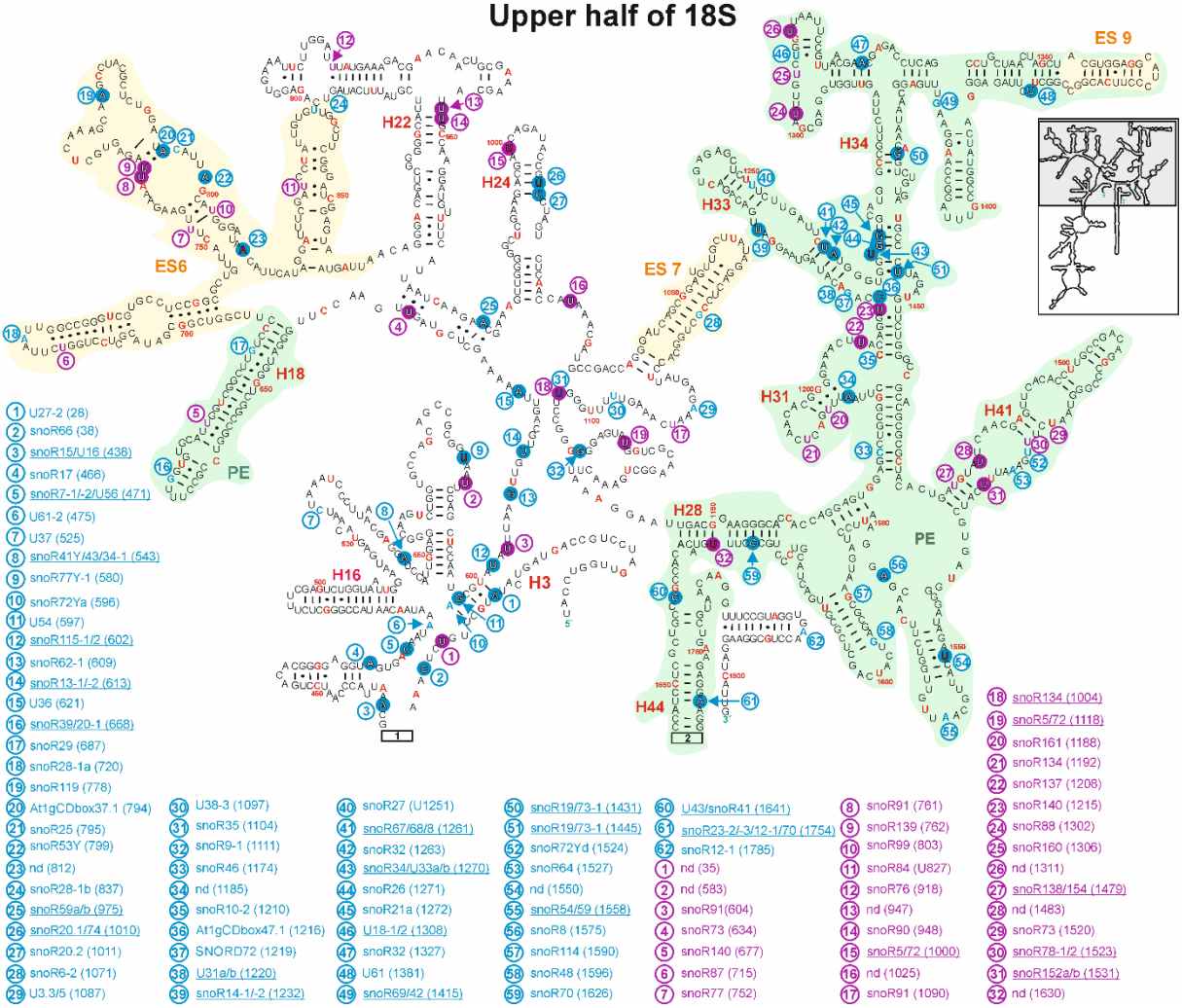

Figure S1. Secondary structure model of 18S rRNA (At2g01010) of *Arabidopsis thaliana*.
Depicted are the positions 1 to 41, 436 to 1655 and 1750 to 1804. The structure was created based on the RNAcentral database (The RNAcentral Consortium, 2019) and http://rna.icmb.utexas.edu. The 2´-O-methylation sites for predicted (blue letters) and verified positions (blue circle with white letters) and pseudouridylation sites for predicted (violet letters) and verified positions (violet circles with white letters) are shown. Next to modified positions, numbers in blue circles (C/D box) or violet circles (H/ACA box) indicate the snoRNA guiding the modification. Guiding snoRNAs were found using the snoRNA database snOPY (Yoshihama et al., 2013). If several snoRNAs are annotated to guide the modification, the name is underlined. Predicted and verified sites were obtained from Barneche et al. (2001), Brown et al. (2001), Qu et al. (20001), Sun et al. (2019) and Azevedo-Favory et al. (2020). Every tenth nucleotide is marked in red and every 50th nucleotide is labeled with the according number. Helices are labeled in red and the number (H1 etc.) A small illustration of the complete 40S rRNA in the higher right half is showing the position (grey) of the illustrated region. Framed large numbers indicate the position of the connections in Figure S2. PE annotates a pivoting element and ES expansion segments previously identified (Paci and Fox, 2015) Adapted from Streit and Schleiff, (2021).

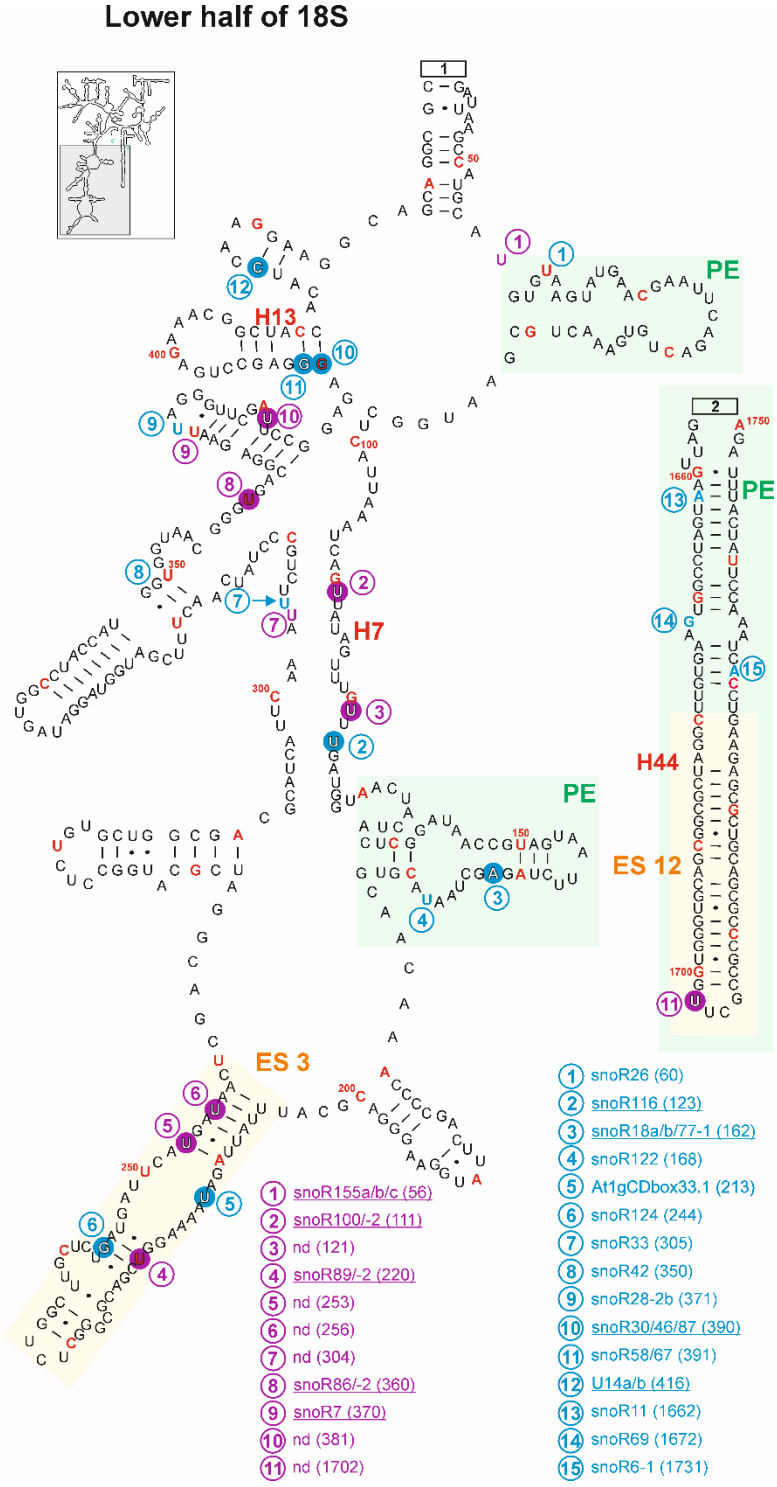

Figure S2. Secondary structure model of 18S rRNA (At2g01010) of *Arabidopsis thaliana*. Structure was created according to The RNA central Consortium (2019). All information is listed in the legend of Figure S1. Adapted from Streit and Schleiff (2021).

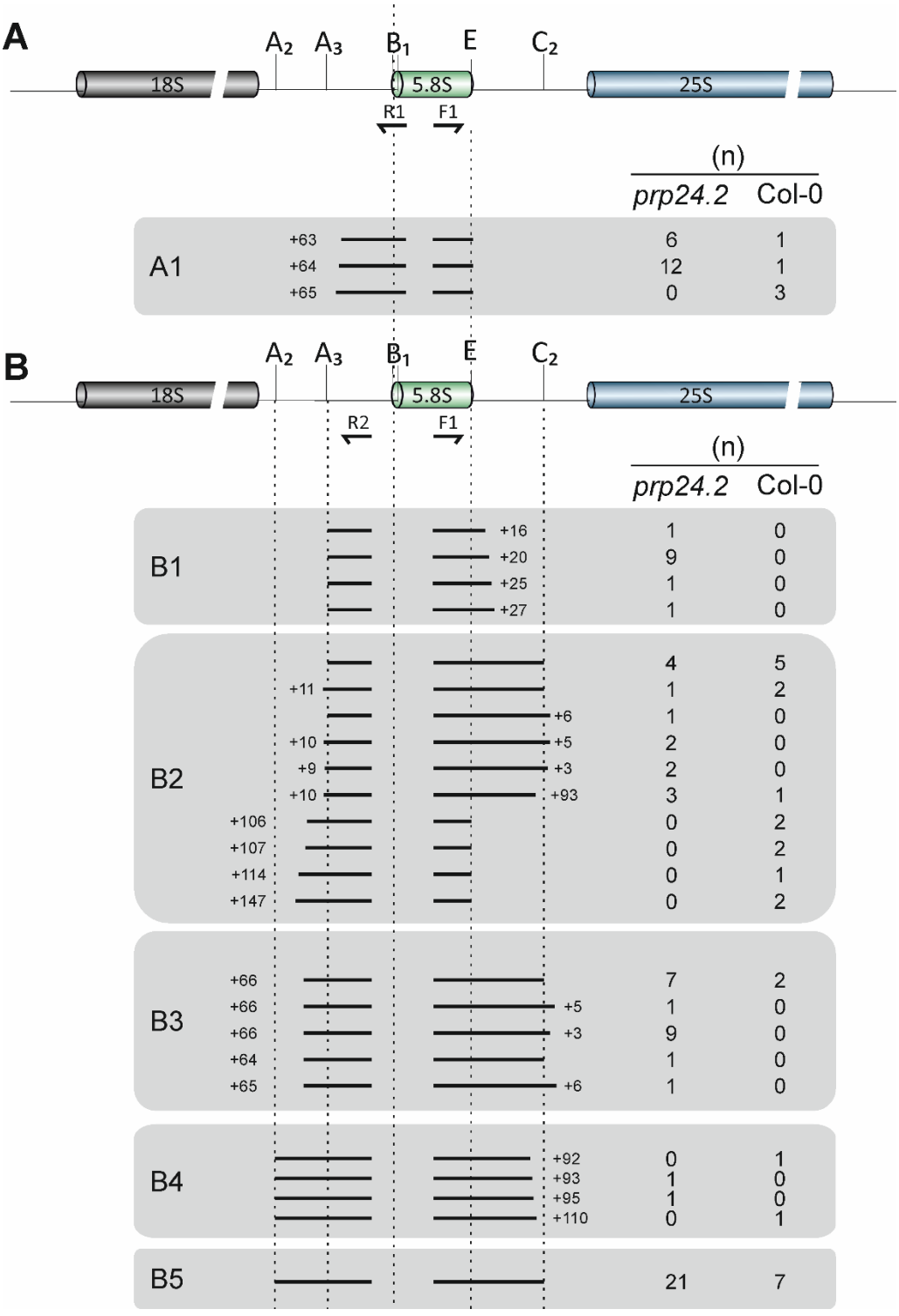

Figure S3. Heterogenous PCR products from 5.8S precursor screening.
A) PCR products that were sequenced when F1 and R1 oligos were used for circular RT-PCR. **B)** PCR products that were sequenced when F1 and R2 were used for circular RT-PCR. Numbers of identified precursors is given (n).

Table S1. Known snoRNAs with identified novel coding region.

Adapted from Streit et al. 2020

	Mapped region			NGS results				RFAM prediction							
snoRNA	Chr	Start	End	Nuc1	Nuc2	Nuc3	TotalCell	Best Hit RFAM	START snoRNA	END snoRNA	Rfam Box	predicted target RNA	start	end	Modified site
U3_1	1	3995022	3995162	0	2	0	0	Plant_U3 (p-val 0.00012)	3995063	3995114	H/ACA	25S rRNA	3267	3276	3270
snoR134	1	9241208	9241396	7	4	6	7	snoR134 (p-val 0.49)	9241298	9241394	C/D	unknown			
SNORD33	1	10300227	10300802	12679	9715	28644	5174	SNORD33 (p-val 9.1e^-10)	10300227	10300312	C/D	25S rRNA	3276	3287	G3280
snoR110	1	12388173	12388313	0	1	0	0	snoR110 (p-val 0.0029)	12388233	12388311	C/D	unknown			
snoU13	1	16992940	16993080	1	2	0	15	snoU13 (p-val 0.37)	16992993	16993017	C/D	unknown			
SNORD72	1	28212605	28213181	306	58	618	515	SNORD72 (p-val 0.000024)	28212629	28212706	C/D	18S rRNA	1211	1226	C1216/ G1219
snR58	2	3336759	3339906	0	2	1	0	snR58 (p-val 0.38)	3336761	3336799	H/ACA	25S rRNA	2254	2263	2259
SNORD57	2	4009331	4009472	0	2	3	5	SNORD57 (p-val 0.000063)	4009339	4009393	H/ACA	25S rRNA	2597	2626	2604
SNORD49	2	7520426	7520566	2144	2089	4050	957	SNORD49 (p-val 0.0016)	7520456	7520513	H/ACA	25S rRNA	682	703	690
snoR442	2	12114089	12114233	7	16	15	77	snoR442 (p-val 0.28)	12114120	12114139	C/D	unknown			
SNORD75	2	12585429	12585569	0	0	2	0	SNORD75 (p-val 0.000064)	12585440	12585505	H/ACA	25S rRNA	1969	1980	1974
snoR98	2	16294265	16294405	1	1	0	3	snoR98 (p-val 0.25)	16294303	16294376	C/D	unknown			
snR83	3	5156268	5156501	0	2	0	5	snR83 (p-val 0.33)	5156316	5156389	H/ACA	18S rRNA	1532	1546	1534
U3_3	3	11313455	11313612	194	133	366	101	Plant_U3 (p-val 0.00000018)	11313455	11313545	H/ACA	18S rRNA	1082	1094	1086
SNORD74	3	12520720	12520860	1	0	1	0	SNORD74 (p-val 0.39)	12520783	12520859	C/D	unknown			
snoR160	3	14203961	14205223	8	9	20	12	snoR160 (p-val 5.7)	14203983	14204044	H/ACA	25S rRNA	271	292	272
snoR12	3	16503994	16504134	0	0	1	2	snoR12 (p-val 0.44)	16504058	16504085	C/D	unknown			
snR77	4	5968737	5968877	3	6	9	8	snR77 (p-val 0.37)	5968764	5968790	H/ACA	18S rRNA			
SNORD27	4	7683700	7684093	85	75	200	104	SNORD27(p-val 2.4e^-9)	7683700	7683783	H/ACA	18S rRNA	1102	1122	1116
SNORD86	4	11458938	11459078	0	1	0	3	SNORD86(p-val0.0095)	11459053	11459078	H/ACA	25S rRNA	944	958	954
snoR135	4	13958526	13958666	15	28	55	228	snoR135 (p-val 3.4)	13958589	13958612	C/D	unknown			
SNORD10	4	14998215	14998534	1	4	7	60	SNORD10 (p-val 0.12)	14998244	14998288	C/D	unknown			
snoR66	4	16091572	16091712	21	23	27	34	snoR66 (p-val 0.069)	16091625	16091661	C/D	unknown			
snoR127	5	4345379	4345519	2	2	4	11	snoR127 (p-val 0.23)	4345464	4345909	C/D	unknown			
SNORD86	5	5473737	5473877	0	0	0	1	SNORD86 (p-val 0.0095)	5473852	5473877	C/D	unknown			
snR86_1	5	7777490	7777630	3	14	8	68	snR86 (p-val 1.3)	7777498	7777596	C/D	unknown			
SNORD98	5	7853192	7853333	0	1	3	12	SNORD98 (p-val 0.000065)	7853220	7853273	H/ACA	25S rRNA	113	133	129
SNORD37	5	9641706	9641913	1	0	0	1	SNORD37 (p-val 0.29)	9641816	9641852	C/D	unknown			
snR86_2	5	13879626	13879766	1	0	1	7	snR86 (p-val 0.28)	13879626	13879665	C/D	unknown			
snoU13	5	15028345	15028485	0	3	1	5	snoU13 (p-val 0.68)	15028384	15028402	C/D	unknown			
SNORD70	5	19991356	19991496	2	0	1	12	SNORD70 (p-val 0.041)	19991362	19991442	C/D	unknown			
snoU85	5	21665872	21666012	1	0	1	2	snoU85 (p-val 0.0036)	21665899	21665953	C/D	unknown			
Plant_U3_5	5	21990591	21990866	1391009	906401	2217271	813011	Plant_U3 (p-val 5.1e^-58)	21990591	21990809	H/ACA	18S rRNA	1082/992	1094 / 1002	1086/994
SNORD24	5	22828847	22829135	8445	7439	19786	5203	SNORD24 (p-val 2.3e^-18)	22828847	22828932	C/D	25S rRNA	1435	1452	C1439

Table S2. List of all mapped/predicted modification sites within 25S rRNA in *A. thaliana.*
Adapted from Streit and Schleiff (2021).

predicted 2´-O-me	snoRNAs	mapped 2´-O-me	predicted Ψ	snoRNAs	mapped Ψ
U36	snoR16-2/U51b		U35	snoT89-1/2	Sun et al., 2019
U44	snoR120	Azevedo-Favory et al., 2020	U132	snoR94	
U48	snoR16-1/2	Azevedo-Favory et al., 2020	377	nd	Sun et al., 2019
A63	snoR107		U397	snoT155a/b/c	
A64	U55		U536	snoR135a/b	
U67	snoR31		U654	snoR162	
U144	At4gCDbox108.1	Azevedo-Favory et al., 2020	U783	snoR82	Sun et al., 2019
U145	snoR36		U826	snoR77	Sun et al., 2019
C335	snoR101		892	nd	Sun et al., 2019
U378	nd	Azevedo-Favory et al., 2020	899	nd	Sun et al., 2019
G386	U38-1/2		967	nd	Sun et al., 2019
U397	U14a		U973	snoR151	Sun et al., 2019
G398	snoR65	Azevedo-Favory et al., 2020	U999	snoR80-1/2/3	
U401	snoR106		U1013	snoR81-1/2	Sun et al., 2019
A660	U18-1/2	Azevedo-Favory et al., 2020	U1050	snoR141	
C674	snoR58Y-1/2	Azevedo-Favory et al., 2020	U1052	snoR141	Sun et al., 2019
U769	R72b/2		U1060	nd	Sun et al., 2019
U784	snoR52/snoR70	Barneche et al., 2001	U1130	snoR80-1/2/3	Sun et al., 2019
U801	snoR14-1/2		U1131	nd	Sun et al., 2019
U803	At1gCDbox31.1/At1g CDbox31.2	Azevedo-Favory et al., 2020	U1246	snoR96	Sun et al., 2019
G812	39BYa/b	Brown et al., 2001; Azevedo-Favory et al., 2020	U1255	snoR144	
A814	U51a/b	Brown et al., 2001; Azevedo-Favory et al., 2020	U1296	nd	Sun et al., 2019
A824	U80-1/2	Brown et al., 2001; Azevedo-Favory et al., 2020	U1465	snoR156	Sun et al., 2019
A883	snoR72Ya/b/c/d	Azevedo-Favory et al., 2020	U1473	nd	Sun et al., 2019
G915	At3gCDbox91.1/At3g CDbox91.2	Azevedo-Favory et al., 2020	U1897	snoR144	Sun et al., 2019
A943	snoR12-1a/b/2a/30	Liang-Hu et al.,2001; Azevedo-Favory et al., 2020	U2028	nd	Sun et al., 2019
A959	R79b/-2/c		U2093	snoR141	Sun et al., 2019
G1002	snoR105		U2124	nd	Sun et al., 2019
A1006	snoR23-2		U2126	snoR87	Sun et al., 2019
U1050	snoR23-3		U2174	snoR150	
U1064	snoR41Y	Azevedo-Favory et al., 2020	U2181	snoR135	Sun et al., 2019
U1089	snoR28-2b		U2201	snoR99	Sun et al., 2019
A1105	snoR81	Barneche et al., 2001	U2244	snoR92	
U1140	U38-1/2/3	Azevedo-Favory et al., 2020	U2248	snoR79-1/2/3	Sun et al., 2019
A1161	snoR107		U2250	U19	Sun et al., 2019
G1191	snoR114		U2304	snoR83	Sun et al., 2019

U1218	snoR36		U2337	nd	Sun et al., 2019
A1248	R72b/2/72c/s/e		U2339	snoR83	Sun et al., 2019
A1260	snoR22-2/3a/3b	Barneche et al., 2001; Azevedo-Favory et al., 2020	U2406	nd	Sun et al., 2019
U1275	snoR22-2/3a/3b	Barneche et al., 2001; Azevedo-Favory et al., 2020	U2422	nd	Sun et al., 2019
C1280	snoR118		U2436	nd	Sun et al., 2019
A1312	snoR69Y		U2445	snoR138	
G1356	snoR106		U2487	nd	Sun et al., 2019
A1372	snoR7-1/2		U2489	nd	Sun et al., 2019
A1377	At3gCDbox102.1/At5 gCDbox102.2	Azevedo-Favory et al., 2020	U2555	snoR86-1/2	
C1439	U24-1/2	Brown et al., 2001; Azevedo-Favory et al., 2020	U2587	nd	Sun et al., 2019
G1446	snoR113		U2604	nd	Sun et al., 2019
A1451	U24-1/2	Brown et al., 2001; Azevedo-Favory et al., 2020	U2620	snoR78-1/2	
G1452	U24-1/2	Brown et al., 2001; Azevedo-Favory et al., 2020	U2703	snoR95	Sun et al., 2019
U1459	snoR28-1a	Brown et al., 2001;	U2707	snoR97-1/2	
C1471	snoR147	Azevedo-Favory et al., 2020	U2735	nd	Sun et al., 2019
C1498	snoR72Yb		U2773	snoR93	
C1510	U49-1/2/3/ snoR121	Brown et al., 2001; Azevedo-Favory et al., 2020	U2816	U65-1	Sun et al., 2019
A1511	snoR33		U2833	snoR136	Sun et al., 2019
U1634	nd	Brown et al., 2001	U2844	nd	Sun et al., 2019
U1679	U35		U2855	snoR160	Sun et al., 2019
U1680	snoR68Y		U2870	U65-2/3	Sun et al., 2019
A1793	snoR21a		U2884	snoR142	Sun et al., 2019
C1837	At5gCDbox123.1	Azevedo-Favory et al., 2020	U2913	snoR74-1/2	Sun et al., 2019
C1840	Z42	Brown et al., 2001	U2945	nd	Sun et al., 2019
G1845	snoR59a/b	Brown et al., 2001	U2964	snoR97-2	Sun et al., 2019
C1850	snoR15/U55/U61-2	Brown et al., 2001; Azevedo-Favory et al., 2020	U2965	snoR97-2	Sun et al., 2019
A1861	snoR33	Brown et al., 2001; Azevedo-Favory et al., 2020	U3100	nd	Sun et al., 2019
U1882	U34a/b/c/d	Brown et al., 2001; Barneche et al., 2001; Azevedo-Favory et al., 2020	U3177	nd	Sun et al., 2019
G1913	U40-2				
U1918	nd	Brown et al., 2001			
G1997	R72d				
U2103	snoR117	Azevedo-Favory et al., 2020			
A2114	U60-1F/2F	Barnache et al., 2000; Azevedo-Favory et al., 2020			
G2116	snoR12-1a/b/2	Liang-Hu et al., 2001; Azevedo-Favory et al., 2020			
A2130	U34a				
U2176	snoR10-1/2				
C2187	snoR118	Azevedo-Favory et al., 2020			
A2204	U37	Brown et al., 2001; Azevedo-Favory et al., 2020			
A2210	U36-1/2/3	Brown et al., 2001; Azevedo-Favory et al., 2020			
G2226	U36a-1/2/3	Azevedo-Favory et al., 2020			

A2246	U46-1/2	Azevedo-Favory et al., 2020
C2247	U40-2	
A2271	U15-1a/b/2	Brown et al., 2001; Barneche et al., 2001; Azevedo-Favory et al., 2020
G2278	U15-1a/b/2	Brown et al., 2001; Azevedo-Favory et al., 2020
C2283	nd	Azevedo-Favory et al., 2020
A2311	U30	Brown et al., 2001; Azevedo-Favory et al., 2020
A2316	snoR44-1a/b/2/3	Brown et al., 2001; Barneche et al., 2001
C2319	R79b/-2/c	
A2324	U14b	
C2327	snoR44-1a/b/2/3	Brown et al., 2001; Barneche et al., 2001; Azevedo-Favory et al., 2020
C2340	snoR77Y-1	
A2351	At2gCDbox63.1	Azevedo-Favory et al., 2020
C2355	snoR37-1/2/U53	Barneche et al., 2001; Azevedo-Favory et al., 2020
G2381	snoR29-1/2	Azevedo-Favory et al., 2020
G2385	nd	Azevedo-Favory et al., 2020
G2399	nd	Azevedo-Favory et al., 2020
U2400	snoR53Y	Barneche et al., 2001; Azevedo-Favory et al., 2020
G2404	snoR29-1/2	Barneche et al., 2001
U2411	snoR37-1/2/U53	Azevedo-Favory et al., 2020
U2445	snoR16-1	Azevedo-Favory et al., 2020
U2483	snoR123a/b	Azevedo-Favory et al., 2020
U2486	R72e	
A2550	nd	Azevedo-Favory et al., 2020
G2610	snoR35/U31a/b	Brown et al., 2001; Azevedo-Favory et al., 2020
A2631	snoR27/68Y	Brown et al., 2001; Azevedo-Favory et al., 2020
U2641	snoR10-1/2	Brown et al., 2001; Azevedo-Favory et al., 2020
G2642	nd	Brown et al., 2001; Azevedo-Favory et al., 2020
C2660	snoR26	
C2673	snoR148	Azevedo-Favory et al., 2020
A2712	R72c	
U2726	snoR68	Azevedo-Favory et al., 2020
G2781	snoR1a/b	Brown et al., 2001; Barneche et al., 2001; Azevedo-Favory et al., 2020
G2783	nd	Brown et al., 2001; Azevedo-Favory et al., 2020
G2805	snoR38Y-2	Azevedo-Favory et al., 2020
C2826	snoR24a/b/c/d	Brown et al., 2001; Barneche et al., 2001; Azevedo-Favory et al., 2020
C2847	nd	Brown et al., 2001
C2856	nd	Brown et al., 2001
C2869	U49-1/2/3	Brown et al., 2001; Barneche et al., 2001; Azevedo-Favory et al., 2020
U2873	snoR64	Barneche et al., 2001; Azevedo-Favory et al., 2020
A2901	snoR31	Azevedo-Favory et al., 2020
G2907	snoR34	Azevedo-Favory et al., 2020

U2911	nd	Azevedo-Favory et al., 2020
G2912	nd	Brown et al., 2001; Azevedo-Favory et al., 2020
A2924	snoR18a/b	Azevedo-Favory et al., 2020
A2936	U29	Azevedo-Favory et al., 2020
C2938	snoR69Y	Azevedo-Favory et al., 2020
G2942	nd	Brown et al., 2001
U2943	nd	Brown et al., 2001; Azevedo-Favory et al., 2020
C2949	U35	Brown et al., 2001; Azevedo-Favory et al., 2020
A3095	snoR58Y-1	
A3221	snoR105	
G3271	U51a	
A3273	snoR6-1/2	
G3280	U33a/b	Azevedo-Favory et al., 2020
U3289	snoR13-1/2	Azevedo-Favory et al., 2020
G3310	snoR72Yc	

Table S3. List of all mapped/predicted modification sites within 18S rRNA in *A. thaliana.*
Adapted from Streit and Schleiff (2021).

predicted 2´-O-me	snoRNAs	mapped 2´-O-me	predicted Ψ	snoRNAs	mapped Ψ
A28	U27-2	Azevedo-Favory et al., 2020	U35	nd	Sun et al., 2019
C38	snoR66	Azevedo-Favory et al., 2020	U56	snoR155a/b/c	
U60	snoR26		U111	snoR100-2	Sun et al., 2019
U123	snoR116	Azevedo-Favory et al., 2020	U121	nd	Sun et al., 2019
A162	snoR18a/b/77-1	Azevedo-Favory et al., 2020	U220	snoR89/-2	Sun et al., 2019
U168	snoR122		U253	nd	Sun et al., 2019
U213	At1gCDbox33.1	Azevedo-Favory et al., 2020	U256	nd	Sun et al., 2019
G244	snoR124	Azevedo-Favory et al., 2020	U304	nd	Sun et al., 2019
U305	snoR33		U360	snoR86/-2	Sun et al., 2019
U350	snoR42		U370	snoR7	
U371	snoR28-2b		U381	nd	Sun et al., 2019
G390	snoR30/46/87	Barneche et al., 2001; Azevedo-Favory et al., 2020	U583	nd	Sun et al., 2019
G391	snoR58/67	Barneche et al., 2001	U604	snoR91	Sun et al., 2019
C416	U14a/b	Azevedo-Favory et al., 2020	U634	snoR73	Sun et al., 2019
A438	snoR15/U16	Brown et al., 2001; Barneche et al., 2001; Azevedo-Favory et al., 2020	U677	snoR140	
A466	snoR17	Brown et al., 2001; Azevedo-Favory et al., 2020	U715	snoR87	
C471	snoR7-1/2/U56	Brown et al., 2001; Azevedo-Favory et al., 2020	U752	snoR77	

A475	U61-2		U761	snoR91	Sun et al., 2019
C525	U37		U762	snoR139	Sun et al., 2019
A543	snoR41Y/43/34-1	Barneche et al., 2001; Azevedo-Favory et al., 2020	U803	snoR99	
U580	snoR77Y-1	Azevedo-Favory et al., 2020	U827	snoR84	
A596	snoR72Ya		U918	snoR76	
G597	U54	Azevedo-Favory et al., 2020	U947	nd	Sun et al., 2019
U602	snoR115-1/2	Azevedo-Favory et al., 2020	U948	snoR90	Sun et al., 2019
G609	snoR62-1	Barneche et al., 2001	U1000	snoR5/72	Sun et al., 2019
U613	snoR13-1/2	Azevedo-Favory et al., 2020	U1025	nd	Sun et al., 2019
U621	U36	Azevedo-Favory et al., 2020	U1090	snoR91	
G668	snoR39/20-1		U1104	snoR134	Sun et al., 2019
G687	snoR29		U1118	snoR5/72	Sun et al., 2019
A720	snoR28-1a		U1188	snoR161	
A778	snoR119	Azevedo-Favory et al., 2020	U1192	snoR134	
A794	At1gCDbox37.1	Azevedo-Favory et al., 2020	U1208	snoR137	Sun et al., 2019
C795	snoR25		U1215	snoR140	Sun et al., 2019
A799	snoR53Y	Brown et al., 2001; Azevedo-Favory et al., 2020	U1302	snoR88	Sun et al., 2019
A810	nd	Azevedo-Favory et al., 2020	U1306	snoR160	
U837	snoR28-1b		U1311	nd	Sun et al., 2019
G995	U3.5		U1479	snoR138/154	
A975	snoR59a/b	Brown et al., 2001; Azevedo-Favory et al., 2020	U1483	nd	Sun et al., 2019
U1010	snoR20-1/74	Liang-Hu et al.,2001; Barneche et al., 2001; Azevedo-Favory et al., 2020	U1520	snoR73	
C1011	snoR20-2	Liang-Hu et al.,2001	U1523	snoR78-1/2	
G1071	snoR6-2		U1531	snoR152a/b	Sun et al., 2019
A1087	U3.3/U3.5		U1630	nd	Sun et al., 2019
U1097	U38-3		U1702	nd	Sun et al., 2019
U1104	snoR35				
G1111	snoR9-1	Barneche et al., 2001			
C1174	snoR46				
A1185	nd	Azevedo-Favory et al., 2020			
C1210	snoR10-2				
C1216	At1gCDbox47.1	Azevedo-Favory et al., 2020			
G1219	SNORD72				
A1220	U31a/b				
U1232	snoR14-1/2	Azevedo-Favory et al., 2020			
U1251	snoR27				
U1261	snoR67/68/8				
U1263	snoR32	Liang-Hu et al.,2001; Azevedo-Favory et al., 2020			
U1261	At3gCDbox95.1/At3gCDbox95.2/At5gCDbox144.1	Azevedo-Favory et al., 2020			
U1270	snoR34/U33a/b	Brown et al., 2001; Azevedo-Favory et al., 2020			

G1271	snoR26	Barneche et al., 2001
G1272	snoR21a	Brown et al., 2001; Azevedo-Favory et al., 2020
U1308	U18-1/2	
A1327	snoR32	Azevedo-Favory et al., 2020
U1381	U61	Azevedo-Favory et al., 2020
G1415	snoR69/42	
G1431	snoR19/73-1	Azevedo-Favory et al., 2020
U1445	snoR19/73-1	Barneche et al., 2001; Azevedo-Favory et al., 2020
U1524	snoR72Yd	
A1527	snoR64	
U1550	nd	Azevedo-Favory et al., 2020
A1558	snoR54/59	
A1575	snoR8	Azevedo-Favory et al., 2020
G1590	snoR114	
G1596	snoR48	
C1626	snoR70	Barneche et al., 2001
C1641	U43/snoR41	Azevedo-Favory et al., 2020
A1662	snoR11	
G1672	snoR69	
A1731	snoR6-1	
A1754	snoR23-1/3/12-1/70	Barneche et al., 2001; Azevedo-Favory et al., 2020
A1785	snoR12-1	

Table S4. List of all mapped/predicted modification sites within 5.8S rRNA in *A. thaliana.*
Adapted from Streit and Schleiff (2021).

predicted 2´-O-me	snoRNAs	mapped 2´-O-me	predicted Ψ	snoRNAs	mapped Ψ
Am47	snoR9-1/2	Brown et al., 2001, Liang-Hu et al.,2001; Barneche et al., 2001; Azevedo-Favory et al., 2020	U78	nd	Sun et al., 2019
Gm79	39BYa/b	Brown et al., 2001; Azevedo-Favory et al., 2020	U22	nd	Sun et al., 2019

Danksagung

Zunächst möchte ich mich herzlichst bei Prof. Dr. Enrico Schleiff bedanken, der mir die Möglichkeit gegeben hat, die äußerst spannende und komplexe Welt der pflanzlichen bzw. eukaryotischen Ribosomenbiogenese zu entdecken und mir auf meiner Reise durch diesen Dschungel immer mit Rat und Tat zur Seite stand.

Ebenfalls möchte ich mich bei Prof. Dr. Michaela Müller-McNicoll für ihre Bereitschaft als Zweitgutachterin meine Dissertation zu lesen, bedanken.

Ich möchte mich auch beim der gesamten AK Schleiff bedanken für die wunderschöne Zeit und die vielen interessanten und wertvollen Seminare, die wir über die Jahre zusammen hatten. Insbesondere möchte ich meinem Kollegen und Freund Thiruvenkadam danken, der immer ein offenes Ohr hatte und mir stets hilfreich mit konstruktiver Kritik zur Seite stand. Ich danke Denise Palm und Jelena Kovacevic, die mich herzlichst in das RiboBio-Labor aufgenommen haben und mir alle wichtigen Techniken und Methoden beigebracht haben.

Des Weiteren danke ich Akis für sein stets offenes Ohr und seine aufmunternden Worte und Unterstützung während meines Studiums. Ich danke auch den vielen Postdocs, insbesondere Stefan und Roman und Rafa, für Ihre stete Unterstützung, wenn ich Fragen hatte. Danke auch an Misgana und Karin, die mir die letzten Wochen und Monate die Zeit im Labor versüßt haben. Ein besonderer Dank geht an Uwe, der immer für ein Späßchen zu haben war und den Tag erhellt hat. Bleib so wie du bist mein Lieber. Ich möchte auch Dr. Peter Kötter danken für seine konstruktiven Kritiken während der *thesis commitee* Sitzungen und Hilfestellungen für Experimente. Außerdem danke ich Dr. Andreas Schlundt für seine Hilfestellungen in der Strukturbiologie und mir sehr gute Anhaltspunkte gegeben hat, wie eine verlängerte 5.8S rRNA im Ribosom aussehen könnte.

Ein großer Dank geht an das gesamte Gärtner-Team um Holger herum, für die unzähligen Töpfe und der Pflege der Pflanzen, die ich für die Experimente benötigt habe.

Ich danke meiner Familie aus tiefstem Herzen für ihre Unterstützung und Beistand, wenn ich sie brauchte. Insbesondere danke ich meinem Vater, der mich immer zu höheren motiviert hat und mich damit zu der Person gemacht, die ich heute bin. Leider kannst du das alles nicht mehr miterleben, aber ich weiß, dass du immer bei mir sein wirst. Ich danke meiner Schwester Ebru, für ihre Worte und Zusprüche und ihrer motivierenden Art. Ich danke meinem Mann Roland, dass er immer für mich da war und natürlich meinem größten Geschenk Alexis, der mein Leben um einiges reicher und lebenswerter gemacht hat, seit dem Tag seiner Geburt.

Publications

Parts of chapter 5.1, 5.2, 6.1 and XX of this thesis were published in the following publications, and the work of each author is indicated:

Streit, D., Shanmugam, T., Garbelyanski, A., Simm, S., & Schleiff, E. (2020). The Existence and Localization of Nuclear snoRNAs in *Arabidopsis thaliana* Revisited. ***Plants*** *(Basel, Switzerland)*, *9*(8), 1016.

Streit D:	Oligo design for FISH and northern blot, RNA extraction, cell culture growth, fractionation of cell culture, northern hybridization, FISH analysis, computational prediction of snoRNA binding sites, manuscript preparation
Shanmugam T:	Oligo design for FISH and northern blot, FISH analysis, northern hybridization, fractionation of cell culture, manuscript preparation
Garbelyanski A:	Northern blotting and hybridization
Simm S:	Analysis of NGS results, computational prediction of snoRNA binding sites
Schleiff E:	Data validation, supervision and manuscript preparation

Streit, D., & Schleiff, E. (2021). The Arabidopsis 2'-O-Ribose-Methylation and Pseudouridylation Landscape of rRNA in Comparison to Human and Yeast. ***Frontiers in plant science***, *12*, 684626.

Streit D:	Creation of secondary structure maps of rRNA, analysis of modified sites
Schleiff E:	Validation data, supervision and manuscript preparation

Further publications on ribosome biogenesis in plants

1. Palm, D., Streit, D., Ruprecht, M., Simm, S., Scharf, C., & Schleiff, E. (2018). Late ribosomal protein localization in *Arabidopsis thaliana* differs to that in *Saccharomyces cerevisiae*. *FEBS open bio*, *8*(9), 1437–1444.
2. Palm, D., Streit, D., Shanmugam, T., Weis, B. L., Ruprecht, M., Simm, S., & Schleiff, E. (2019). Plant-specific ribosome biogenesis factors in Arabidopsis thaliana with essential function in rRNA processing. *Nucleic acids research*, *47*(4), 1880–1895.
3. Shanmugam, T., Streit, D., Schroll, F., Kovacevic, J., & Schleiff, E. (2021). Dynamics and thermal sensitivity of ribosomal RNA maturation paths in plants. *Journal of experimental botany*, erab434. Advance online publication.
4. Shanmugam, T., Chaturvedi, P., Streit, D., Ghatak, A., Bergelt, T., Simm, S., Weckwerth, W., & Schleiff, E. (2022). Low dose ribosomal DNA P-loop mutation affects development and enforce autophagy in Arabidopsis. EMBO reports. In submission
5. Streit, D., Shanmugam, T., Schlundt, A., Simm, S., & Schleiff, E. (2022). The processing of 5.8S in plants. Draft

Erklärung

Ich erkläre hiermit, dass ich mich bisher keiner Doktorprüfung unterzogen habe.

Frankfurt am Main, den ……..…….. …….

Eidesstattliche Versicherung

Ich erkläre hiermit an Eides Statt, dass ich die vorgelegte Dissertation über

„ Plant specificities in rRNA processing - From snoRNA to rRNA variations - ”

selbständig angefertigt und mich anderer Hilfsmittel als der in ihr angegebenen nicht bedient habe, insbesondere, dass alle Entlehnungen aus anderen Schriften mit Angabe der betreffenden Schrift gekennzeichnet sind.

Ich versichere, die Grundsätze der guten wissenschaftlichen Praxis beachtet, und nicht die Hilfe einer kommerziellen Promotionsvermittlung in Anspruch genommen zu haben.

Frankfurt am Main, den ……..…….. …….